

READING THE RECORDED HISTORY OF SOIL MANTLED HILLSLOPES

By

Simon Marius Mudd

Dissertation

Submitted to the Faculty of the
Graduate School of Vanderbilt University

in partial fulfillment of the requirements

for the degree of

DOCTOR OF PHILOSOPHY

in

Environmental Engineering

May, 2006

Nashville, Tennessee

Approved:

Professor David J. Furbish

Professor James H. Clarke

Professor Kaye S. Savage

Professor Florence Sanchez

To my wife Robin, my mother Monika, and my father Brian

ACKNOWLEDGMENTS

This work was made possible through the financial support of the National Science Foundation, the Florida State University, and Vanderbilt University.

I am grateful to my peers, colleagues, and mentors with whom I have had countless hours of discussion about geomorphology that have shaped my ideas about the physics of the Earth's surface. I wish to give special thanks to the people with whom I have generally looked for beautiful landscapes to work in and understand. These people include (in semi-chronological order) Ian MacMillan, Manny Gabet, Mike Singer, Daniel Malmon, Tom Dunne, Steve Lancaster, Ryosuke Akahori, Jeroen Sonke, Jiun-Yee Yen, Sergio Fagherazzi, Andrea D'Alpaos, Mark Schmeekle, and Kyungsoo Yoo.

Finally, and perhaps most significantly, I wish to acknowledge David Furbish, my advisor and mentor. It will be my pleasure to carry on David's intellectual legacy, and will strive in my career to be his equal in ability and enthusiasm for both teaching and creating knowledge in the field of earth surface processes.

TABLE OF CONTENTS

	Page
DEDICATION	ii
ACKNOWLEDGMENTS	iii
LIST OF TABLES	vii
LIST OF FIGURES	viii
 Chapter	
I. INTRODUCTION	1
1. Overview	1
2. Components of the Thesis	7
3. Summary	14
3. References	16
II. THE INFLUENCE OF CHEMICAL DENUDATION ON HILLSLOPE MORPHOLOGY	19
Abstract	19
1. Introduction	20
2. A Depth-Integrated Equation of Hillslope Mass Conservation Incorporating Chemical Denudation and Deposition	25
2.1. Previous Work	25
2.2. General Statement of Mass Conservation	26
2.3. Depth-Integration of the Statement of Mass Conservation ..	28
2.4. Kinematic Conditions at the Soil Surface and the Soil-Bedrock Boundary	29
2.5. The Depth-Integrated Equation for Mass Conservation of Soil on a Hillslope	31
2.6. Simplifying Assumptions for Conservation of Mass Equation	32
3. The Steady-State, Chemically Denuding Hillslope: 1-D Analysis	33
3.1. Derivation of Governing Equations	33
3.2. Denudation Rates	36
3.2.1. Mechanical Denudation Rate	36
3.2.2. Chemical Denudation Rate	36
3.3. Curvature, Slope, and Profile of the 1-D Steady- State Hillslope	39

3.3.1. Features of the 1-D Steady-State Hillslope	40
3.4. Non-Dimensionalization	43
4. Discussion	46
4.1 Effect of Chemical Weathering on the Morphology of Steady-State Hillslopes	46
4.2. Conceptual Explanation of the Steady-State Convex-Concave Hillslope	47
4.3. Conditions for Steady-State Hillslopes with Convex-Concave Profiles	48
4.4. Transport Ratios for Steady-State Hillslopes With Convex-Concave Profiles	50
4.5. Comparison of Theoretical Transport Ratios with Transport Ratios Calculated From Field Data	51
4.6. The Occurrence of Hillslopes with Denudation Ratios Greater Than 0.5	54
5. Conclusions	55
Appendix 1	56
Appendix 2	57
Appendix 3	58
6. List of Symbols	60
7. References	62

III. USING CHEMICAL TRACERS IN HILLSLOPE SOILS TO ESTIMATE THE IMPORTANCE OF CHEMICAL DENUDATION UNDER CONDITIONS OF DOWNSLOPE SEDIMENT TRANSPORT.....68

Abstract	68
1. Introduction	69
2. A Coupled Model of Hillslope Evolution	72
2.1. Conservation of Total Soil Mass	72
2.2. Conservation of a Soil Phase	74
3. A 1-D, Two Phase Model of Hillslope Weathering and Transport	77
3.1. Simplifying assumptions	78
3.2. Flux Laws	79
3.3. Lagrangian Coordinate System	80
3.4. The Governing Equations for a Hillslope Soil Composed of Two Phases	81
3.5. Non-Dimensionalization and Scaling	84
4. On the Use of the Two Phase Hillslope System	87
4.1. Steady State Solution of the Two Phase Hillslope Model	90
4.2. Quantifying the Changes in the Concentration of the Immobile Phase Related to Transient Incision or Deposition	99
5. Conclusions	105
Appendix A	107
6. List of Symbols	109

7. References	111
IV. LATERAL MIGRATION OF HILLCRESTS IN RESPONSE TO CHANNEL INCISION IN SOIL MANTLED LANDSCAPES.....	117
Abstract	117
1. Introduction	118
2. A 1-D Model of Hillcrest Migration	122
2.1. Governing Equations	122
2.2. Scaling and Nondimensionalization of the Governing Equations	126
2.3. Dimensionless Governing Equations	128
3. Analytical Solutions of Hillcrest Migration	129
3.1. Hillcrest Offset Due to Channel Elevation Differences at Topographic Steady State	129
3.2. Migrating Hillcrest Due to Steady But Unequal Channel Incision Rates	135
4. Numerical Simulations of Transient Hillcrest Migration	142
4.1. The Effect of Delayed Knickpoint Migration	143
4.1.1. Linear Flux Law	144
4.1.2. Linear-Critical Flux Law	151
4.1.3. Soil Storage and Thickness Effects	153
4.2. The Effect of Variations in Amplitude and Frequency of Incision Rates	155
5. Conclusions	161
6. List of Symbols	163
7. References	166
V. RESPONSES OF SOIL MANTLED HILLSLOPES TO TRANSIENT CHANNEL INCISION RATES.....	171
Abstract	171
1. Introduction	171
2. Mass Conservation of Eroding Hillslope Soils.....	174
3. Timescales of Adjustment to Transient Channel Incision for aSimplified Soil Mantled Hillslope.....	176
4. Timescales of Hillslope Response for Soil Thickness, Soil Production,and Hillslope Erosion Rate.....	184
4.1. Numerical Simulations.....	186
4.1.1. Linear Flux Law.....	187
4.1.2. Depth-Slope Flux Law.....	189
5. Conclusions.....	191
6. List of Symbols.....	192
7. References.....	194
VI. CONCLUSIONS AND FUTURE DIRECTIONS.....	198

LIST OF TABLES

Table	Page
CHAPTER II	
1. Values of the transport ratio (θ_T) for naturally occurring rates of total denudation (R_T), average soil depth ($\langle h \rangle$), hillslope length (λ), and sediment diffusivity (D).....	53
2. Denudation ratios (θ_d) from selected river basins.....	55
CHAPTER IV	
1. Measured incision ratios of adjacent basins.....	140

LIST OF FIGURES

Figure	Page
 CHAPTER I	
1. A soil mantled landscape in Marin County, California.	2
2. Two hillslopes experiencing a reduction in the downcutting rate in the channel (at $x = 50\text{m}$). These different flux laws lead to different soil depth profiles. [Modified from <i>Furbish</i> , 2003].	3
3. Conceptual diagram of the effect of chemical denudation on hillslope morphology.	8
4. Schematic showing the different mechanisms by which hillslope soils may become enriched in an chemically immobile mineral (such as zircon).	10
5. Plots of the difference in elevations between two channels on each side of a hillcrest (dotted lines) and the lateral motion of the hillcrest (solid line) that results from different channel incision rates.....	12
6. The surface topography and erosion rate of a hillslope that is responding to a change in the rate of incision of the channel at its base.....	14
 CHAPTER II	
1. The convex upward portion of an idealized convex-concave hillslope has negative curvature by convention, and the concave portion has positive curvature.....	21
2. Idealized simulation of a soil mantled landscape using a traditional form of the sediment continuity equation.....	23
3. Diagrams of coordinate system adopted for soil-mantled hillslopes.....	28
4. Diagram of denudation balance.....	38
5. Non-dimensional surface elevation, slope, and curvature for hillslopes with varying parameter values.....	47
6. Diagram of a convex-concave slope and the denudation balance as a function of distance from the divide.....	48
7. Dimensionless depth of soil at the divide (h_*) for hillslopes with	

	an inflection point at the hillslope outlet ($x = \lambda$) and hillslopes with an inflection point three quarters of the length of the hillslope from the divide.....	49
8.	Contour plot of the transport ratio (θ_T) for an inflection point of $\xi_* = 0.5$ and $\xi_* = 0.75$ and dimensionless soil depth $h_* = 0.1, h_* = 0.05, \text{ or } h_* = 0.01$	51
9.	Hillslope profiles for various values of the transport ratio (θ_T), dimensionless soil depth at the divide (h_*), rate of increase in soil depth away from the divide (m), and denudation ratio (θ_d).....	52
CHAPTER III		
1.	Schematic of a 2-D hillslope.....	73
2.	Schematic of the 1-D hillslope.....	78
3.	Schematic showing mechanisms for changing the elevation of the soil-saprolite boundary relative to base level.....	82
4.	Schematic showing mechanisms for changing the elevation of the soil surface relative to base level.....	83
5.	Schematic of the mechanisms that change the concentration of the chemically immobile phase within the soil layer.....	86
6.	Schematic of the a. integrated denudation rates and b. local denudation rates. c. Spatial variations in the local denudation ratio and the integrated denudation ratio.....	89
7.	Schematic showing a. linear variation in space of the dimensionless mass loss rate due to chemical weathering (\hat{S}) and its relationship to the spatial variation in the local denudation ratio (Θ_{dl}).....	93
8.	Plots of enrichment of the immobile phase in the soil (\hat{c}) and the chemical depletion fraction (CDF) for steady state solutions of the two phase hillslope system where there is no spatial variation in the local chemical denudation rate ($\Phi_{sl} = 0$).....	94
9.	Plots of enrichment of the immobile phase in the soil (\hat{c}) and the chemical depletion fraction (CDF) for steady state solutions of the two phase hillslope system where there is no spatial variation in the enrichment of the immobile phase at the soil-saprolite boundary ($\sigma = 0$).....	95

10.	Normalized difference between the true local ratio of chemical to total denudation rate (Θ_{dl}) and this ratio estimated using the chemical depletion fraction (CDF).....	96
11.	Contour plots of the fractional difference between the integrated denudation ratio and the denudation ratio estimated by the chemical depletion fraction (e.g., all plots show contours of $\delta_1 = (\theta_d - \text{CDF})/\theta_d$).....	99
12.	Diagram showing the response of a hillslope to increasing or decreasing incision rates.....	105

CHAPTER IV

1.	Two scenarios for erosion in a basin.....	119
2.	Schematic of the coordinate system.....	123
3.	Dimensionless hillslope profiles.....	130
4.	Contours of the dimensionless hillcrest offset ($\hat{\Omega}$) as a function of hillslope relief and vertical channel offset.....	134
5.	Pseudo steady state hillcrest migration.....	137
6.	The dimensionless time to stream capture (\hat{t}_{sc}) as a function of the incision ratio θ_l and the density ratio τ_d	139
7.	Transient behavior of a hillslope subjected to two knickpoints of the same elevation.....	144
8.	Relaxation time of hillcrest migration as a fraction of hillslope relaxation time (κ).....	146
9.	Hillcrest offset through dimensionless time for hillslopes with linear sediment transport, $\tau_d=2$, and $\theta_{kp}=0.3$	151
10.	Hillcrest offset as a function of dimensionless time. All runs use a linear-critical sediment flux law unless where labeled.....	152
11.	Change in soil storage ratio through time.....	154
12.	Vertical channel offset and hillcrest offset for hillslopes bounded by channels with oscillating incision rates.....	157
13.	Soil thickness as a function of time and space for a	

hillslope bounded by channels with oscillating incision rates.....	160
--	-----

CHAPTER V

1. Schematic of the soil profile.....	175
2. Schematic of the 1-D hillslope.....	178
3. Analytical solutions of equation (6) for surface topography (a.) and erosion rate (b.).....	179
4. The true erosion rate (solid lines) and erosion rate predicted by fitting equation (11) (dashed grey lines) as a function of time at the divide (a. , $x = 0$) and a point near the channel (b. $x = 32\text{m} = 0.8\lambda$).....	180
5. Erosion rate due to individual harmonics on a perturbed hillslope as a function of time.....	182
6. Values of M_E (see equation 11) as a function of wavenumber.....	184
7. Plots of normalized (by τ_0 in a. and τ_a in b.) response timescale for the soil thickness and erosion rate.....	187
8. Difference between hillslope response timescale τ and approximate hillslope response timescale τ_a normalized by τ_a for hillslopes whose sediment flux is linearly proportional to the hillslope gradient.....	188
9. Difference between hillslope response timescale τ and approximate hillslope response timescale τ_a normalized by τ_a for hillslopes whose sediment flux is proportional to the hillslope gradient times the soil thickness.....	190

CHAPTER I

INTRODUCTION

“Hillslopes have the distinction of being the commonest and, at the same time, least studied geomorphic features, especially in terms of the processes acting upon them. In some ways it is their very ubiquity which is responsible for this neglect because researchers have preferred to study unique or restricted features instead of facing the massive sampling problem which is involved in characterizing slopes. In addition, hillslopes present difficult research problems because their forms change either slowly or infrequently, particularly when compared to rivers.”

-Carson and Kirkby, 1972

1. Overview

Landscapes are formed over thousands to tens of millions of years through the complex interactions between climate and tectonics. These two forcing factors drive both mechanical and chemical processes that act to denude the landscape. The nature and intensity of these processes acting upon the landscape, when integrated over geologic time, determine the morphology and chemical composition of the landscape.

Soil mantled hillslopes (Figure 1) make up a significant portion of the terrestrial landscape, and are the subject of this thesis. The production of mobile sediment on hillslopes, and chemical dissolution within hillslope soils, are the primary source of sediment and nutrients within many landscapes. Hillslope soils also serve as the thin layer upon which biota thrive, and serve to store and cycle nutrients essential to life on the surface of the Earth.

A fundamental goal of geomorphologists is to be able to predict how hillslopes react to changes in climatic and tectonic forcings. For example, on a global scale, we



Figure 1. A soil mantled landscape in Marin County, California.

would like to be able to predict how climate change affects the supply of nutrients to the ocean. The nutrients are derived from eroded bedrock, temporarily stored on hillslopes, and hillslope processes determine the rate and nature of their delivery to the fluvial system, which then transports the nutrients to the ocean. On a more local scale, a watershed manager might want to predict how erosion rates and sediment supply to a river might change with changes in land use, or if erosion rates measured over human timescales are similar to long term average erosion rates.

Making predictions of how changes in climatic and tectonic forcings will affect erosion rates requires an understanding of how the processes that combine to erode the landscapes vary with climate and tectonic forcing. Early geomorphologists recognized that hillslope forms and the processes acting upon them are linked. For example, G. K. Gilbert [1909] proposed that the rate of sediment transport increases with increasing

slope. Further, Gilbert [1909] observed that the convexity of hillslopes could be explained because slope must increase as one moves from the hillcrest because all sediment that is produced upslope of a point on the hillslope must be transported through that point. Such observations led to much research in the field of geomorphology, but without quantifying the processes using sediment flux laws (e.g. an equation that describes the sediment flux as a function of some landscape property, such as slope), using mathematical and theoretical models was impossible. Later, R. E. Horton [1945] published seminal papers in the field of process geomorphology by quantifying sediment transport as a function of slope and hydrology based on field experiments. W. E. H. Culling [1960] then combined a hillslope sediment flux law with a statement of mass conservation. This was the first rigorous statement of mass conservation applied to a hillslope soil, and gave birth to modern hillslope geomorphology.

Using conservation of mass, the most basic tool of physical scientists, in conjunction with sediment flux laws, geomorphologists were able to show how different hillslope processes affected hillslope morphologies [e.g., *Ahnert*, 1970; *Armstrong*, 1976; *Carson and Kirkby*, 1972; *Culling*, 1963; *Hirano*, 1975; *Kirkby*, 1971], and how changes in the nature and intensity of these processes could lead to dynamic hillslope behavior [e.g., *Ahnert*, 1987; *Armstrong*, 1987; *Arrowsmith et al.*, 1996; *Dunne*, 1991; *Gossmann*, 1976; *Kirkby*, 1985]. In addition, a number of researchers have used the assumption that the landscape has approached a condition where base level fall matches erosion to investigate the interactions between climate, tectonics, and hillslope form (called a steady state or steady topographic form assumption) [e.g., *Heimsath et al.*, 1997; *Howard*, 1988; *Riebe et al.*, 2003; *Roering et al.*, 1999; *Small et al.*, 1999].

In many of these studies of hillslope form and process, it has been implicitly assumed that a unique suite of processes and forcings will generate unique topography. Recently, the usefulness of using topography alone to investigate the relationships between climate, tectonics, and hillslope morphology has been questioned [Furbish, 2003; Roering *et al.*, 2004]. Regardless of whether the landscape is at steady state or not, the linkages between process and form may not be unique. For example, Dunne [1991] demonstrated that hillslopes with different processes acting at different intensities can result in similar topography. If a steady state assumption is made, the dynamics of hillslope evolution may be discounted, and one only needs a direct observation of topography to relate form and process. While there is evidence of steady state in some landscapes [e.g., Reneau and Dietrich, 1991], many landscapes have been the subject to changes in climate or tectonics over the history of the hillslope [e.g., Arrowsmith *et al.*, 1996; Gabet and Dunne, 2003; Roering *et al.*, 2004]. The morphologies of many hillslopes are determined by the integrated history of their dynamic evolution [e.g., Howard, 1997]. Unfortunately, the time over which hillslopes develop is 10^4 - 10^7 years [Fernandes and Dietrich, 1997; Roering *et al.*, 2001], meaning that direct observation of significant hillslope evolution is rarely possible. Geomorphologists are not without recourse, however, because as Furbish [2003] and Roering *et al.* [2004] demonstrate, the use of other variable hillslope quantities (such as soil depth and the concentration of a chemical tracer) can be used to constrain the dynamics of hillslope evolution (Figure 2).

Chemical weathering is another process that denudes landscapes, but this process has been largely ignored by geomorphologists. Soil scientists, however, have long recognized that hillslope soils vary in their mineralogical and chemical properties as a

function of topography [Milne, 1935a, 1935b]. Soil toposequences [Jenny, 1941] have been descriptively associated with hillslope processes of soil erosion [e.g., Schimel *et al.*, 1985] and solute transport via subsurface water flow [Sommer and Schlichting, 1997], and soil properties have been statistically linked to topographic attributes such as slope gradient and curvature [e.g. Gessler *et al.*, 2000; Park *et al.*, 2001]. Despite the rapid progress in quantitatively characterizing the spatial variability in soil properties [McBratney *et al.*, 2003], only recently have process-based geomorphic models been applied to understand how spatial and temporal variations in soil biogeochemistry develop [Rosenbloom *et al.*, 2001; Yoo *et al.*, 2005, in press].

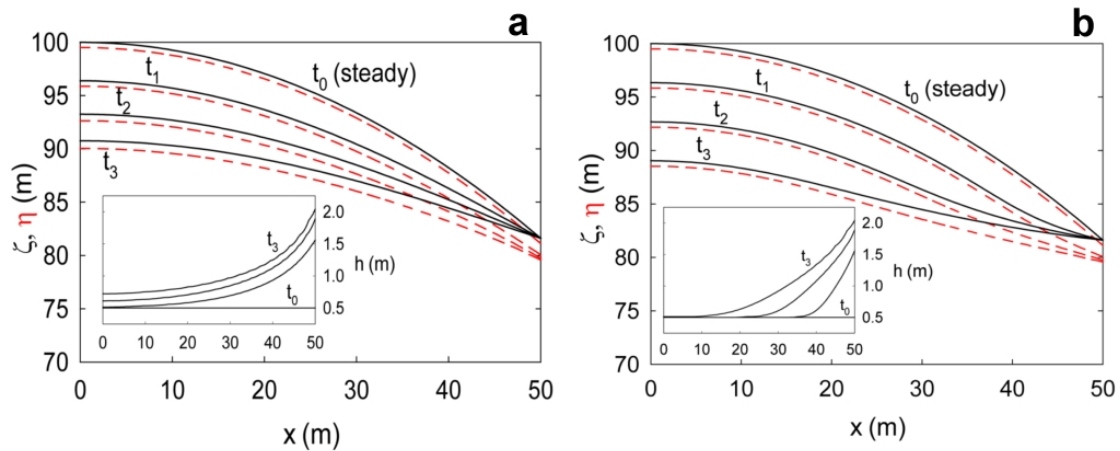


Figure 2. Two hillslopes experiencing a reduction in the downcutting rate in the channel (at $x = 50\text{m}$). In **a.**, sediment flux is linearly proportional to slope, whereas in **b.** sediment flux is proportional to the product of the soil thickness and the slope. These different flux laws lead to different soil depth profiles. [Modified from Furbish, 2003]

Whereas short term measurements of both sediment transport and mineral dissolution kinetics exist, it may not be feasible or appropriate to apply these measurements to the spatial and temporal scales intrinsic to hillslope soils. In this thesis I

approach the problem using a phenomenological rather than reductionist approach. By this I mean simply that I seek constitutive equations for mechanical and chemical processes acting on hillslopes that may be used to accurately predict the denudation rates, hillslope form, and the chemical composition of hillslope soils that function at the appropriate length and timescales (e.g., over the length of typical hillslope and on the timescale of their evolution). This approach leads to several tasks. First, the sediment transport processes that dominate in the formation of a hillslope must be identified. Constitutive laws for those processes must then either be proposed heuristically or measured directly. Third, novel techniques must be developed to make predictions of the spatial and temporal distribution of hillslope properties, such as their topography or chemistry, and then be compared with field data.

It is germane to the study of processes causing the denudation of the landscape to seek properties of hillslope soils that contain information about the spatial distribution of the rates of mechanical and chemical denudation, as well as their changes through time. The information stored on hillslopes comes in two forms, each with its own characteristic timescale. The first form of information relates to the particles that make up the soil. Particles are entrained from a soils' parent material and then transported downslope until they reach either a sediment sink (such as an abandoned terrace or inactive colluvial hollow) or a channel (which transports sediment either within water or a debris flow). Information contained within the particles is stored over their residence time on the hillslope. In the last several years, with the advent of modern analytical techniques, a number of different properties of soil particles can be quantified. These quantities include the time elapsed since the particle has been exposed to the surface (measured using

optically stimulated luminescence), the concentration of cosmogenic radionuclides contained within the particle (using atomic mass spectroscopy), the concentration of fallout radionuclides (using gamma detectors), the chemical composition of the particles (using x-ray fluorescence or inductively coupled plasma mass spectrometry), the mineralogy of the particles (using x-ray diffraction).

The second form of information stored in a hillslope soil relates to the topographic features of that soil. These topographic features include both the elevation of the soil surface and the elevation of the soil-saprolite boundary. The difference in these two elevations is the soil thickness. This topographic information adjusts to changes in the rate of mechanical and chemical denudation, and topography and soil thickness may maintain characteristic spatial patterns for periods longer than the individual soil particles reside within the soil layer.

2. Components of the Thesis

The following four chapters of the thesis are investigations focusing on developing analytical and numerical techniques to better understand how soil mantled landscapes respond to climatic and tectonic changes.

In Chapter II, entitled ‘The Influence of chemical denudation on hillslope morphology’, I explore how changes in the rates of incision of the channels bounding hillslope profiles affect topography and soil thickness. I have shown how downslope changes in soil lowering due to chemical processes will be reflected in the hillslope morphology, leading to hillslopes that have different relief, slope, and shape than

hillslopes undergoing only with mechanical sediment transport. This chapter demonstrates that hillslopes under certain conditions may have a convex-concave profile at steady state, which previously was thought to be possible only sediment transport due to overland flow or if the hillslope had sediment deposition at its base. An important

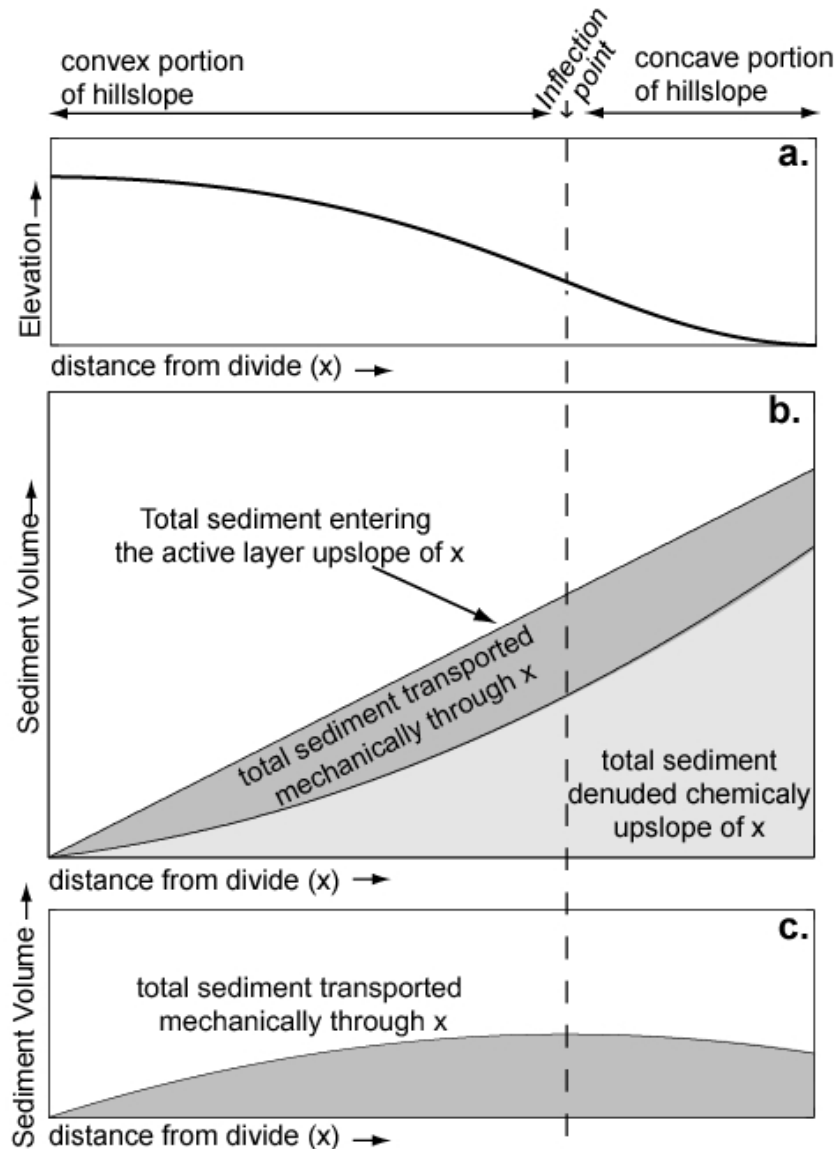


Figure 3. Conceptual diagram of the effect of chemical denudation on hillslope morphology. Sediment created through soil production must be removed from the hillslope by either mechanical or chemical denudation. If the chemical denudation rate increases downslope, this can accommodate a greater proportion of the sediment produced on the slope, leading to systematic changes in the topography of the hillslope.

condition for the existence of a hillslope with a convex-concave profile at steady state is that the chemical denudation rate must exceed the mechanical denudation rate on the hillslope (Figure 3).

In this second chapter, I define a ratio, called the denudation ratio, which is the ratio of the denudation rate due to chemical weathering to the total landscape denudation rate. Taking data from the literature, I found that in many natural basins the denudation ratio approaches the same magnitude as the mechanical denudation rate. In such basins chemical denudation will play as great a role in shaping the landscape as mechanical sediment transport processes. This work was published in 2004 in the *Journal of Geophysical Research-Earth Surface* [Mudd and Furbish, 2004].

In chapter III, entitled 'Using chemical tracers in hillslope soils to estimate the importance of chemical denudation under conditions of downslope sediment transport', I investigate the enrichment of insoluble minerals within hillslope soils due to chemical weathering of soluble minerals (Figure 4). Mass conservation equations are derived that can be used to predict concentrations of this chemically immobile phase. I have found that under simplifying assumptions that are relevant to certain field situations, the spatial distribution of the enrichment of this immobile phase can be solved analytically.

Chemical denudation rates in a hillslope soil can be measured using the concentration of immobile elements, but in turn the enrichment of these immobile elements are influenced by spatial variations in chemical denudation rates and the chemical composition of the material from which the soil is derived.

A fundamental finding of this chapter is that these considerations cloud the use of elemental depletion factors and cosmogenic nuclide-based determination of total denudation rates that have been used previously in identifying the relationship between physical erosion and chemical weathering. Although the method using elemental

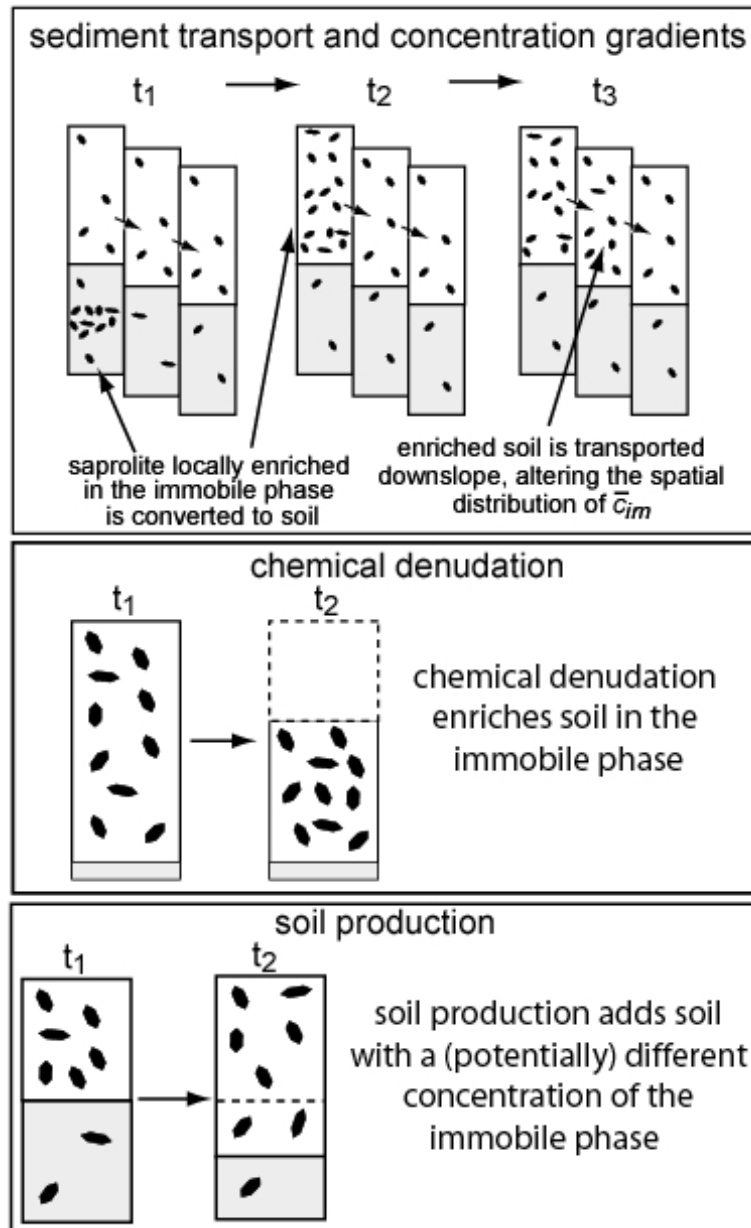


Figure 4. Schematic showing the different mechanisms by which hillslope soils may become enriched in an chemically immobile mineral (such as zircon).

depletion fractions may be inadequate in regions where the chemical denudation rate is only a small fraction of the total denudation rate, it is still useful in locations where the chemical denudation rate is a significant portion of the total denudation rate (e.g., >50%) and where sediment transport and spatial variations in chemical denudation rates only introduce small (<10%) errors in the chemical denudation rates estimated using measurements that do not take sediment transport into account. In regions where the chemical denudation rate is a significant proportion of the total denudation rate, spatially distributed measurements of the enrichment of immobile soil phases are required to accurately quantify the relationship between physical erosion and chemical weathering.

Chapter III also presents several possible responses of chemical weathering rates in the soil, such as the expected distribution of particle ages, to unsteady channel incision rates. Depositional parts of a hillslope system have locally greater particle ages, which might be expected to reduce the local rate of chemical denudation. These areas of deposition would also coincide with topographic hollows, however, where there is an increased likelihood of groundwater flow, which might be expected to increase weathering. Using immobile minerals to quantify weathering rates in such locations of transient deposition could allow researchers to assess the relative importance of hydrology and particle exposure ages on the rate of chemical weathering in hillslope soils. This work will be published in 2006, with David Furbish as coauthor, in the *Journal of Geophysical Research-Earth Surface* (at the time of this writing, the article is in press).

The fourth chapter, entitled ‘Lateral migration of hillcrests in response to channel incision in soil mantled landscapes’ explores how changing rates of channel incision

affect hillslope soil thickness and topography. Specifically, this chapter investigates the behavior of lateral hillcrest offset and migration under conditions of vertical offsets in the elevation of channels bounding a hillcrest and locally varying incision rates in the bounding channels. When the channel at the base of a hillslope experiences a change in

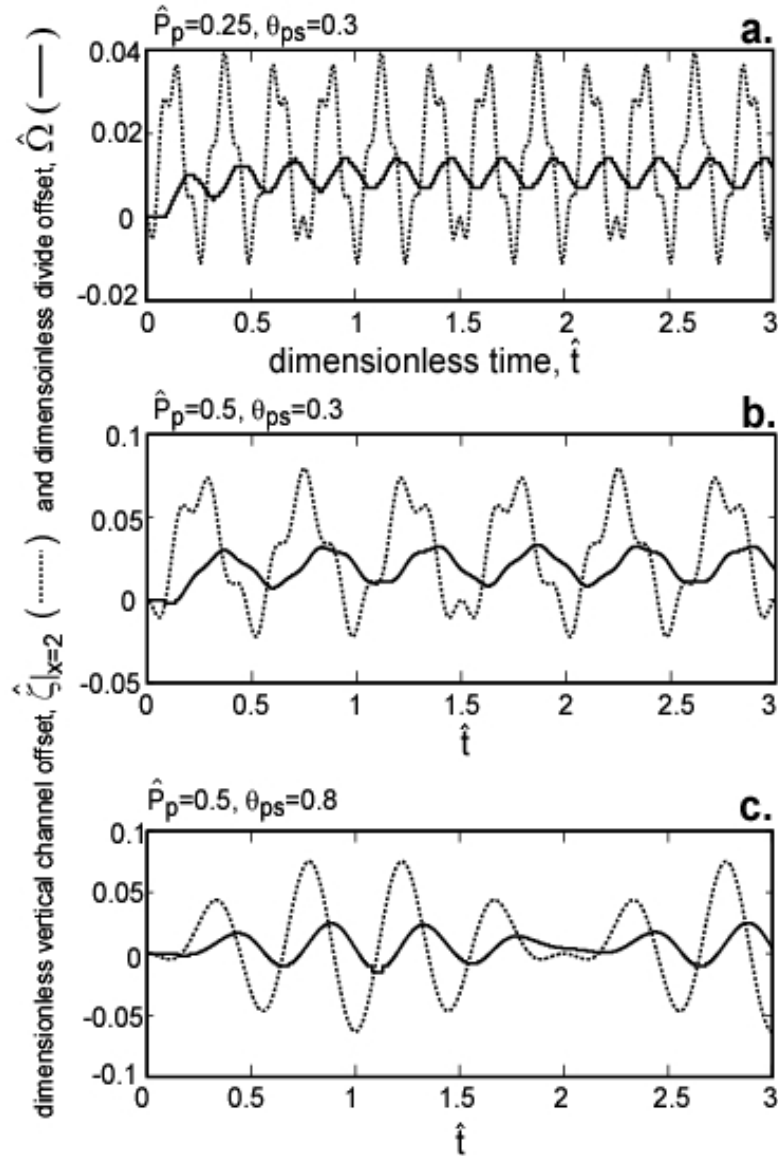


Figure 5. Plots of the difference in elevations between two channels on each side of a hillcrest (dotted lines) and the lateral motion of the hillcrest (solid line) that results from different channel incision rates. Hillcrests migrate in response to spatially varying rates of channel incision across a landscape.

incision rate, most of the divide migration takes place early after disturbance of a channel. All else being equal, shorter hillslopes, lower background incision rates, greater soil diffusivities, and greater soil production will lead to faster hillcrest migration.

Chapter IV also explores hillslopes that are bounded by channels whose incision rates vary in time. In this case the response of the hillslope topography reflects the vertical channel offset generated by the transient channel downcutting rates. Higher frequency oscillations in the channel downcutting rate are less likely to influence the position of the hillcrest than low frequency oscillations. The oscillation of the hillcrest will be out of phase with the oscillation of the vertical offset of the channels, and we have found that the hillcrest can be in an asymmetric position when there is no difference in the elevation in the channels (Figure 5). I have found that if channels bounding a hillcrest are at the same elevation, but the hillcrest is not equidistant from the two channels, this could be a indication of an imbalance in the erosion rates of the two channels bounding the hillslope. This work was published in 2005 in the *Journal of Geophysical Research-Earth Surface* [Mudd and Furbish, 2005].

Chapter V, entitled ‘Responses of soil mantled hillslopes to transient channel incision rates’ examines how hillslopes respond to changes in the rate of channel incision at their base. When channel incision rates change, signals from such changes propagate away from the channel (Figure 6). Chapter V demonstrates that these signals operate on a number of timescales, and that two of these timescales are particularly important. The first timescale determines how much time must pass after a change in the channel incision rate before the entire hillslope equilibrates to this new condition. The second timescale is the time it takes a signal caused by a change in the channel incision rate to

propagate from the channel to the divide. Chapter V shows that these timescales are proportional to the square of the length of the hillslope divided by a measure of the efficacy of sediment transport on that hillslope, the hillslope diffusivity.

Through the analysis in chapter V, it is demonstrated that the response timescale of the entire hillslope is nine times greater than the time it takes a signal of changing erosion rate to propagate from the channel to the divide for hillslopes whose soil is the same density as the underlying parent material of that soil. On hillslopes where soil is not the same density as the material from which the soil is derived, the ratio between the two densities is of first order importance in determining the hillslope response to a change in the channel incision rate. In addition, it is shown that the erosion rate, the soil production rate, and the soil thickness respond to changes in channel incision rates on different timescales. The difference in the adjustment timescales for soil thickness and soil erosion rate is sensitive to the ratio between the initial channel incision rate and the channel incision rate after it has been perturbed. This difference in timescales is greater as the difference between the initial and final channel incision rate increases for hillslopes that

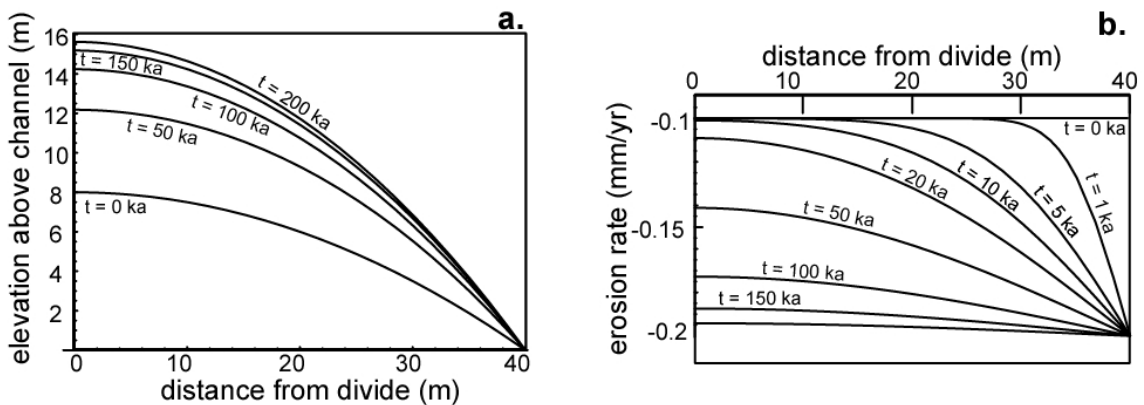


Figure 6. The surface topography (a.) and erosion rate (b.) of a hillslope that is responding to a change in the rate of incision of the channel at its base (at $x = 40\text{m}$).

experience a linear sediment flux law, whereas this relationship is reversed for hillslopes experiencing sediment flux that is proportional to the product of the soil thickness and the hillslope gradient. I will submit Chapter V to the *Journal of Geophysical Research-Earth Surface* in 2006 with coauthor David Furbish.

Finally, a summary of how these four components may be synthesized and applied in a field setting is presented in Chapter VI. This chapter also describes how I intend to apply the results of Chapters II through V in my future investigations of soil mantled hillslopes.

4. References

- Ahnert, F. (1970), Functional Relationships Between Denudation, Relief, and Uplift in Large Mid-Latitude Drainage Basins, *American Journal of Science*, 268 (3), 243-263.
- Ahnert, F. (1987), Approaches to Dynamic Equilibrium in Theoretical Simulations of Slope Development, *Earth Surface Processes and Landforms*, 12 (1), 3-15.
- Armstrong, A.C. (1976), A three-dimensional simulation of slope forms, *Z. Geomorph. Suppl. Bd.*, 25, 20-28.
- Armstrong, A.C. (1987), Slopes, Boundary-Conditions, and the Development of Convexo- Concave Forms - Some Numerical Experiments, *Earth Surface Processes and Landforms*, 12 (1), 17-30.
- Arrowsmith, J.R., D.D. Pollard, and D.D. Rhodes (1996), Hillslope Development in Areas of Active Tectonics, *Journal of Geophysical Research-Solid Earth*, 101 (B3), 6255-6275.
- Carson, M.A., and M.J. Kirkby (1972), *Hillslope Form and Process*, 475 p. pp., Cambridge University Press, Cambridge.
- Culling, W.E.H. (1960), Analytical Theory of Erosion, *Journal of Geology*, 68 (3), 336-344.
- Culling, W.E.H. (1963), Soil Creep and the Development of Hillside Slopes, *Journal of Geology*, 71 (2), 127-161.

- Dunne, T. (1991), Stochastic aspects of the relations between climate, hydrology, and landform evolution, *Transactions, Japanese Geomorphological Union*, 12 (1), 1-24.
- Fernandes, N.F., and W.E. Dietrich (1997), Hillslope evolution by diffusive processes: The timescale for equilibrium adjustments, *Water Resources Research*, 33 (6), 1307-1318.
- Furbish, D.J. (2003), Using the dynamically coupled behavior of the land-surface geometry and soil thickness in developing and testing hillslope evolution models, in *Prediction in Geomorphology*, edited by P.R. Wilcock, and R.M. Iverson, American Geophysical Union, Washington, D. C.
- Gabet, E.J., and T. Dunne (2003), A stochastic sediment delivery model for a steep Mediterranean landscape, *Water Resources Research*, 39 (9), 1237, doi:10.1029/2003WR002341.
- Gessler PE, Chadwick OA, Chamran F, Althouse L, Holmes K (2000), Modeling soil-landscape and ecosystem properties using terrain attributes. *Soil Science Society of America Journal* 64: 2046-56.
- Gilbert, G.K. (1909), The convexity of hilltops, *Journal of Geology*, 17, 344-350.
- Gossmann, H. (1976), Slope modelling with changing boundary conditions - effects of climate and lithology, *Z. Geomorph. Suppl. Bd.*, 25, 72-88.
- Green, E.G., W.E. Dietrich, and J.F. Banfield (2003), The Quantification of mass loss via geochemical weathering in hillslope processes, *Eos Trans. AGU, Fall Meet. Suppl.*, 84 (46), Abstract H51E-1128.
- Heimsath, A.M., W.E. Dietrich, K. Nishiizumi, and R.C. Finkel (1997), The Soil Production Function and Landscape Equilibrium, *Nature*, 388 (6640), 358-361.
- Hirano, M. (1975), Simulation of Developmental Process of Interfluvial Slopes With Reference to Graded Form, *Journal of Geology*, 83 (1), 113-123.
- Horton, R.E. (1945), Erosional development of streams and their drainage basins; hydrophysical approach to quantitative geomorphology, *GSA bulletin*, 56, 275-370.
- Howard, A.D. (1988), Equilibrium models in geomorphology, in *Modeling in Geomorphic Systems*, edited by M.G. Anderson, pp. 49-72, John Wiley, New York.
- Howard, A.D. (1997), Badland Morphology and Evolution: Interpretation Using a Simulation Model, *Earth Surface Processes and Landforms*, 22 (3), 211-227.
- Jenny H (1941), *The Factors of Soil Formation*. New York: McGraw-Hill, 281 pp.

- Kirkby, M.J. (1971), Hillslope process-response models based on the continuity equation, Institute of British Geographers Special Publication, 3, 15-30.
- Kirkby, M.J. (1985), A model for the evolution of regolith-mantled slopes, in *Models in Geomorphology*, edited by M.J. Woldenberg, pp. 213-237, Allen and Unwin.
- McBratney AB, Santos MLM, Minasny B (2003), On digital soil mapping. *Geoderma* 117: 3-52.
- Mudd, S.M., and D.J. Furbish (2004), The Influence of chemical denudation on hillslope morphology, *Journal of Geophysical Research*, 109 (F02001), doi:10.1029/2003JF000087.
- Mudd, S.M., and D.J. Furbish (2005), Lateral migration of hillcrests in response to channel incision in soil mantled landscapes, *Journal of Geophysical Research*, 110 (12), F04026, doi:10.1029/2005JF000313.
- Park SJ, McSweeney K, Lowery B (2001), Identification of the spatial distribution of soils using a process-based terrain characterization. *Geoderma* 103: 249-72.
- Riebe, C.S., J.W. Kirchner, and R.C. Finkel (2003), Long-term rates of chemical weathering and physical erosion from cosmogenic nuclides and geochemical mass balance, *Geochimica Et Cosmochimica Acta*, 67 (22), 4411-4427.
- Roering, J.J., P. Almond, P. Tonkin, and J.A. Mckean (2004), Constraining climatic controls on hillslope dynamics using a coupled model for the transport of soil and tracers: Application to loess-mantled hillslopes, South Island, New Zealand, *Journal of Geophysical Research*, 109 (F01010), doi:10.1029/2003JF000034.
- Roering, J.J., J.W. Kirchner, and W.E. Dietrich (1999), Evidence for Nonlinear, Diffusive Sediment Transport on Hillslopes and Implications for Landscape Morphology, *Water Resources Research*, 35 (3), 853-870.
- Roering, J.J., J.W. Kirchner, and W.E. Dietrich (2001), Hillslope Evolution by Nonlinear, Slope-Dependent Transport: Steady State Morphology and Equilibrium Adjustment Timescales, *Journal of Geophysical Research-Solid Earth*, 106 (B8), 16499-16513.
- Rosenbloom NA, Doney SC, Schimel DS (2001), Geomorphic evolution of soil texture and organic matter in eroding landscapes. *Global Biogeochemical Cycles* 15: 365-81.
- Schimel D, Stillwell MA, Woodmansee RG (1985), Biogeochemistry of C,N, and P in a soil catena of the shortgrass steppe. *Ecology* 66(1): 276-82.
- Small, E.E., R.S. Anderson, and G.S. Hancock (1999), Estimates of the Rate of Regolith Production Using Be-10 and Al-26 From an Alpine Hillslope, *Geomorphology*, 27

(1-2), 131-150.

Sommer M, Schlichting E. (1997), Archetypes of catenas in respect to matter-a concept for structuring and grouping catenas. *Geoderma* 76: 1-33.

Yoo K, Amundson R, Heimsath AM, Dietrich WE. Rates of Soil Chemical Weathering and Sediment Transport on Hillslopes: Integrating Geochemical Mass Balance with Hillslope Sediment Transport Processes, in preparation.

CHAPTER II

THE INFLUENCE OF CHEMICAL DENUDATION ON HILLSLOPE MORPHOLOGY

Abstract

Models of hillslope evolution involving diffusion-like sediment transport conventionally are presented as an equation in which the changes in land-surface elevation or soil thickness are balanced by the divergence of soil transport and either tectonic uplift or soil production, or both. These models typically do not include the loss or gain of mass in hillslope soils due to processes of chemical weathering and deposition. We formulate a more general depth-integrated equation for the conservation of soil mass on a hillslope that includes a term representing chemical deposition or denudation. This general depth-integrated equation is then simplified to determine the one-dimensional form of a steady-state hillslope which experiences both mechanical and chemical denudation. The differences in morphology between hillslopes only experiencing diffusion-like mechanical sediment transport and hillslopes experiencing both diffusion-like mechanical sediment transport and chemical denudation are explored. Under the conditions of a downslope increase in local soil lowering rate due to chemical weathering the hillslope profile will depart from the parabolic shape predicted by models that incorporate only linear diffusion-like mechanical sediment transport. In addition, hillslopes that experience both chemical and mechanical denudation may have a convex-concave profile at steady state. A necessary condition for such steady-state profiles is that the chemical denudation rate must exceed the mechanical denudation rate. We further suggest that

combinations of other physical parameter values (such as total denudation rate, average soil depth, sediment diffusivity, and the increase in soil depth away from the divide) that lead to steady-state convex-concave hillslope profiles may exist in a wide variety of natural settings.

1. Introduction

Landscapes that contain topographic relief are often mantled with soil. In a seminal paper, *G. K. Gilbert* [1909] remarked that downslope motion of sediment on a hillslope is impelled by gravity, which depends on slope for its effectiveness. Furthermore, *Gilbert* [1909] noted that in order to accommodate increasing downslope sediment flux the transport rate of sediment should increase away from the hillslope divide, and therefore the local slope should steepen away from the divide. The result of this steepening slope is the presence of a convex hillslope (Figure 1). *Culling* [1960] formalized this observation mathematically by combining a sediment flux law and a statement of mass conservation. The flux law used by *Culling* [1960], in which the sediment flux is a linear function of the surface elevation gradient, was analogous to the heat flux law introduced by *Fourier* [1822]; such gradient-driven processes are referred to as diffusive. Since the publication of *Culling's* [1960] work, other researchers have proposed non-linear flux laws [e.g., *Anderson*, 2002; *Andrews and Bucknam*, 1987; *Carson and Kirkby*, 1972; *Furbish and Fagherazzi*, 2001; *Gabet*, 2000; *Gabet*, 2003; *Gabet et al.*, 2003; *Kirkby*, 1967; *Roering et al.*, 1999]. Because the analogy to heat or chemical diffusion is not perfect, the family of flux laws describing hillslope sediment transport is now more appropriately referred to as dispersive or 'diffusion-like.'

The equations of diffusion-like hillslope sediment transport have been used to investigate the dynamics and implications of hillslope morphology and evolution. Some researchers have used these equations to explore the characteristic forms of steady-state or equilibrium hillslopes and the adjustment times from transient profiles to steady-state profiles [e.g., *Ahnert, 1976; Ahnert, 1987; Armstrong, 1976; Armstrong, 1980; Armstrong, 1987; Arrowsmith et al., 1996; Fernandes and Dietrich, 1997; Furbish and Fagherazzi, 2001; Hirano, 1976; Roering et al., 1999*]. In these studies steady state refers to a situation in which the elevation of the soil surface does not change through time. This surface elevation can be the elevation in a moving reference frame in the case of steady base-level fall or in a fixed reference frame in the case of steady uplift. Others have used a steady-state assumption to investigate the mechanics and nature of soil

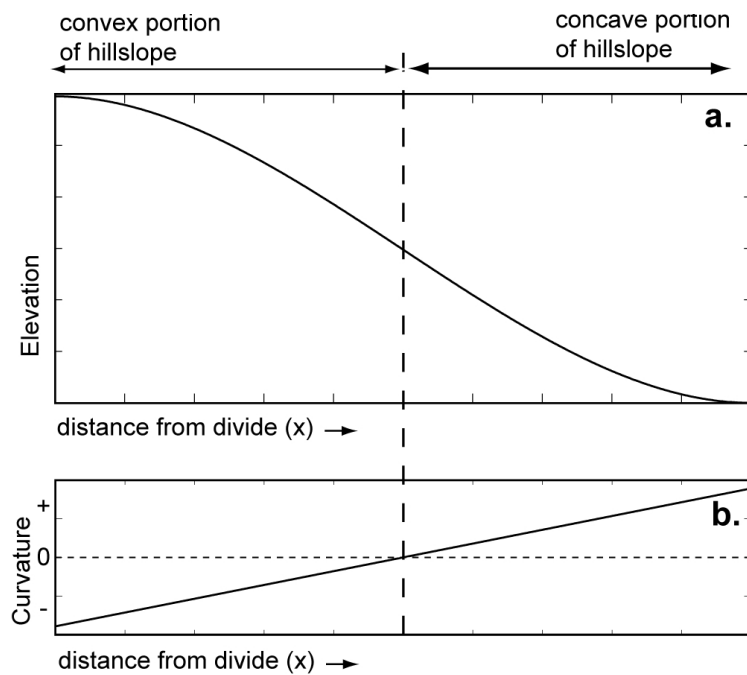


Figure 1. The convex upward portion of an idealized convex-concave hillslope (**a**) has negative curvature by convention, and the concave portion has positive curvature. Slope curvature is shown in (**b**).

production [e.g., *Heimsath et al.*, 1999]. These studies assume that soil depth does not change through time. As pointed out by *Braun et al.* [2001], this definition of steady state does not necessarily imply topographic steady state. Others [e.g., *Anderson and Dietrich*, 2001] have defined steady state as a condition in which a broad range of physical characteristics of the soil, such as soil density, soil chemistry, and soil depth, in addition to surface elevation, do not vary with time.

Another group of researchers have used the most basic forms of the equations of hillslope sediment transport (typically linear flux laws with threshold slopes) in models of landscape evolution [e.g., *Anderson*, 1994; *Braun and Sambridge*, 1997; *Howard*, 1994; *Howard*, 1997; *Kooi and Beaumont*, 1994; *Tucker and Slingerland*, 1996; *Willgoose et al.*, 1991]. *Tucker and Bras* [1998] found that a landscape's morphology is highly sensitive to the suite of mechanisms of sediment transport operating within it.

As anticipated by *Gilbert* [1909], analytic and numerical solutions of the equation of mass conservation on hillslopes with diffusion-like sediment transport have shown that, with steady base-level fall, hillslope profiles will have negative curvature (indicating a convex hillslope, see Figure 1). Predicted hillslope curvature can approach zero (a locally planar hillslope) if a non-linear diffusion-like sediment flux law is used [*Roering et al.*, 1999]. In rapidly uplifting landscapes such as the Oregon Coast Range or Central Range of Taiwan the hillslopes are commonly convex near the divide and planar downslope [*Roering et al.*, 1999]. Concavity on hillslopes with steady base-level fall may be caused by processes such as sheetwash [e.g., *Ahnert*, 1976; *Kirkby*, 1971], but in landscapes with gentler slopes or high infiltration capacities, overland flow is uncommon and not an effective process of geomorphic change.

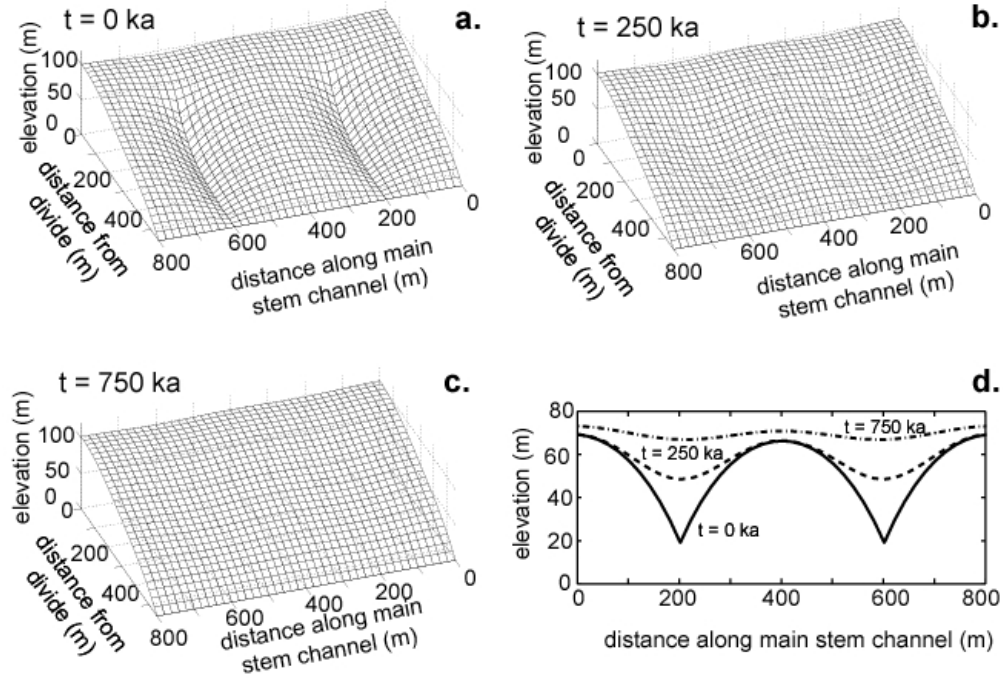


Figure 2. Idealized simulation of a soil mantled landscape using a traditional form of the sediment continuity equation, $\rho_s(\partial\zeta/\partial t) - K\nabla^2 \zeta - \rho_s U_z = 0$. Terms are defined in the text. Values for the parameters are $\rho_r = 2000 \text{ kg m}^{-3}$, $\rho_s = 1000 \text{ kg m}^{-3}$, $R_T = 1 \times 10^{-5} \text{ m yr}^{-1}$, and $K = 10 \text{ kg yr}^{-1} \text{ m}^{-2}$ ($D = 1 \times 10^{-2} \text{ m}^2 \text{ yr}^{-1}$). The domain represents a straight main stem channel that is eroding at the rate of uplift ($\partial\zeta/\partial t = 0$) and transporting all sediment delivered to it. Two additional tributary channels with exponential profiles are initially imposed on the hillslope, these channels are also eroding at the rate of uplift and transporting all sediment delivered to them. This landscape is then brought to steady state ($\partial\zeta/\partial t = 0$ everywhere), as shown in (a). The tributary channels then recede (no fluvial erosion or transport) and only the main stem channel erodes at the rate of uplift. The valleys fill significantly by 250 ka (b) and the unchanneled valleys almost completely disappear from the landscape by 750 ka after imposition of the new conditions (c). d shows profiles parallel to the main stem at a distance of 250m from the divide. At steady state, the curvature of the side slopes are negative resulting in a convex hillslope form. Only when the tributary channels are removed does there appear a concave section of the side slope, representing deposition and filling of the unchanneled valleys (d).

Hillslope concavity is often seen in landscapes where overland flow is uncommon. In such landscapes the concavity has been identified as a location of sediment deposition and storage [e.g., *Armstrong*, 1987]. The deposition of sediment reflects a transient state. In a two-dimensional numerical model, *Rinaldo et al.* [1995]

investigated unchanneled valleys, where there is landscape concavity but no fluvial channel to maintain the concavity. *Rinaldo et al.* [1995] described these unchanneled valleys as indicators of climatic or tectonic change. If the climate becomes ‘drier’ (in *Rinaldo et al.* [1995] a drier climate simply indicated that a greater drainage area was required for fluvial erosion), uplift is reduced, or the runoff threshold (the amount of rain that must fall before overland flow is generated) is increased due to changes in the biota present on the landscape, the fluvial system retreats downstream and diffusion-like hillslope processes begin depositing sediment and filling unchanneled valleys. Unless the sediment filling these valleys is evacuated by a fluvial network that has expanded due to climate change, the valleys will be smoothed from the landscape (Figure 2).

The timescale of the gradual smoothing away of landscape concavities (such as an unchanneled valley in the 2-D case, Figure 2) on hillslopes experiencing only diffusion-like sediment transport is dictated by the relaxation time of the hillslope. The relaxation time of a hillslope has been defined as the time it takes for a hillslope to approach an equilibrium state after a change in climate (represented by a change in the sediment diffusivity) or a change in base-level lowering rate [*Fernandes and Dietrich* 1997; *Roering et al.* 2001]. Relaxation times for hillslopes with typical diffusivities have been found to be on the order of 10^4 to 10^6 years [*Fernandes and Dietrich* 1997; *Roering et al.* 2001; *Anderson* 2002]. Many ancient landscapes, such as the Piedmont of the eastern United States, have widespread landscape concavities. Why have the unchanneled valleys and landscape concavities in these ancient landscapes not been filled by hillslope processes? Are landscapes containing unchanneled valleys diffusing away to a Davisian [*Davis* 1889] peneplain? Despite a drastically reduced rate of base-level fall, can

landscape concavities persist solely due to the effects of climatic fluctuations?

One explanation for the presence of long-lived landscape concavity is that it is periodically rejuvenated by episodes of wet weather or other climatic or biotic changes that cause the expansion of the channel network and erosion of sediment filled valleys [Rinaldo *et al.*, 1995]. We suggest, however, that in addition to the theory of Rinaldo *et al.* [1995], there exists another plausible explanation of concavity in landscapes older than the hillslope relaxation time. We show that the convex-concave hillslope can exist in an equilibrium state due to a process that has been largely ignored in previous hillslope evolution studies. This process is mass loss in the soil due to chemical weathering. We derive an depth-integrated equation of mass conservation in hillslope soils that includes the mass lost or gained through chemical processes. This equation is simplified to 1-D and used to investigate how chemical processes may affect the curvature, slope, and form of hillslopes. We explore the combinations of physical parameter values including total denudation rate, sediment diffusivity, the increase in soil depth away from the divide, and the ratio of the mechanical to chemical denudation rate that lead to a convex-concave profile at steady state. We further suggest that these combinations of parameters associated with a steady-state convex-concave hillslope profile may exist in a wide variety of natural settings.

2. A Depth-Integrated Equation of Hillslope Mass Conservation Incorporating Chemical Denudation and Deposition

2.1. Previous Work

Before the implications of chemical weathering on hillslope morphology can be

investigated, the equation of hillslope sediment transport incorporating this process must be derived. Few researchers have addressed the processes of chemical weathering, denudation, or deposition in their analysis. *Furbish and Fagherazzi* [2001] proposed a heuristic alteration of the soil production function as described by *Heimsath et al.* [1997] to account for weathering. *Ahnert* [1987] included dissolved load denudation derived from slopewash, but calculated this chemical denudation as a function of the overland flow, and not as weathering and transport occurring within the soil profile. *Small et al.* [1999] used a dissolution term in a steady-state form of the equation of mass conservation on a hillslope to show dissolution can affect ages determined by cosmogenic radionuclides, but did not explore the implications of denudation on hillslope morphology. Likewise *Kirkby* [1977; 1985] modeled soil chemistry evolution within a creeping soil, but only reported modeled vertical soil profiles and did not comment on the expression of these processes on the morphology of the hillslopes in question.

2.2. General Statement of Mass Conservation

Researchers typically report the hillslope diffusion-like equations as a specific case of a more general statement of local mass conservation. This specific case is generally assumed a priori. Here we derive the equation for conservation of mass on a hillslope directly from a local statement of mass conservation. We begin with the familiar continuum element with a surface A (L^2), a volume V (L^3), and a vector normal to the surface \mathbf{n} (L). A generalized form of the local conservation of mass in this element is

$$\int_V \frac{\partial}{\partial t} \rho_s \, dV + \int_A (\rho_s \mathbf{v}) \cdot \mathbf{n} \, dA - \int_V S_v \, dV = 0, \quad (1)$$

where ρ_s ($M L^{-3}$) is the dry bulk density of the soil, and \mathbf{v} ($L T^{-1}$) is the velocity vector of the material at the surface of the element. The velocity will be an ensemble average velocity of the discrete particles crossing the surface of the continuum element (Figure 3). The first term is the change in mass per unit volume per unit time of the material in the continuum element, and the second term is the flux of mass per unit volume across the surface of the element. S_v ($M L^{-3} T^{-1}$) is a mass source or sink per unit volume per time, and will be referred to as the chemical denudation and/or deposition rate. Equation (1) is used here to describe the local conservation of mass in the solid phase of a hillslope soil. The local soil mass can change due to dissolution into or precipitation from the aqueous phase, which is described by the source or sink term. This term allows the equation of soil mass conservation to be coupled to advection-dispersion-reaction (ADR) equations, which describe solute concentration for chemical species in the aqueous phase. This coupling is beyond the scope of this contribution but will be important in future research. Coupling equation (1) to the ADR equations is not necessary for significant details of hillslope form and process to be interpreted through equation (1).

The velocity vector in equation (1) can be decomposed into tectonic velocity, \mathbf{U} ($L T^{-1}$), and local soil velocity, \mathbf{v}_s ($L T^{-1}$):

$$\int_V \frac{\partial}{\partial t} \rho_s \, dV + \int_A [\rho_s (\mathbf{v}_s + \mathbf{U})] \cdot \mathbf{n} \, dA - \int_V S_v \, dV = 0. \quad (2)$$

Invoking Gauss' law, the flux term (the second term) is converted to a volume integral,

after which the resulting integral can be differentiated to:

$$\frac{\partial \rho_s}{\partial t} + \nabla \cdot (\rho_s \mathbf{v}_s) + \nabla \cdot (\rho_s \mathbf{U}) - S_v = 0. \quad (3)$$

Equation (3) may be written in component form:

$$\frac{\partial \rho_s}{\partial t} + \frac{\partial (\rho_s v_{sx})}{\partial x} + \frac{\partial (\rho_s v_{sy})}{\partial y} + \frac{\partial (\rho_s v_{sz})}{\partial z} + \frac{\partial (\rho_s U_x)}{\partial x} + \frac{\partial (\rho_s U_y)}{\partial y} + \frac{\partial (\rho_s U_z)}{\partial z} - S_v = 0, \quad (4)$$

where the subscripts x , y , and z denote the components of the sediment and tectonic velocity vectors in the x , y , and z directions, respectively (Figure 3).

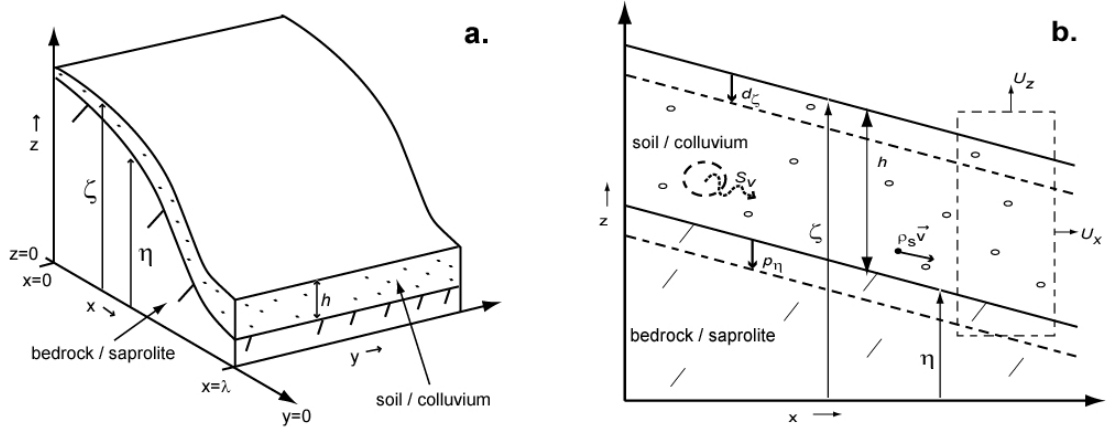


Figure 3. Diagrams of coordinate system adopted for soil-mantled hillslopes. If the surfaces $z = \eta$ and $z = \zeta$ change as shown in (b), then the production rate (p_η) is positive and that deposition rate (d_ζ) is negative.

2.3. Depth-Integration of the Statement of Mass Conservation

Coordinates for the surface of the soil ($z = \zeta$) and the base of the active soil ($z = \eta$)

are adopted (Figure 3). Soil scientists, geomorphologists, and geologists may use different definitions for the words regolith, soil, saprolite, and bedrock. The definition of soil adopted here is that part of the material at the near surface that is being actively disturbed by mechanical means — the active layer. The active layer will extend to the deepest of the rooting depth, burrowing depth, creep depth, shrink-swell depth, or frost-heave depth. This is different from the traditional definitions of soil and bedrock, but here the definitions reflect the emphasis on the physics of transport. The terms ‘mechanically active layer’ and ‘mechanically inactive layer’ may be more appropriate, but in many natural settings the soil and the saprolite (or bedrock) coincide with the active and inactive layers, respectively, so these terms are retained.

Equation (4) may then be depth-integrated between ζ and η :

$$\int_{\eta}^{\zeta} \frac{\partial \rho_s}{\partial t} dz + \int_{\eta}^{\zeta} \frac{\partial (\rho_s v_{sx})}{\partial x} dz + \int_{\eta}^{\zeta} \frac{\partial (\rho_s v_{sy})}{\partial y} dz + \int_{\eta}^{\zeta} \frac{\partial (\rho_s v_{sz})}{\partial z} dz + \int_{\eta}^{\zeta} \frac{\partial (\rho_s U_x)}{\partial x} dz + \int_{\eta}^{\zeta} \frac{\partial (\rho_s U_y)}{\partial y} dz + \int_{\eta}^{\zeta} \frac{\partial (\rho_s U_z)}{\partial z} dz - \int_{\eta}^{\zeta} S_v dz = 0. \quad (5)$$

The soil depth h , is the distance between the surface and base of the soil:

$$h = \zeta - \eta. \quad (6)$$

The integrals in equation (5) are evaluated using the mean value theorem and Leibniz’s rule (Appendix 1).

2.4. Kinematic Conditions at the Soil Surface and the Soil-Bedrock Boundary

The use of Leibniz’s rule in equation (5) results in a number of terms that are

evaluated at the coordinates $z = \zeta$ and $z = \eta$. These terms must be addressed by assigning kinematic boundary conditions. These are the conditions that describe the motion of the soil surface and the soil-bedrock boundary. The kinematic boundary condition at $z = \zeta$ is

$$\frac{\partial \zeta}{\partial t} = (v_{sz} + U_z)|_{\zeta} - (v_{sx} + U_x)|_{\zeta} \frac{\partial \zeta}{\partial x} - (v_{sy} + U_y)|_{\zeta} \frac{\partial \zeta}{\partial y} + d_{\zeta}. \quad (7)$$

The first term to the right of the equality is the vertical velocity at the soil surface. The second and third terms result from the fact that a particle must remain on the soil surface even if it has horizontal velocity. If a particle that remains on the surface moves to a location with a different surface coordinate, it must have some component of vertical velocity. The last term to the right of the equality, d_{ζ} ($L T^{-1}$), is a deposition or erosion term. This term can describe deposition from organic or aeolian sources, or erosion from overland flow. It should be noted that this term describes mass being transported in or out of the hillslope sediment system. This term allows coupling of the hillslope sediment transport equation to transport equations for overland flow. Processes in which sediment only briefly leaves the system but over the long term resides on the hillslope, such as rainsplash, should be accounted for in the flux terms in the hillslope sediment conservation equation. Additionally, in some cases the leaf layer may not be considered part of the soil profile. Organic carbon in the soil is left by the decay of roots within the soil and leaching of carbon from the leaf litter layer into the underlying soil. In these cases the mass contributed to the soil from organic carbon would be encompassed by the chemical denudation and deposition term.

The kinematic boundary condition at the soil-bedrock interface is

$$\frac{\partial \eta}{\partial t} = U_z|_{\eta} - U_x|_{\eta} \frac{\partial \eta}{\partial x} - U_y|_{\eta} \frac{\partial \eta}{\partial y} - p_{\eta}. \quad (8)$$

The sediment velocities in the x , y , and z directions at this boundary are zero, but tectonic velocities are non-zero. The term p_{η} ($L T^{-1}$) will be positive if the active layer lowers in the absence of tectonic velocities. One cause of lowering of the active layer is soil production, which is the conversion of bedrock or saprolite to soil through chemical, biological, or mechanical processes [e.g., *Heimsath 1997*].

2.5. The Depth-Integrated Equation for Mass Conservation of Soil on a Hillslope

After depth integration, the equation for mass conservation of soil on a hillslope is

$$\begin{aligned} & \frac{\partial}{\partial t} (\overline{h \rho_s}) + \frac{\partial}{\partial x} (\overline{h \rho_s v_{sx}}) + \frac{\partial}{\partial y} (\overline{h \rho_s v_{sy}}) + \\ & \frac{\partial}{\partial x} (\overline{h \rho_s U_x}) + \frac{\partial}{\partial y} (\overline{h \rho_s U_y}) - \overline{h S_v} - \rho_s|_{\eta} (p_{\eta}) - \rho_s|_{\zeta} (d_{\zeta}) = 0. \end{aligned} \quad (9)$$

The overbar denotes a depth-integrated quantity. The quantity d_{ζ} is positive for deposition and negative for erosion, and the quantity S_v is negative in the case of dissolution and positive in the case of precipitation. Figure 3 shows the coordinate system and components of equation (9). The dry bulk density at the soil-bedrock boundary, or $\rho_s|_{\eta}$, is renamed ρ_r . The dry bulk density of the soil at the surface, or $\rho_s|_{\zeta}$, is renamed ρ_{ζ} .

The second and third terms in equation (9) contain sediment flux terms

$$\overline{\rho_s v_{sx}} = q_{sx}, \quad (10a)$$

$$\overline{\rho_s v_{sy}} = q_{sy}. \quad (10b)$$

The sediment fluxes q_{sx} and q_{sy} have units ($M L^{-2} T^{-1}$). The subscripts x and y denote flux in the x - and y -directions, respectively. Substituting equations (10a) and (10b) into equation (9) yields

$$\frac{\partial}{\partial t}(h\bar{\rho}_s) + \frac{\partial}{\partial x}(hq_{sx}) + \frac{\partial}{\partial y}(hq_{sy}) + \frac{\partial}{\partial x}(h\bar{\rho}_s\overline{U_x}) + \frac{\partial}{\partial y}(h\bar{\rho}_s\overline{U_y}) - h\overline{S_v} - \rho_r p_\eta - \rho_\zeta d_\zeta = 0. \quad (11)$$

Equation (11) may be written in vector form

$$\frac{\partial}{\partial t}(h\bar{\rho}_s) + \nabla_2 \cdot (h\mathbf{q}_s) + \nabla_2 \cdot (h\bar{\rho}_s\overline{\mathbf{U}}) - h\overline{S_v} - \rho_r p_\eta - \rho_\zeta d_\zeta = 0. \quad (12)$$

In equation (12), all vectors and vector operators are in the x - and y -directions only, for example $\nabla_2 = \mathbf{i} \partial/\partial x + \mathbf{j} \partial/\partial y$, where \mathbf{i} is the unit vector in the x -direction and \mathbf{j} is the unit vector in the y -direction.

2.6. Simplifying Assumptions for Conservation of Mass Equation

Equation (12) is a general form of the equation of hillslope sediment continuity. Various forms of this equation may be derived using simplifying assumptions. An almost universal assumption in studies of hillslope geomorphology is that the local horizontal tectonic motions are zero, or $U_x = U_y = 0$. There are some examples of research at the mountain belt scale in which horizontal tectonic velocities have been incorporated into a surface processes model [e.g., *Ellis et al.*, 1999; *Willett et al.*, 2001], but to the authors' knowledge none at the hillslope scale. The assumption of zero horizontal tectonic velocities may be inappropriate in some settings, such as small folds or basins in which the folding or extension is occurring at the scale of the hillslope. A hillslope growing over a low angle blind thrust fault should have significant horizontal tectonic velocities

relative to vertical velocities [e.g., *Keller et al.*, 1998]. For many situations, however, an assumption of zero horizontal tectonic velocities, such as landscapes undergoing long wavelength flexure or isostatic rebound, will be appropriate.

It is typically assumed a priori that deposition from organic or aeolian sources is zero. Additionally, slopewash is often not considered because it is a channelizing process rather than a diffusion-like process [e.g., *Ahnert*, 1987], (although it has been shown that overland flow can lead to landscape convexity under the proper conditions [*Dunne*, 1991]). In either of the above cases the deposition term is set to zero. Setting deposition to zero and assuming no horizontal tectonic velocities leads to:

$$\frac{\partial}{\partial t}(h\bar{\rho}_s) + \nabla_2 \cdot (h\mathbf{q}_s) - h\bar{S}_v - \rho_r p_\eta = 0. \quad (13)$$

A version of equation (13) expressed in terms of the rate of change in the land surface elevation is presented in Appendix 2.

3. The Steady-State, Chemically Denuding Hillslope: 1-D Analysis

We investigate the effects of chemical processes on hillslope form by using the limited but illustrative case of the one-dimensional hillslope at steady state (to be defined below).

3.1. Derivation of Governing Equations

Equation (13) may be cast in its one dimensional form:

$$\frac{\partial}{\partial t}(h\bar{\rho}_s) + \frac{\partial}{\partial x}(hq_{sx}) - h\bar{S}_v - \rho_r p_\eta = 0. \quad (14)$$

This equation can be simplified by making steady-state assumptions. The first of these

assumptions is that the depth-integrated dry bulk density of the soil is spatially and temporally homogenous. This implies (if the density of the mineral grains that make up the soil is not changing) that the porosity of the soil remains constant in time and space. Soils may be maintained at a constant porosity because mechanical disturbances such as bioturbation will collapse excess porosity created by mass losses due to chemical weathering [Brimhall *et al.*, 1992]. The second assumption is that the soil depth does not change in time ($\partial h/\partial t$). This eliminates the first term in equation (14). The next assumption involves defining elevations relative to a local base-level:

$$\frac{\partial \eta_{bl}}{\partial t} = \frac{\partial \eta}{\partial t} - \frac{\partial \eta_\lambda}{\partial t}, \quad (15a)$$

$$\frac{\partial \zeta_{bl}}{\partial t} = \frac{\partial \zeta}{\partial t} - \frac{\partial \eta_\lambda}{\partial t}, \quad (15b)$$

where the subscript _{bl} indicates an elevation relative to base-level and η_λ is the elevation of the base level. The second assumption in our definition of steady state is that the elevations relative to base level are not changing in time, or $\partial \eta_{bl}/\partial t, \partial \zeta_{bl}/\partial t = 0$. This is the case of steady topographic form implied by *Gilbert* [1909]. The result of this assumption is that the elevation of the soil-bedrock boundary and the elevation of the soil surface anywhere on the hillslope are changing at the same rate as the elevation of local base level. It is assumed that the tectonic uplift rate is spatially homogenous at the hillslope scale. If U_z and $\partial \eta/\partial t$ are spatially homogenous, then p_η is also spatially homogenous.

To maintain the steady state defined above, all the soil entering the active layer on the hillslope must be removed by either mechanical or chemical processes. In other

words, p_η will equal the total denudation rate:

$$p_\eta = R_c + R_m = R_T, \quad (16)$$

where R_c is the chemical denudation rate ($L T^{-1}$), R_m is the mechanical denudation rate ($L T^{-1}$), and R_T is the total denudation rate ($L T^{-1}$). Incorporating the assumptions stated above, equation (14) becomes:

$$\frac{\partial}{\partial x}(h q_{sx}) = h \bar{S}_v + \rho_r R_T. \quad (17)$$

At this point a constitutive equation for sediment flux must be chosen. Two field studies have found evidence for a linear sediment transport law on gentle slopes [Mckean *et al.*, 1993; Small *et al.*, 1999]. A linear formulation also allows analytic solutions for equation (17). Although there is evidence that non-linear sediment transport laws may be operating on many natural hillslopes [Roering *et al.*, 1999], a linear sediment transport law is a reasonable approximation on gently sloping hillslopes, and is used in this study. The linear sediment transport equation is

$$h \mathbf{q}_s = -\bar{\rho}_s D \nabla_2 \zeta, \quad (18)$$

where D ($L^2 T^{-1}$) is a sediment diffusivity. (Another coefficient occasionally reported in the literature, K , is in units of $M L^{-1} T^{-1}$. This coefficient is related to D by $K = \bar{\rho}_s D$). It is assumed that D is spatially homogenous. Equation (18) is inserted into equation (17) and the resulting equation is divided by $\bar{\rho}_s$ to give

$$D \frac{\partial^2 \zeta}{\partial x^2} + \frac{h \bar{S}_v}{\bar{\rho}_s} + \frac{\rho_r}{\bar{\rho}_s} R_T = 0. \quad (19)$$

Each of the three terms in equation (19) are rates in units $L T^{-1}$. These are the local rates of change of the surface elevation due to diffusion-like sediment transport, chemical denudation or deposition, and p_η . Again, p_η is replaced by the total denudation rate because we have assumed steady topographic form. The total denudation rate represents a rate of lowering for material with density ρ_r , whereas terms in equation (19) represent soil lowering rates. This is why the total denudation rate in the third term of equation (19) is multiplied by a density ratio. The modeled hillslope has a divide at $x = 0$ and a lower boundary (the base of the hillslope) at $x = \lambda$.

3.2. Denudation Rates

Soil produced on the hillslope must be removed by some combination of mechanical and chemical denudation (equation (16)). This can be measured as denudation rates, which represent the rate of landscape lowering due to mechanical and chemical processes.

3.2.1. Mechanical Denudation Rate

The mechanical denudation rate averaged over the hillslope is the rate of lowering caused by mechanical hillslope processes and is related to the mechanical flux through the lower boundary of the hillslope by

$$R_m = -\frac{D \bar{\rho}_s}{\rho_r \lambda} \left(\frac{\partial \zeta}{\partial x} \Big|_\lambda \right), \quad (20)$$

where R_m ($L T^{-1}$) is the slope-averaged mechanical denudation rate and λ (L) is the hillslope length. The quantity in parenthesis is the slope at the hillslope base.

3.2.2. Chemical Denudation Rate

The local chemical denudation rate must be integrated over the length hillslope to find the slope-averaged rate, because precipitation from or dissolution into the aqueous phase is occurring at all points on the hillslope (Figure 4). The slope-averaged chemical denudation rate, R_c ($L T^{-1}$) is:

$$R_c = -\frac{\bar{\rho}_s}{\rho_r \lambda} \int_0^\lambda \frac{h \bar{S}_v}{\bar{\rho}_s} dx. \quad (21)$$

Carson and Kirkby [1972] argue that in humid environments soil depth (h) tends to increase away from the divide and in arid regions the soil thins away from the divide. Recent work [e.g., *Heimsath et al.*, 1997; *Small et al.*, 1999] has shown that soil production is a function of soil depth, so if soil depth varies in space so will soil production. If soil production is the dominant mechanism driving p_η , then spatially varying soil production will violate the assumption of steady topographic form, because the bedrock surface will be lowering at different rates at different points on the hillslope. *Furbish and Fagherazzi* [2001], however, proposed that the soil production function may vary as a function of distance from the divide. It is assumed here that soil production function does vary with x . This variation is assumed to lead to spatially constant p_η , despite spatial variations in soil depth. The simplest approximation of the soil depth that still can describe whether it is thinning, thickening, or remaining constant as a function of distance from the divide is:

$$h = mx + h_0, \quad (22)$$

where m (dimensionless) is the slope of the soil depth function and h_0 (L) is the soil depth

at the divide.

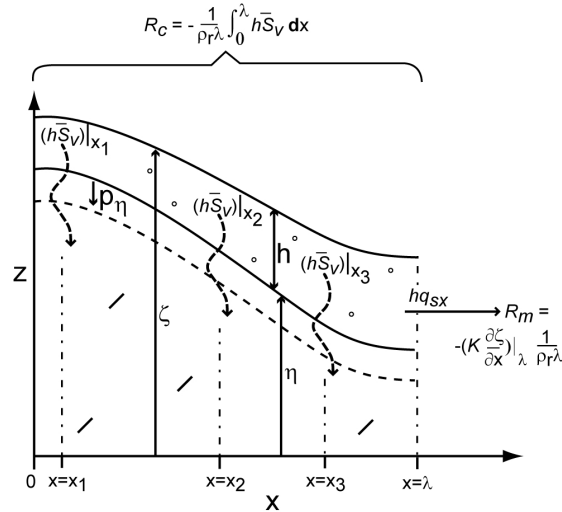


Figure 4. Diagram of denudation balance. A linear sediment transport law is shown. The quantity $h\bar{S}_v$ varies over the hillslope, so this quantity must be integrated over the hillslope to find the chemical denudation rate.

The depth-averaged mass loss rate due to chemical processes must also be described. The spatial and temporal distribution of mineral weathering, particularly in the vadose zone, is still largely unknown and is an area of active research [e.g., *Anderson et al.*, 2002; *Egli et al.*, 2001; *Millot et al.*, 2002; *Sander*, 2002; *Stonestrom et al.*, 1998; *White et al.*, 1999]. A spatially homogenous weathering rate is simply assumed from the onset of the analysis in *Small et al.* [2001]. In this contribution we also assume that the depth-averaged mass loss rate due to chemical processes is spatially uniform over the hillslope, in the interest of simplicity. A more general form of the local lowering rate due to chemical processes is described in Appendix 3.

Inserting equation (22) into equation (21) and integrating gives

$$R_c = \frac{\bar{S}_v}{2 \rho_r} (\lambda m + 2 h_0). \quad (23)$$

A ratio between the chemical denudation rate and the total denudation rate may be defined. This ratio, θ_d (dimensionless) is named the denudation ratio:

$$\theta_d = \frac{R_c}{R_c + R_m}. \quad (24)$$

Equations (16) and (24) can be inserted into equation (23) and solved for \bar{S}_v :

$$\bar{S}_v = \frac{2 R_T \theta_d \rho_r}{\lambda m + 2 h_0}. \quad (25)$$

3.3. Curvature, Slope, and Profile of the 1-D Steady-State Hillslope

When equations (22) and (25) are inserted into (19), an equation for the curvature of the hillslope as a function of distance from the divide may be found:

$$\frac{\partial^2 \zeta}{\partial x^2} = a x - b, \quad (26a)$$

where

$$a = \frac{2 R_T \theta_d \rho_r m}{D \bar{\rho}_s (\lambda m + 2 h_0)}, \quad (26b)$$

and

$$b = \frac{\rho_r R_T}{D \bar{\rho}_s} \left(1 - \frac{2 \theta_d h_0}{\lambda m + 2 h_0} \right). \quad (26c)$$

The local slope and land-surface elevation of the hillslope may be determined by applying the appropriate boundary conditions. The slope at the base may be found by combining equations (20), (23), and (24).

$$\left. \frac{\partial \zeta}{\partial x} \right|_{\lambda} = - \frac{R_T \rho_r \lambda}{D \bar{\rho}_s} (1 - \theta_d). \quad (27)$$

If the slope at the lower boundary is zero then there is no mechanical transport out of the system. Such a hillslope could be said to be ‘disconnected mechanically’ from the fluvial system and would have a denudation ratio of one. A hillslope that has as its base a fluvial terrace would be one example of this.

By integrating equation (26) and using the above boundary condition (equation (27)), the equation for the slope as a function of distance from the divide is found to be

$$\frac{\partial \zeta}{\partial x} = \frac{a x^2}{2} - b x, \quad (28)$$

where a and b were defined in equation (26b,c). The surface coordinate at the base of the hillslope is chosen to be $\zeta(\lambda) = 0$. Integrating equation (28) gives the equation for the surface of the hillslope:

$$\zeta = \frac{a(x^3 - \lambda^3)}{6} - \frac{b(x^2 - \lambda^2)}{2}. \quad (29)$$

The maximum elevation on the hillslope will be at $x = 0$.

3.3.1. Features of the 1-D Steady-State Hillslope

The curvature of the hillslope is linear with respect to distance from the divide when chemical denudation or deposition is occurring in the hillslope soil. This is a departure from the end-member case when there is no chemical denudation ($\theta_d = 0$), where the curvature is constant. There are several important features to equation (26). In the end-member case where there is no chemical denudation ($\theta_d = 0$), the curvature will be constant and the equation reduces to the familiar equation:

$$D \frac{\partial^2 \zeta}{\partial x^2} = \frac{\rho_r R_T}{\bar{\rho}_s}. \quad (30)$$

If the soil depth is not changing with distance from the divide ($m = 0$), the curvature is again constant but is less than the curvature found in the case of $\theta_d = 0$.

$$D \frac{\partial^2 \zeta}{\partial x^2} = \frac{\rho_r R_T}{\bar{\rho}_s} (1 - \theta_d). \quad (31)$$

Equation (31) has the important implication that if one measures the sediment diffusivity and estimates the soil production rate without accounting for the chemical denudation one will underestimate (or overestimate, if there is precipitation of solutes in the soil) the production rate by a factor of $(1 - \theta_d)$.

The curvature at the divide is

$$\left. \frac{\partial^2 \zeta}{\partial x^2} \right|_{x=0} = -\frac{\rho_r R_T}{D \bar{\rho}_s} \left(1 - \frac{2 \theta_d h_0}{\lambda m + 2 h_0} \right). \quad (32)$$

For the curvature to be negative, or in other words for the hillslope to be convex at the

divide, the parameters must satisfy the following condition:

$$\frac{2 h_0 \theta_d}{\lambda m + 2 h_0} < 1. \quad (33)$$

For hillslopes in which there is either net chemical deposition (θ_d is negative) or the soil thins with distance from the divide (m is negative), or both, there may be concave slopes at the divide. This would mean that the greatest slope would be at the divide. Many hillslopes, however, have soils that thicken away from the divide (m positive) and net chemical denudation (θ_d is positive), and therefore most hillslopes that are both mechanically and chemically weathering should be convex at the divide. This is the same result as in the case of the hillslope that is denuding through mechanical means only, and is the typical morphology of natural hillslopes in humid climates.

If curvature is a linear function of distance from the divide, it is possible that there will be a point some distance from the divide where curvature equals zero and the hillslope transitions from negative to positive curvature, or vice versa. This point separates the convex portion of the hillslope from the concave portion of the hillslope. Setting the curvature equal to zero in equation (26), the location of this inflection point, ξ (L), may be calculated:

$$\xi = \frac{m \lambda + 2 h_0 (1 - \theta_d)}{2 m \theta_d}, \quad (34)$$

There is no inflection point on hillslopes with $\xi > \lambda$, because the predicted location of the inflection point lies farther from the divide than the hillslope base. Such hillslopes will be only concave or convex. When $0 < \xi < \lambda$ the hillslope is convex-concave. The condition

for a convex-concave slope may be stated as:

$$\frac{m\lambda + 2h_0}{2m\lambda + 2h_0} < \theta_d. \quad (35)$$

If $2h_0 \gg m\lambda$, then θ_d will approach unity, and a convex-concave slope may only be maintained at steady state if all denudation is occurring through the mechanism of chemical weathering. If $2h_0 \ll m\lambda$, then θ_d approaches 0.5. Thus the chemical denudation rate must be at least as great as the mechanical denudation rate if a convex-concave slope is to exist at steady state.

If the hillslope has a convex-concave form, the slope with the maximum absolute value (S_{max}) will occur at the inflection point. This slope is:

$$S_{max} = \left| - \left(\frac{R_T \rho_r}{D \bar{\rho}_s} \right) \frac{(2h_0[1 - \theta_d] + m\lambda)^2}{4\theta_d m (m\lambda + 2h_0)} \right|. \quad (36)$$

3.4. Non-Dimensionalization

In the above analysis, important quantities such as the shape of the hillslope ($\zeta(x)$), the maximum slope, the inflection point, and the curvature are described in terms of several parameters. These relationships can be collapsed into relationships between a smaller number of parameters through non-dimensionalization. All terms that have dimension length may be scaled by the hillslope length, λ :

$$\zeta_* = \frac{\zeta}{\lambda}, \quad \eta_* = \frac{\eta}{\lambda},$$

$$x_* = \frac{x}{\lambda}, \quad \xi_* = \frac{\xi}{\lambda}, \quad h_* = \frac{h_0}{\lambda}, \quad (37)$$

where the star indicates a dimensionless quantity. Two timescales may also be identified. The first is the mean residence time of a particle on the hillslope (T_R (T)), which is the average depth of the soil on the hillslope ($\langle h \rangle$ (L)), divided by the total denudation rate:

$$\langle h \rangle = \frac{1}{\lambda} \int_0^\lambda (h_0 + mx) dx = h_0 + \frac{m\lambda}{2}, \quad (38)$$

$$T_R = \frac{\langle h \rangle}{R_T}. \quad (39)$$

Another timescale is the relaxation timescale. *Fernandes and Dietrich* [1997] and *Roering et al.* [2001] explored this numerically, but here we use the analytical relaxation timescale that is commonly seen in the analysis of heat and chemical diffusion, as well as in *Furbish and Fagherazzi* [2001], *Jyotsna and Haff* [1997], and *Koons* [1989]:

$$T_D = \frac{\lambda^2}{D}. \quad (40)$$

The ‘diffusive’ timescale, T_D (T), is the square of the system size (in this case the hillslope length) and the inverse of its diffusivity (which is a measure of the effectiveness of the transport process). A nondimensional ratio may be defined that is the ratio of the residence timescale to the diffusive timescale:

$$\theta_T = \frac{T_R}{T_D}. \quad (41)$$

This ratio will be called the transport ratio, as it is a proxy for the ratio of sediment entering the active layer to the sediment transported through diffusion-like mechanical processes. If no other parameters change, increasing the total denudation rate will result in a smaller value of θ_T , whereas increasing the diffusivity of the hillslope will increase θ_T .

Finally, a density ratio may be formed:

$$\tau_d = \frac{\overline{\rho_s}}{\rho_r}. \quad (42)$$

Important quantities may now be recast in nondimensional terms. The non-dimensional inflection point is:

$$\xi_* = \frac{m - 2 h_* (\theta_d - 1)}{2 m \theta_d}. \quad (43)$$

The maximum slope as a function of non-dimensional parameters is:

$$S_{\max} = \frac{(m - 2 h_* [\theta_d - 1])^2}{8 m \theta_d \theta_T \tau_d}. \quad (44)$$

The equation for the non-dimensional hillslope profile is:

$$\zeta_* = \frac{a_* (x_*^3 - 1)}{6} - \frac{b_* (x_*^2 - 1)}{2}, \quad (45a)$$

where

$$a_* = \frac{\theta_d m}{\theta_T \tau_d}, \quad (45b)$$

and

$$b_* = \frac{m + 2 h_* (1 - \theta_d)}{2 \theta_T \tau_d}. \quad (45c)$$

4. Discussion

4.1 Effect of Chemical Weathering on the Morphology of Steady-State Hillslopes

In the end-member case when both m and θ_d equal zero, the hillslope profile will be parabolic and the curvature will be uniform, as predicted qualitatively by *Gilbert* [1909]. This end-member hillslope morphology may be compared with the morphology of hillslopes that experience chemical weathering in the soil. Figure 5 shows morphologies of hillslopes with varying denudation ratios and m values. If all other parameters are constant, increasing denudation ratios lead to gentler slopes and less relief. The hillslopes that have chemical weathering diverge from the parabolic shape of the end-member case ($m = 0, \theta_d = 0$); for hillslope with spatially homogenous \bar{S}_v and finite m values the curvature increases linearly as a function from the divide. The increase is due to the linear increase in the local lowering rate due to chemical denudation as a function of distance from the divide, which is a result of the assumptions used in the development of the governing equations. Appendix 3 addresses the possibility of nonlinearities in the local soil lowering rate due to chemical processes as a function of

distance from the divide. If $m = 0$ and θ_d is nonzero, hillslope curvature will be constant and the profile will be parabolic as in the end-member case of no chemical denudation, but the presence of chemical denudation will reduce the relief and lead to gentler slopes than in the purely mechanical case.

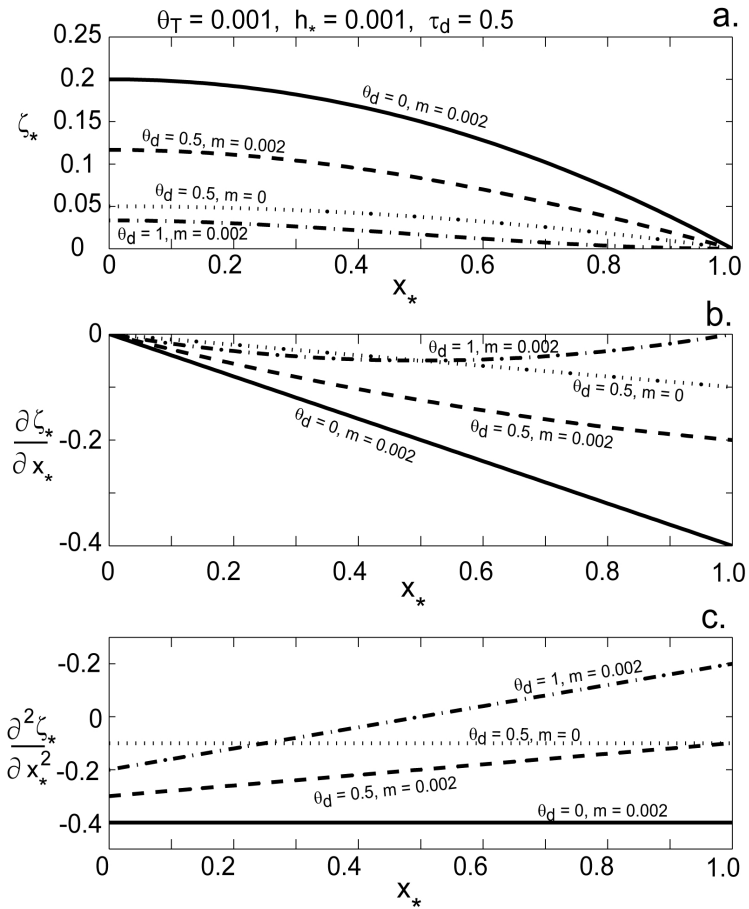


Figure 5. Non-dimensional surface elevation (a), slope (b), and curvature (c) for hillslopes with varying parameter values.

4.2. Conceptual Explanation of the Steady-State Convex-Concave Hillslope

Figure 6 shows the relationship between sediment entering the active layer and

sediment transport and removal due to the two denudation mechanisms. If the total amount of sediment dissolved chemically upslope of a point is increasing less than the total amount of sediment entering the active layer, then the amount of sediment that must be transported mechanically is increasing at that point, and therefore the hillslope will be steepening away from the divide. If, however, the denudation ratio is greater than 0.5, at some point on the slope the amount of sediment denuded chemically will be increasing faster than the amount of sediment entering the active layer from upslope. Downslope of this point, the sediment transported mechanically must decrease in the downslope direction, and the slope will become gentler, giving concave topography.

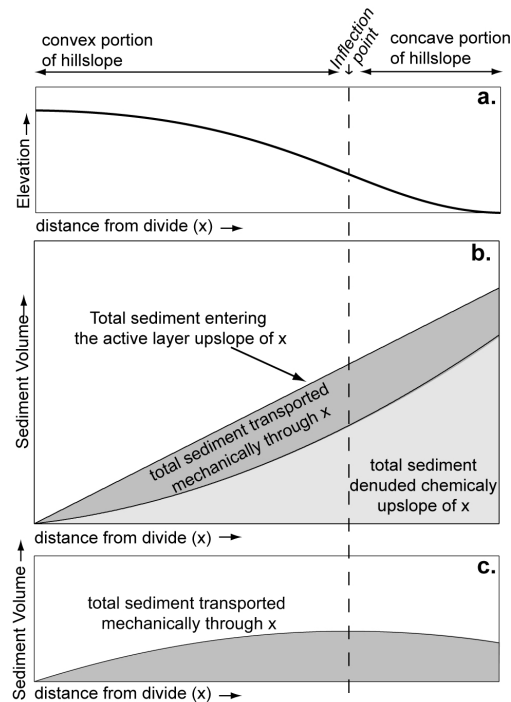


Figure 6. Diagram of a convex-concave slope (a) and the denudation balance as a function of distance from the divide. The total sediment denuded chemically is a non-linear function of the distance from the divide (b). Below the inflection point, the total amount of sediment denuded chemically above x begins to increase more quickly than the corresponding increase in total sediment entering the active layer upslope, and the sediment that must pass through x mechanically decreases with increasing distance from the divide (c).

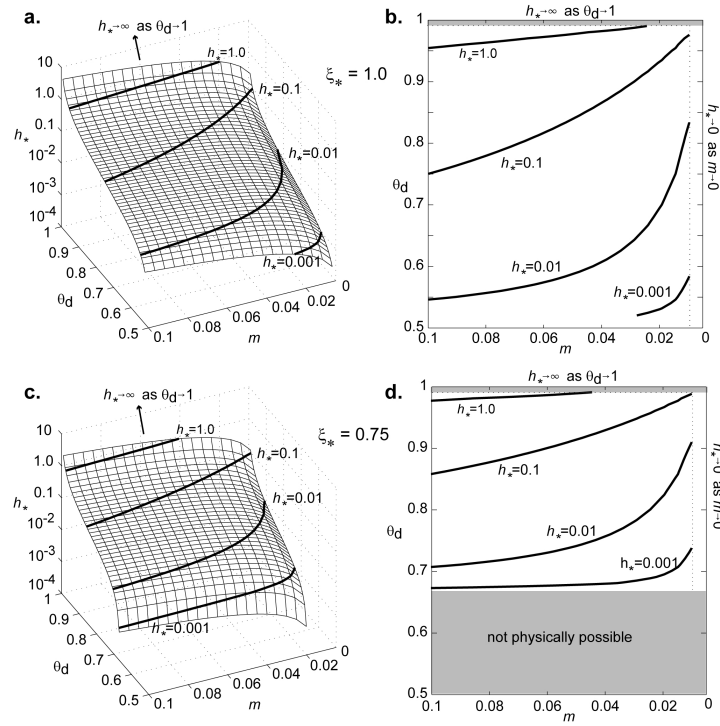


Figure 7. Dimensionless depth of soil at the divide (h_*) for hillslopes with an inflection point at the hillslope outlet ($x = \lambda$) (a,b) and hillslopes with an inflection point three quarters of the length of the hillslope from the divide (c,d). Surfaces (a, c) and contour plots (b,d) are shown. Any hillslope with a combination of h_* , denudation ratio (θ_d), and rate of the increase of soil depth away from the divide (m) that plots below the surface in a has a convex-concave slope.

4.3. Conditions for Steady-State Hillslopes With Convex-Concave Profiles

Equation (43) may be used to predict the combinations of dimensionless soil depth at the divide (h_*), the rate of increase in soil depth away from the divide (m), and the denudation ratio (θ_d) that occur on steady-state hillslopes with convex-concave profiles. The parameter values of a hillslope with an inflection point at the base of the hillslope can be represented as a surface. Two such surfaces are shown in Figure 7.

The surface in Figure 7a represents the parameter values at which the inflection point is at the base of the hillslope. Parameter values plotting below this surface have

convex-concave profiles at steady state. Hillslopes that have higher denudation ratios and for which soil depth increases faster away from the divide are favored to have convex-concave slope profiles. Smaller values of the dimensionless soil depth at the divide, h_* , also favor convex-concave slope profile. Thus, hillslopes with shallower soils at the divide and longer slope lengths are more likely to have convex-concave profiles at steady state. As noted by inspection of equation (35), the value of the denudation ratio must be greater than 0.5 for a convex-concave slope to exist. A hillslope with $\theta_d = 1$, or in other words a hillslope in which all the denudation is occurring through chemical means, always has a convex-concave profile and the inflection points of these hillslopes are located halfway between the divide and the outlet ($\lambda / 2$). Mechanical sediment transport still functions on these hillslopes, and particles entrained from the bedrock at and away from the divide still move downslope, but the slope at the hillslope outlet is zero, so the horizontal mechanical sediment transport there must be zero, and all mass converted to soil from the underlying bedrock is removed through chemical means as it moves towards the base of the hillslope.

4.4. Transport Ratios for Steady-State Hillslopes With Convex-Concave Profiles

We may assume that in many landscapes climate and tectonics combine to form an initial drainage network. If these conditions then change, causing the drainage network to retreat (that is to decrease the drainage density or reduce the total length of the channels in the fluvial system), the now unchanneled valleys will begin to fill with sediment. At some time after the retreat of the drainage network, the unchanneled valleys may relax to a steady-state convex-concave shape. In this situation the antecedent

drainage network has set the length of the hillslopes. The climatic and tectonic regime that lead to the steady-state unchanneled valleys are also external influences that help to set the shape of the hillslope. These external influences are contained within the transport ratio, θ_T , along with the depth of the soil at the divide and the soil depth increase away from the divide (m), which are set by hillslope processes. For a range of maximum slopes (S_{max} , or the slope at the inflection point) and m values, the transport ratio can vary over several orders of magnitude. The predicted transport ratios (see Figure 8) may be compared to physically realistic θ_T values.

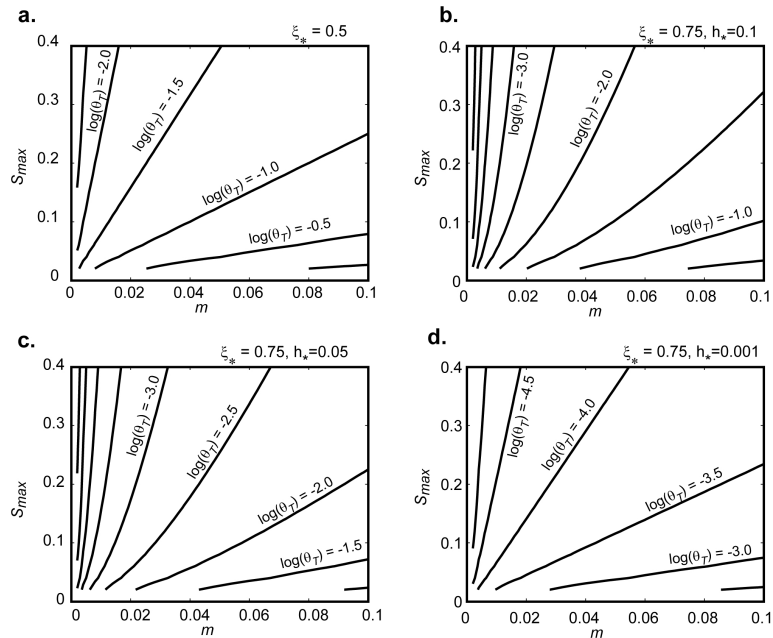


Figure 8. Contour plot of the transport ratio (θ_T) for an inflection point of $\xi_* = 0.5$ (a), and $\xi_* = 0.75$ (b, c, d) and dimensionless soil depth $h_* = 0.1$ (b), $h_* = 0.05$ (c), and (d). $h_* = 0.01$ The density ratio (τ_d) for these plots is 0.5.

4.5. Comparison of Theoretical Transport Ratios with Transport Ratios Calculated From Field Data

Physically realistic ranges of the transport ratio may be obtained from measured

values for diffusivities, total denudation rates, hillslope length scales, and reasonable soil parameters (Figure 8). The relatively small number of field studies of hillslope diffusivities have reported values of D ranging from order 10^{-4} to order 10^{-1} $\text{m}^2 \text{yr}^{-1}$ (see Table 1 in *Fernandes and Dietrich [1997]*). More humid regions will typically have higher values of D , although D also depends on the biota, temperature, and the nature of sediment in a given landscape [*Anderson, 2002*].

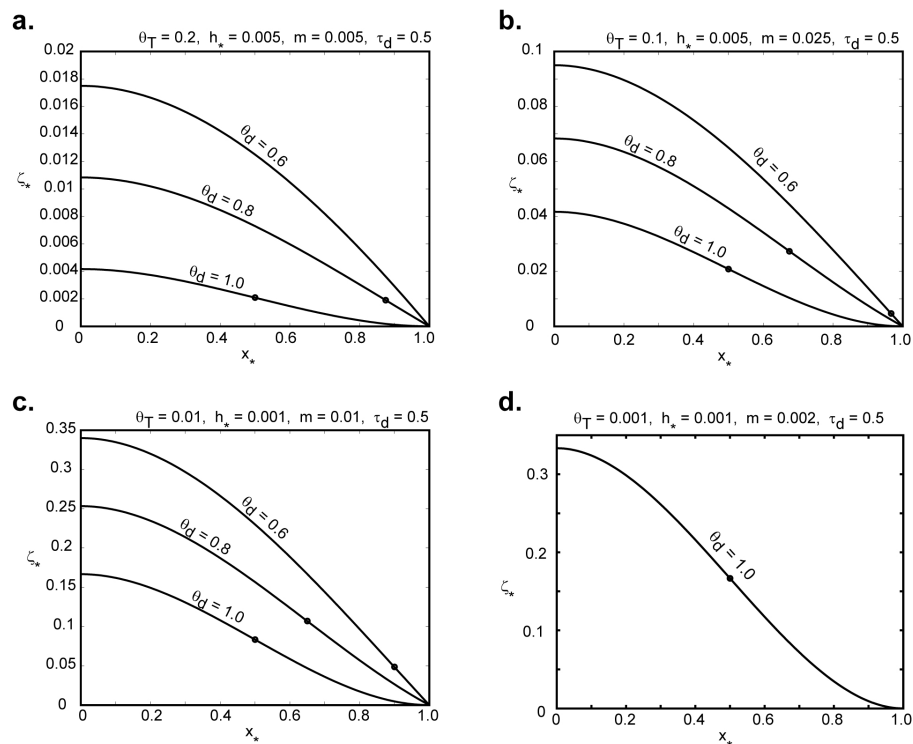


Figure 9. Hillslope profiles for various values of the transport ratio (θ_T), dimensionless soil depth at the divide (h_*), rate of increase in soil depth away from the divide (m), and denudation ratio (θ_d). The value of the density ratio (τ_d) is 0.5 for all plots. Note the change in vertical scale. Black dots indicate the inflection point (transition from negative to positive curvature). The curve in **a.** without a black dot has a predicted inflection point at $x_* > 1$.

The upper range on exhumation rate is 1.0×10^{-2} m yr^{-1} [*Burbank, 2002*], but the

most rapid documented chemical denudation rate is $5.8 \times 10^{-5} \text{ m yr}^{-1}$ [White *et al.*, 1998]. Exhumation must balance denudation at steady state. Because the mechanical denudation rate must be less than the chemical denudation rate in order for a convex-concave slope to be in steady state, the upper limit on total denudation rate that allows this hillslope form is $\sim 10^{-4} \text{ m yr}^{-1}$. Such a denudation rate, although several orders of magnitude lower than the fastest known denudation rates, is nevertheless a rate of denudation that is representative of areas of active tectonics. The Oregon Coast Range near the experimental site of Anderson *et al.* [2002] has been estimated to have a long term uplift rate (which should be similar to the total denudation rate at steady state) of $10^{-4} \text{ m yr}^{-1}$. The lowest denudation rate is (trivially) zero, but as a point of reference, the time-averaged uplift due to tectonic flexure on the Atlantic margin of the U.S. is estimated to be $2 \times 10^{-6} - 1 \times 10^{-5} \text{ m yr}^{-1}$ [Pazzaglia and Gardner, 1994].

Table 1. Values of the transport ratio (θ_T) for naturally occurring rates of total denudation (R_T), average soil depth ($\langle h \rangle$), hillslope length (l), and sediment diffusivity (D). Note that these values are slightly different than the end-member values and have been chosen because they are presumably representative of a larger number of natural hillslopes.

θ_T	R_T (m yr ⁻¹)	$\langle h \rangle$ (m)	l (m)	D (m ² yr ⁻¹)	Convex-concave profile possible?
6.25×10^2	2×10^{-6}	5	20	10^{-1}	no
10^{-2}	5×10^{-6}	5	500	10^{-3}	yes
10^{-4}	10^{-4}	1	100	10^{-3}	yes

Hillslopes are typically tens to hundreds of meters long. Soil depth can be zero, but the upper limit of soil depth is harder to quantify. As researchers in the Amazon basin

have found rooting depths of 8 meters [Nepstad *et al.*, 1994], and root growth causes mechanical disturbance of the soil [e.g., Gabet *et al.*, 2003], it is presumed that the upper limit on soil depths is on the order of 10 meters.

With this information, physically meaningful values may be established for T_R , T_D , and θ_T . For a very deep soil and a total denudation rate similar to the estimated uplift rate of the Atlantic margin of the United States, T_R will be on the order of 10^8 years. Low hillslope lengths and high diffusivities give a T_D of order 10^3 years, and a θ_T of order 10^5 . This value is several orders of magnitude larger than the highest values calculated for θ_T in Figure 8. Therefore the end-member combination of the residence and relaxation time will not have convex-concave slopes at steady state. In landscapes with low total denudation and thick soils, hillslopes must either be longer or have lower diffusivities than the end-member hillslopes in order to have steady-state convex-concave slopes. With a hillslope length of order 10^3 m and a diffusivity of 10^{-2} m² yr⁻¹ the T_D value will be of order 10^8 years, and θ_T will be of order unity. This is in the range of θ_T values predicted in Figure 8 for slopes of low relief. Lowlands are, by definition, low-relief landscapes. Steady-state convex-concave hillslopes of higher relief will have thinner soils, lower diffusivities, shorter slopes, and faster total denudation rates. For example, a hillslope with a total denudation rate of order 10^{-4} m yr⁻¹, a diffusivity of order 10^{-3} m² yr⁻¹, an average soil depth of order 1m, and a length of order 100m will have a θ_T value of 10^{-3} . Table 1 shows the values of θ_T for selected combinations of naturally occurring soil depths, uplift rates, diffusivities, and hillslope lengths.

Some representative hillslope profiles are plotted in Figure 9. These hillslopes range from high relief (**a**), to moderate relief (**b**, **c**), to low relief (**d**). As shown in Figure

9, hillslopes with a wide range of parameter values may have convex-concave profiles at steady state.

4.6. The Occurrence of Hillslopes with Denudation Ratios Greater Than 0.5

It is required that $\theta_d > 0.5$ for the existence of steady-state hillslopes with convex-concave profiles. Is this condition physically realistic? In studies of river basin denudation rates, *Summerfeld and Hulton* [1994] and *Gaillardet et al.* [1997] found denudation ratios of 0.5 or greater (see Table 2). As stated earlier, the highest measured chemical denudation rate is on the order of 10^{-4} m yr⁻¹. As local erosion rates can be

Table 2. Denudation ratios (θ_d) from selected river basins. Superscripts indicate source: ¹*Summerfeld and Hulton* [1994]; ²*Gaillardet et al.* [1997].

θ_d	River Basin	Location
0.857	Dnepr ¹	Ukraine, Belarus, Russia
0.759	Lena ¹	Russia
0.647	Ob ¹	Russia
0.944	St. Lawrence ¹	Canada
0.783	Yenisei ¹	Russia
0.5	Urucara (Amazon sub-basin) ²	Brasil
0.5	Tapajos (Amazon sub-basin) ²	Brasil

several orders of magnitude greater than the fastest measured chemical denudation rate, if a basin includes one or more sub-basins that are undergoing rapid physical erosion this will skew the basin-averaged denudation ratio in favor of mechanical erosion. We also

note that chemical denudation rates calculated by solute fluxes incorporate dissolution that occurs in both bedrock and the soil mantle. Nonetheless, *Anderson et al.* [2002], found that chemical weathering is much more vigorous in soil than in bedrock, due to the fact that more water may flush the soil due to its higher porosity, and because minerals in the soil have larger available surface area for reactions to occur.

5. Conclusions

Chemical denudation can affect the curvature, slope, and profile of hillslopes. Downslope changes in soil lowering due to chemical processes will be reflected in the hillslope morphology, leading to hillslopes that have different relief, slope, and shape (e.g., non-parabolic) than hillslopes undergoing only diffusion-like sediment transport. We have shown that hillslopes under certain conditions may have a convex-concave profile at steady state. This is in contrast to slopes only experiencing diffusion-like mechanical sediment transport wherein only slopes that are transient and are storing sediment at their base may have a convex-concave profile. Hillslopes with a variety of lengths, soil depths, variations in soil depth as a function of distance from the divide, total denudation rates, sediment diffusivities, and density changes as soil is converted to bedrock, may have a convex-concave profile. An important condition for the existence of a hillslope with a convex-concave profile at steady state is that the chemical denudation rate must exceed the mechanical denudation rate on the hillslope. Although there is evidence that chemical denudation is greater than physical denudation in some large river basins, further work is required to quantify both mechanical and chemical denudation rates at the hillslope scale. It will be important at this scale to measure the

chemical denudation that occurs in the soil, as dissolution in the bedrock does not directly affect the hillslope topography. Chemical weathering in soils is an area of active research, but the spatial variation in the local rate of soil lowering due to chemical processes at the hillslope is not well understood. Further research in this area is needed in order to better understand the impact of chemical weathering on hillslope morphology.

Appendix 1.

The mean value theorem may be stated as, for example:

$$\bar{f} = \frac{1}{\zeta - \eta} \int_{\eta}^{\zeta} f(x, y, z, t) dz = \frac{1}{h} \int_{\eta}^{\zeta} f(x, y, z, t) dz, \quad (\text{A1.1})$$

where the overbar denotes a depth-averaged quantity, and f is some function of position (x , y , and z) and time (t). Leibniz's rule may be stated as

$$\int_{\eta(x, y, t)}^{\zeta(x, y, t)} \frac{\partial}{\partial x} f(x, y, z, t) dz = \frac{\partial}{\partial x} \int_{\eta(x, y, t)}^{\zeta(x, y, t)} f(x, y, z, t) dz - f(\zeta(x, y, t), x, y, t) \frac{\partial \zeta}{\partial x} + f(\eta(x, y, t), x, y, t) \frac{\partial \eta}{\partial x}. \quad (\text{A1.2})$$

Appendix 2.

Equation (13) allows one to track changes in the soil depth, h . In some cases it may be more desirable to track the change in surface elevation, ζ . One method yielding a relatively simple equation is carried out by multiplying equation (8) by the depth-averaged dry bulk soil density (and with the assumption of no horizontal tectonic

velocities):

$$\bar{\rho}_s \frac{\partial \eta}{\partial t} - \bar{\rho}_s U_z |_{\eta} + \bar{\rho}_s p_{\eta} = 0. \quad (\text{A2.1})$$

Because the terms to the left of the equality in equation (A2.1) equal zero, these terms may be added to equation (13). Equation (6) is also inserted into the unsteady term in equation (13) such that the soil depth h in this term is cast in terms of ζ and η . The chain rule is then used to arrive at:

$$\bar{\rho}_s \frac{\partial \zeta}{\partial t} + h \frac{\partial \bar{\rho}_s}{\partial t} + \nabla_2 \cdot (h \mathbf{q}_s) - h \bar{S}_v - (\rho_r - \bar{\rho}_s) p_{\eta} - \bar{\rho}_s U_z = 0, \quad (\text{A2.2})$$

or in component form

$$\bar{\rho}_s \frac{\partial \zeta}{\partial t} + h \frac{\partial \bar{\rho}_s}{\partial t} + \frac{\partial}{\partial x} (h q_{sx}) + \frac{\partial}{\partial y} (h q_{sy}) = h \bar{S}_v + (\rho_r - \bar{\rho}_s) p_{\eta} + \bar{\rho}_s U_z. \quad (\text{A2.3})$$

Appendix 3.

Equation (24) contains three terms which are local rates of soil surface lowering due to mechanical sediment transport, chemical denudation, and total denudation (which has replaced soil production due to the steady-state assumptions). By assuming spatial homogeneity of S_v and a linear increase in soil depth away from the divide the local rate of soil lowering due to chemical weathering, r_c (L T^{-1}), was cast as a linear function of distance from the divide:

$$r_c = \frac{h \bar{S}_v}{\bar{\rho}_s} = \frac{(m x + h_0) \bar{S}_v}{\bar{\rho}_s}. \quad (\text{A3.1})$$

A more general formulation could simply treat the local rate of soil lowering due to chemical weathering as a power law function of x :

$$r_c = \alpha x^\beta + r_0, \quad (\text{A3.2})$$

where α and β are empirical coefficients and r_0 is the local rate of soil lowering due to chemical weathering at the divide. If $\beta = 1$, then equation (A3.2) reduces to equation (A3.1) where

$$r_0 = \frac{h_0 \bar{S}_v}{\bar{\rho}_s}, \quad (\text{A3.3a})$$

$$\alpha = \frac{m \bar{S}_v}{\bar{\rho}_s}. \quad (\text{A3.3b})$$

The chemical denudation rate may be calculated by integrating the local chemical denudation rate as done in equation (26). This gives

$$R_c = -\frac{\bar{\rho}_s}{\rho_r} \left(\frac{\alpha x^\beta}{1 + \beta} + r_0 \right). \quad (\text{A3.4})$$

Equation (29) may be inserted into equation (A3.4), which may then be solved for r_0 :

$$r_0 = -\frac{\bar{\rho}_s}{\rho_r} R_T \theta_d - \frac{\alpha \lambda^\beta}{1 + \beta}. \quad (\text{A3.5})$$

Inserting equations (A3.5) and (A3.2) into equation (24) gives the hillslope curvature:

$$\frac{\partial^2 \zeta}{\partial x^2} = \frac{\alpha}{D} x^\beta + \frac{1}{D} \left(\frac{\rho_r}{\bar{\rho}_s} R_T (1 - \theta_D) - \frac{\alpha \lambda^\beta}{1 + \beta} \right). \quad (\text{A3.6})$$

If the increase or decrease in r_0 as a function of distance from the divide is non-linear, so too will be the curvature. The empirical coefficients α and β may depend on many factors, including but not limited to climate, hydrology, and the kinetics of chemical reactions within the soil, and are a significant control on hillslope morphology. Recent studies have begun to explore spatial variations in chemical weathering at the hillslope scale [e.g, *Green et al.*, 2003], such studies may be used in the future to better parameterize equation (A3.2).

6. List of Symbols

α	empirical coefficient for power law description of soil surface lowering due to chemical weathering as a function of x .
β	empirical exponent for power law description of soil surface lowering due to chemical weathering as a function of x .
D	sediment diffusivity ($L^2 T^{-1}$)
d_ζ	deposition or erosion at surface of soil ($L T^{-1}$)
η	coordinate of the bedrock-soil interface (L)
η_*	dimensionless bedrock-soil interface coordinate
η_{bl}	elevation of soil-bedrock boundary with respect to base level (L)
η_λ	base-level elevation (L)
h	soil depth (L)
$\langle h \rangle$	average depth of soil over a hillslope (L)
h_0	depth of soil at hillslope divide (L)
K	sediment diffusion coefficient ($M L^{-1} T^{-1}$)

λ	hillslope length (L)
m	slope of soil depth as a function of distance from divide (dimensionless)
p_η	Rate of change of the elevation of the soil-bedrock boundary under conditions of no tectonic velocities (L T ⁻¹)
\bar{q}_s	sediment flux vector (M L ⁻² T ⁻¹)
q_{sx}, q_{sy}	components of sediment flux vector in the x- and y- directions, respectively (M L ⁻² T ⁻¹)
ρ_s	dry bulk density of soil (M L ⁻³)
$\bar{\rho}_s$	depth averaged dry bulk density of soil (M L ⁻³)
ρ_r	dry bulk density of the material at the soil-bedrock boundary (M L ⁻³)
r_c	local rate of soil surface lowering due to chemical weathering (L T ⁻¹)
r_0	value of r_c at the divide (L T ⁻¹)
R_m	mechanical denudation rate (L T ⁻¹)
R_s	chemical denudation rate (L T ⁻¹)
R_T	total denudation rate (L T ⁻¹)
S_{max}	absolute value of maximum slope (dimensionless)
S_v	chemical denudation and deposition (M L ⁻³ T ⁻¹)
\bar{S}_v	depth averaged chemical denudation and deposition (M L ⁻³ T ⁻¹)
T_R	relaxation timescale (T)
T_D	diffusive timescale (T)

θ_d	denudation ratio (dimensionless)
θ_T	transport ratio (dimensionless)
τ_d	density ratio (dimensionless)
\vec{U}	tectonic velocity vector (L T ⁻¹)
U_x, U_y, U_z	components of the tectonic velocity vector in the x,y, and z directions (L T ⁻¹)
\vec{v}_s	sediment velocity vector (L T ⁻¹)
v_{sx}, v_{sy}, v_{sz}	components of sediment velocity vector in x,y, and z directions (L T ⁻¹)
$\overline{v_{sx}}, \overline{v_{sy}}, \overline{v_{sz}}$	depth averaged components of the sediment velocity vector in the x-, y- and z- directions, respectively (L T ⁻¹)
ζ	coordinate of the soil surface (L)
ζ_{bl}	coordinate of the soil surface relative to base level (L)
ζ_*	dimensionless soil surface coordinate
ξ	location of hillslope inflection point (point of zero curvature) (L)
ξ_*	dimensionless location of inflection point

7. References

- Ahnert, F., Brief description of a comprehensive three-dimensional process-response model of landform development, *Z. Geomorph. Suppl. Bd.*, 25, 29-49, 1976.
- Ahnert, F., Approaches to Dynamic Equilibrium in Theoretical Simulations of Slope Development, *Earth Surface Processes and Landforms*, 12 (1), 3-15, 1987.
- Anderson, R.S., Evolution of the Santa-Cruz Mountains, California, Through Tectonic Growth and Geomorphic Decay, *Journal of Geophysical Research-Solid Earth*, 99 (B10), 20161-20179, 1994.

- Anderson, R.S., Modeling the tor-dotted crests, bedrock edges, and parabolic profiles of high alpine surfaces of the Wind River Range, Wyoming, *Geomorphology*, 46 (1-2), 35-58, 2002.
- Anderson, S.P., and W.E. Dietrich, Chemical Weathering and Runoff Chemistry in a Steep Headwater Catchment, *Hydrological Processes*, 15 (10), 1791-1815, 2001.
- Anderson, S.P., W.E. Dietrich, and G.H. Brimhall, Weathering Profiles, Mass-Balance Analysis, and Rates of Solute Loss: Linkages Between Weathering and Erosion in a Small, Steep Catchment, *Geological Society of America Bulletin*, 114 (9), 1143-1158, 2002.
- Andrews, D.J., and R.C. Bucknam, Fitting Degradation of Shoreline Scarps by a Nonlinear Diffusion-Model, *Journal of Geophysical Research-Solid Earth and Planets*, 92 (B12), 12857-12867, 1987.
- Armstrong, A.C., A three-dimensional simulation of slope forms, *Z. Geomorph. Suppl. Bd.*, 25, 20-28, 1976.
- Armstrong, A.C., Simulated Slope Development Sequences in a 3-Dimensional Context, *Earth Surface Processes and Landforms*, 5 (3), 265-270, 1980.
- Armstrong, A.C., Slopes, Boundary-Conditions, and the Development of Convexo-Concave Forms - Some Numerical Experiments, *Earth Surface Processes and Landforms*, 12 (1), 17-30, 1987.
- Arrowsmith, J.R., D.D. Pollard, and D.D. Rhodes, Hillslope Development in Areas of Active Tectonics, *Journal of Geophysical Research-Solid Earth*, 101 (B3), 6255-6275, 1996.
- Braun, J., A.M. Heimsath, and J. Chappell, Sediment Transport Mechanisms on Soil-Mantled Hillslopes, *Geology*, 29 (8), 683-686, 2001.
- Braun, J., and M. Sambridge, Modelling Landscape Evolution on Geological Time Scales: a New Method Based on Irregular Spatial Discretization, *Basin Research*, 9 (1), 27-52, 1997.
- Brimhall, G.H., O.A. Chadwick, C.J. Lewis, W. Compston, I.S. Williams, K.J. Danti, W.E. Dietrich, M.E. Power, D. Hendricks, and J. Bratt, Deformational Mass-Transport and Invasive Processes in Soil Evolution, *Science*, 255 (5045), 695-702, 1992.
- Burbank, D.W., Rates of erosion and their implications for exhumation, *Mineralogical Magazine*, 66 (1), 25-52, 2002.
- Carson, M.A., and M.J. Kirkby, *Hillslope Form and Process*, 475 p. pp., Cambridge

- University Press, Cambridge, 1972.
- Culling, W.E.H., Analytical Theory of Erosion, *Journal of Geology*, 68 (3), 336-344, 1960.
- Davis, W.M., The Rivers and Valleys of Pennsylvania, *Natl. Geog. Mag.*, 1, 183-253, 1889.
- Dunne, T., Stochastic aspects of the relations between climate, hydrology, and landform evolution, *Transactions, Japanese Geomorphological Union*, 12 (1), 1-24, 1991.
- Egli, M., P. Fitze, and A. Mirabella, Weathering and Evolution of Soils Formed on Granitic, Glacial Deposits: Results From Chronosequences of Swiss Alpine Environments, *Catena*, 45 (1), 19-47, 2001.
- Ellis, M.A., A.L. Densmore, and R.S. Anderson, Development of mountainous topography in the Basin Ranges, USA, *Basin Research*, 11 (1), 21-41, 1999.
- Fernandes, N.F., and W.E. Dietrich, Hillslope evolution by diffusive processes: The timescale for equilibrium adjustments, *Water Resources Research*, 33 (6), 1307-1318, 1997.
- Fourier, J.B., *Theorie Analytique de la Chaleur*, Didot. (English translation by A. Freeman: *The Analytical theory of Heat*. Cambridge University Press, Cambridge, 1878. Reprinted by Dover Publications, Inc., New York, 1955), Paris, 1822.
- Furbish, D.J., and S. Fagherazzi, Stability of Creeping Soil and Implications for Hillslope Evolution, *Water Resources Research*, 37 (10), 2607-2618, 2001.
- Gabet, E.J., Gopher Bioturbation: Field Evidence for Non-Linear Hillslope Diffusion, *Earth Surface Processes and Landforms*, 25 (13), 1419-1428, 2000.
- Gabet, E.J., Sediment transport by dry ravel, *Journal of Geophysical Research*, 108 (B1), 22-1 - 22-8, 2003.
- Gabet, E.J., O.J. Reichman, and E.W. Seabloom, The Effects of bioturbation on soil processes and sediment transport, *Annual Reviews of Earth and Planetary Science*, 31, 249-73, 2003.
- Gaillardet, J., B. Dupre, C.J. Allegre, and P. Negrel, Chemical and physical denudation in the Amazon River basin, *Chemical Geology*, 142 (3-4), 141-173, 1997.
- Gilbert, G.K., The convexity of hilltops, *Journal of Geology*, 17, 344-350, 1909.
- Green, E.G., W.E. Dietrich, and J.F. Banfield, The Quantification of mass loss via geochemical weathering in hillslope processes, *Eos Trans. AGU, Fall Meet. Suppl.*,

- 84 (46), Abstract H51E-1128, 2003.
- Heimsath, A.M., W.E. Dietrich, K. Nishiizumi, and R.C. Finkel, The Soil Production Function and Landscape Equilibrium, *Nature*, 388 (6640), 358-361, 1997.
- Heimsath, A.M., W.E. Dietrich, K. Nishiizumi, and R.C. Finkel, Cosmogenic Nuclides, Topography, and the Spatial Variation of Soil Depth, *Geomorphology*, 27 (1-2), 151-172, 1999.
- Hirano, M., Mathematical model and the concept of equilibrium in connection with slope shear ration, *Zeitschrift f. Geomorph. Sppl. Bd*, 25, 50-71, 1976.
- Howard, A.D., A Detachment-Limited Model of Drainage-Basin Evolution, *Water Resources Research*, 30 (7), 2261-2285, 1994.
- Howard, A.D., Badland Morphology and Evolution: Interpretation Using a Simulation Model, *Earth Surface Processes and Landforms*, 22 (3), 211-227, 1997.
- Jyotsna, R., and P.K. Haff, Microtopography as an indicator of modern hillslope diffusivity in arid terrain, *Geology*, 25 (8), 695-698, 1997.
- Keller, E.A., R.L. Zepeda, T.K. Rockwell, T.L. Ku, and W.S. Dinklage, Active tectonics at Wheeler Ridge, southern San Joaquin Valley, California, *Geological Society of America Bulletin*, 110 (3), 298-310, 1998.
- Kirkby, M.J., Measurement and Theory of Soil Creep, *Journal of Geology*, 75 (4), 359-&, 1967.
- Kirkby, M.J., Hillslope process-response models based on the continuity equation, *Institute of British Geographers Special Publication*, 3, 15-30, 1971.
- Kirkby, M.J., Soil Development Models as a Component of Slope Models, *Earth Surface Processes and Landforms*, 2 (2-3), 203-230, 1977.
- Kirkby, M.J., A Basis for Soil-Profile Modeling in a Geomorphic Context, *Journal of Soil Science*, 36 (1), 97-121, 1985.
- Kooi, H., and C. Beaumont, Escarpment Evolution on High-Elevation Rifted Margins - Insights Derived from a Surface Processes Model That Combines Diffusion, Advection, and Reaction, *Journal of Geophysical Research-Solid Earth*, 99 (B6), 12191-12209, 1994.
- Koons, P.O., The Topographic Evolution of Collisional Mountain Belts - a Numerical Look at the Southern Alps, New-Zealand, *American Journal of Science*, 289 (9), 1041-1069, 1989.

- Mckean, J.A., W.E. Dietrich, R.C. Finkel, J.R. Southon, and M.W. Caffee, Quantification of Soil Production and Downslope Creep Rates From Cosmogenic Be-10 Accumulations on a Hillslope Profile, *Geology*, 21 (4), 343-346, 1993.
- Millot, R., J. Gaillardet, B. Dupre, and C.J. Allegre, The global control of silicate weathering rates and the coupling with physical erosion: new insights from rivers of the Canadian Shield, *Earth and Planetary Science Letters*, 196 (1-2), 83-98, 2002.
- Nepstad, D.C., C.R. Decarvalho, E.A. Davidson, P.H. Jipp, P.A. Lefebvre, G.H. Negreiros, E.D. Dasilva, T.A. Stone, S.E. Trumbore, and S. Vieira, The Role of Deep Roots in the Hydrological and Carbon Cycles of Amazonian Forests and Pastures, *Nature*, 372 (6507), 666-669, 1994.
- Pazzaglia, F.J., and T.W. Gardner, Late Cenozoic Flexural Deformation of the Middle United-States Atlantic Passive Margin, *Journal of Geophysical Research-Solid Earth*, 99 (B6), 12143-12157, 1994.
- Rinaldo, A., W.E. Dietrich, R. Rigon, G.K. Vogel, and I. Rodriguez-Iturbe, Geomorphological signatures of varying climate, *Nature*, 374, 632-635, 1995.
- Roering, J.J., J.W. Kirchner, and W.E. Dietrich, Evidence for Nonlinear, Diffusive Sediment Transport on Hillslopes and Implications for Landscape Morphology, *Water Resources Research*, 35 (3), 853-870, 1999.
- Roering, J.J., J.W. Kirchner, and W.E. Dietrich, Hillslope Evolution by Nonlinear, Slope-Dependent Transport: Steady State Morphology and Equilibrium Adjustment Timescales, *Journal of Geophysical Research-Solid Earth*, 106 (B8), 16499-16513, 2001.
- Sander, H., The Porosity of Tropical Soils and Implications for Geomorphological and Pedogenetic Processes and the Movement of Solutions Within the Weathering Cover, *Catena*, 49 (1-2), 129-137, 2002.
- Small, E.E., R.S. Anderson, and G.S. Hancock, Estimates of the Rate of Regolith Production Using Be-10 and Al-26 From an Alpine Hillslope, *Geomorphology*, 27 (1-2), 131-150, 1999.
- Stonestrom, D.A., A.F. White, and K.C. Akstin, Determining Rates of Chemical Weathering in Soils - Solute Transport Versus Profile Evolution, *Journal of Hydrology*, 209 (1-4), 331-345, 1998.
- Summerfield, M.A., and N.J. Hulton, Natural Controls of Fluvial Denudation Rates in Major World Drainage Basins, *Journal of Geophysical Research-Solid Earth*, 99 (B7), 13871-13883, 1994.

- Tucker, G.E., and R.L. Bras, Hillslope Processes, Drainage Density, and Landscape Morphology, *Water Resources Research*, 34 (10), 2751-2764, 1998.
- Tucker, G.E., and R. Slingerland, Predicting Sediment Flux From Fold and Thrust Belts, *Basin Research*, 8 (3), 329-349, 1996.
- White, A.F., A.E. Blum, T.D. Bullen, D.V. Vivit, M. Schulz, and J. Fitzpatrick, The Effect of Temperature on Experimental and Natural Chemical Weathering Rates of Granitoid Rocks, *Geochimica Et Cosmochimica Acta*, 63 (19-20), 3277-3291, 1999.
- White, A.F., A.E. Blum, M.S. Schulz, D.V. Vivit, D.A. Stonestrom, M. Larsen, S.F. Murphy, and D. Eberl, Chemical Weathering in a Tropical Watershed, Luquillo Mountains, Puerto Rico: I. Long-Term Versus Short-Term Weathering Fluxes, *Geochimica Et Cosmochimica Acta*, 62 (2), 209-226, 1998.
- Willett, S.D., R. Slingerland, and N. Hovius, Uplift, shortening, and steady-state topography in active mountain belts, *American Journal of Science*, 301 (4-5), 455-485, 2001.
- Willgoose, G., R.L. Bras, and I. Rodriguez-Iturbe, A Coupled Channel Network Growth and Hillslope Evolution Model .1. Theory, *Water Resources Research*, 27 (7), 1671-1684, 1991.

CHAPTER III

USING CHEMICAL TRACERS IN HILLSLOPE SOILS TO ESTIMATE THE IMPORTANCE OF CHEMICAL DENUDATION UNDER CONDITIONS OF DOWNSLOPE SEDIMENT TRANSPORT

Abstract

We present a model of hillslope soils that couples the evolution of topography, soil thickness, and the concentration of constituent soil phases, defined as unique components of the soil with collective mass equal to the total soil mass. The model includes both sediment transport and chemical denudation. A simplified two phase model is developed; the two phases are a chemically immobile phase, which has far lower solubility than the bulk soil and is not removed through chemical weathering (for example, zircon grains), and a chemically mobile phase that may be removed from the system through chemical weathering. Chemical denudation rates in hillslope soils can be measured using the concentration of immobile elements, but the enrichment of these immobile elements is influenced by spatial variations in chemical denudation rates and spatial variations in the chemical composition of a soil's parent material. These considerations cloud the use of elemental depletion factors and cosmogenic nuclide-based total denudation rates measured at single points on hillslopes to identify the relationship between physical erosion and chemical weathering. The model is used to predict concentrations of chemically immobile phases in hillslope soils; these predictions are used to test the veracity of using point measurements to estimate basin wide chemical denudation rates. Point measurements may be adequate where the chemical denudation rate is a significant fraction of the total denudation rate, but are inadequate in regions where chemical weathering rates are small

compared to the total denudation rate. We also examine relationships between unsteady mechanical and chemical denudation rates. Soil particle exposure ages may affect chemical weathering rates; the relationship between total landscape lowering rates and soil particle ages can thus be quantified.

1. Introduction

Many landscapes are mantled by a mobile layer of soil. This soil is created from weathered bedrock or saprolite through a variety of processes such as penetration by tree roots, burrowing by mammals, or freeze-thaw mechanisms [e.g., see *Birkeland*, 1999]. Once created, mobile soil is removed from the landscape by either mechanical sediment transport [e.g., *Gilbert*, 1877], or by chemical weathering processes [e.g., *White and Brantley*, 1995]. Chemical weathering within a hillslope soil plays an important role in the export of dissolved material from basins; recent work has found that the fluxes of solutes from soils may be equal to or greater than the fluxes from saprolite and weathered bedrock [*Anderson et al.*, 2002; *Green et al.*, 2004].

Chemical weathering of silicate minerals can serve as a sink for atmospheric CO₂ [*Berner et al.*, 1993]; studies of chemical weathering therefore have been motivated in part by the hypothesis that there are feedbacks between chemical weathering and global climate [*Raymo and Ruddiman*, 1992]. In their landmark study *Raymo and Ruddiman* [1992] hypothesized that an increased mechanical denudation rate due to tectonic uplift can result in an increased chemical denudation rate (due to an increase in the rate of production of fresh mineral surfaces) and global cooling (due to reduction in atmospheric CO₂). A number of researchers have demonstrated a coupling between chemical and

mechanical denudation rates using stream gauge data [see *Stallard*, 1995, for review]. Measurements of both chemical and mechanical denudation rates from stream gauges have the advantage of integrating denudation over an entire basin, but have the disadvantage of varying due to the stochastic distribution of floods and brief measurement periods relative to the measurement period needed to fully characterize the full distribution of floods [e.g., *Kirchner et al.*, 2001].

Quantifying the balance between chemical and mechanical denudation in hillslope soils has the advantage of averaging the denudation rate over 10ka-1000ka, as hillslope soils respond more slowly than channels to erosional forcings by storms [e.g., *Furbish and Fagherazzi*, 2001; *Mudd and Furbish*, 2005 *in press*]. In the soil environment, mass balance techniques are useful in determining the extent of chemical weathering [e.g., *April et al.*, 1986; *Brimhall and Dietrich*, 1987]. These mass balance techniques involve measuring the enrichment of minerals in the soil that are relatively insoluble. Until recently, however quantifying rates of chemical denudation within soils has been limited to non-sloping sites where the age of the soil is known [e.g., *Chadwick et al.*, 1990; *Merritts et al.*, 1992; *Taylor and Blum*, 1995]. A recent series of papers, however, has shown that the chemical denudation rate may be estimated in eroding landscapes if the total denudation rate (the sum of the chemical and mechanical denudation rates) is known [*Small et al.*, 1999; *Riebe et al.*, 2001; *Riebe et al.*, 2003; *Riebe et al.*, 2004a; *Riebe et al.*, 2004b]. Measuring the chemical denudation rate using the enrichment of immobile minerals is distinct from solute studies because the estimate of chemical denudation using this method is averaged over the residence time of the soil particles. The total denudation rate of a soil may be determined by measuring inventories of cosmogenic radionuclides at

the soil-saprolite boundary [e.g., *Heimsath et al.*, 1997, *Small et al.*, 1997].

While the techniques of *Riebe et al.* [2001] and *Small et al.* [1999] allow for the estimation of the relative proportion of chemical and mechanical weathering in mobile soils averaged over the residence time of the soil particles, they are limited to soils in which there is no spatial variation in the chemical composition of the parent material, and in which the chemical denudation rate in the soil does not vary spatially. Strong spatial co-variations of chemical weathering and sediment transport processes, however, have been long inferred from routine observations that soil properties systematically vary along hillslopes [e.g. *Birkeland*, 1999]. Recent investigations have found spatial heterogeneity in the degree of chemical weathering in hillslope soils as a function of position using mass balance techniques [*Green et al.*, 2003; *Green et al.*, 2004; *Nezat et al.*, 2004; *Yoo et al.*, 2004].

In this contribution we extend the work of *Small et al.* [1999] and *Riebe et al.* [2001] by developing a model that explicitly includes spatial variations in chemical denudation rates and spatial variations in the chemical composition of the parent material from which the soil is formed. This new model is used to address several questions. First we examine to what extent the chemical composition of the soil is expected to vary under hypothesized spatial variations in the chemical denudation rate. We then address the question of how closely the chemical denudation rate estimated using the technique of *Riebe et al.* [2001] (which is relatively simple, requires few measurements, and is therefore a preferred first alternative to taking spatially distributed measurements in a basin) will match the true basin averaged chemical denudation rate if the chemical composition of the parent material or the chemical denudation rate varies spatially.

Finally, the model is used to examine patterns of soil chemical composition under conditions of transient erosion rates, and how such transient erosion rates may affect the sediment transport and chemical denudation rates of hillslope soils.

2. A Coupled Model of Hillslope Evolution

Our model, which couples the elevation a hillslope surface with the concentration of constitutive phases (to be defined in section 2.2) in the soil, is based on conservation of mass for the total soil layer and for each constitutive phase within the soil. First we derive a statement of mass conservation for the whole soil.

2.1. Conservation of Total Soil Mass

Many authors have derived equations for conservation of mass on hillslopes that contain terms for the mechanical transport of sediment [*Ahnert*, 1976; *Anderson*, 2002; *Armstrong*, 1976; *Culling*, 1960; *Gabet et al.*, 2003; *Kirkby*, 1971; *Roering* 2001]. Others have derived models that explicitly include terms for mass loss due to chemical weathering processes [*Kirkby*, 1977; *Kirkby*, 1985a; *Kirkby*, 1985b, *Mudd and Furbish*, 2004]. Here we use a depth-integrated equation for the conservation of mass of a hillslope soil, one including both chemical and physical processes:

$$\frac{\partial (h \bar{\rho}_s)}{\partial t} + \frac{\partial (h \bar{v}_x \rho_s)}{\partial x} + \frac{\partial (h \bar{v}_y \rho_s)}{\partial y} - h \bar{S}_v - \rho_\zeta d_\zeta - \rho_r p_\eta = 0, \quad (1)$$

where h (L) is soil depth, ρ_s ($L^3 T^{-1}$) is the dry bulk density of the soil, v_x ($L T^{-1}$) is the velocity of the sediment in the x -direction, v_y ($L T^{-1}$) is the velocity of the sediment in the y -direction, S_v ($M T^{-1} L^{-3}$) is a rate of mass loss or gain per unit volume due to chemical or

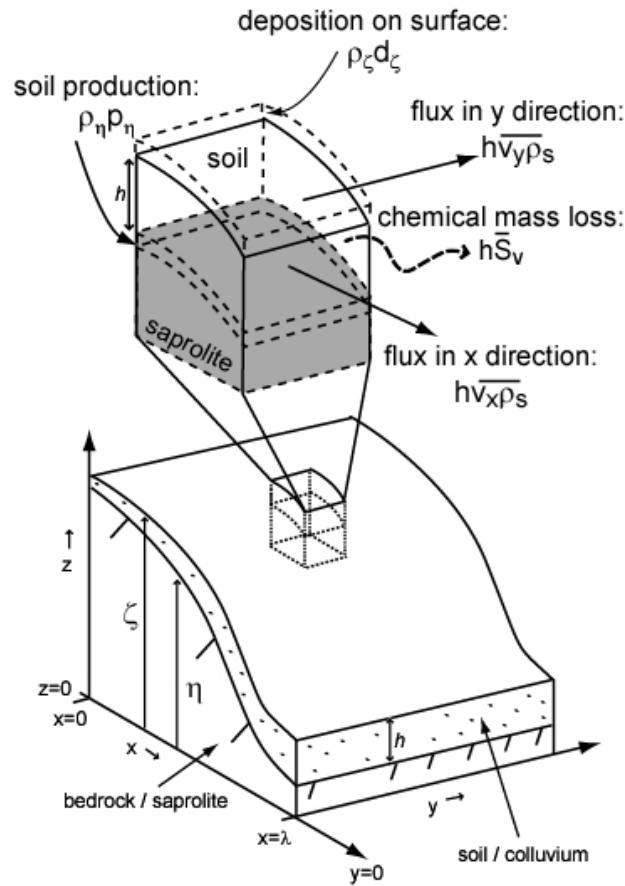


Figure 1. Schematic of a 2-D hillslope.

biological processes, ρ_c ($M L^{-3}$) is the dry bulk density of material deposited at the surface, d_c ($L T^{-1}$) is the deposition rate of material at the surface, ρ_r ($M L^{-3}$) is the density of the parent material, p_r ($L T^{-1}$) is the rate of entrainment of parent material into the active soil layer, and the overbars denote depth-averaged quantities (Figure 1). The derivation of equation (1) is presented in *Mudd and Furbish* [2004]. The first term in equation (1) is the change with respect to time of the mass in a column of soil. The second and third terms are the mass fluxes of sediment in the x and y directions, respectively. The fourth term is the rate of mass lost or gained due to chemical or biological processes (e.g., weathering of minerals, deposition of plant material). The last

two terms are rate of mass losses or gains due to deposition of material on the surface of the soil or production of soil at the soil-saprolite boundary. The soil thickness h is defined as the distance between the elevation of the soil surface, ζ (L), and the elevation of the base of the mechanically active layer of the soil, η (L):

$$h = \zeta - \eta, \quad (2)$$

where the mechanically active layer is the portion of the soil which is experiencing mechanical disturbances.

The deposition and production rate terms (d_ζ and p_η , respectively) represent the change in the elevation of the base of the active layer and the surface if the hillslope sediment velocities v_x , v_y , and v_z are zero (the vertical velocity of the sediment, v_z , does not appear in equation (1) because it has been eliminated by depth integration). If particle motion extends to the base of the soil as defined in a pedological sense, such that η coincides with the soil-bedrock interface, then p_η is the rate of soil production associated with the conversion of bedrock to soil. This is analogous to the production term described by *Kirkby* [1971] and examined empirically using cosmogenic isotopes [e.g., *Heimsath et al.*, 1997; *Riebe et al.*, 2003; *Small et al.*, 1999]. It is important to note that the production term does not include any mass losses due to chemical weathering; these mass losses are subsumed in the term S_v .

2.2. Conservation of a Soil Phase

We now consider conservation of mass for constitutive phases that make up the soil for the general framework outlined in equation (1). We define a phase as any identifiable and unique portion of the soil. By unique we mean that a given phase is

physically separate from all other phases. In a given soil sample, the total mass of the sample is the sum of the masses of the constitutive phases:

$$m_{tot} = \sum_{i=1}^N m_i, \quad (3)$$

where m_i is the mass of phase i (M), m_{tot} is the total mass in the sample (M), and N is the number of phases. The concentration by mass of phase i , c_i (dimensionless), is:

$$c_i = \frac{m_i}{m_{tot}}. \quad (4)$$

Summing the concentrations by mass gives:

$$\sum_{i=1}^N c_i = 1. \quad (5)$$

The mass of a constitutive phase in the soil per unit volume is

$$\frac{m_i}{V} = \frac{m_i}{m_{tot}} \frac{m_{tot}}{V} = c_i \rho_s, \quad (6)$$

where V (L³) is a unit volume. In a control element with a surface area A (L²), a volume V , and a vector normal to the surface \mathbf{n} (L), the conservation of mass of a constitutive phase is:

$$\int_V \frac{\partial}{\partial t} (c_i \rho_s) dV + \int_A (\mathbf{v}_i c_i \rho_s) \cdot \mathbf{n} dA - \int_V S_i dV = 0, \quad (7)$$

where \mathbf{v}_i (L T⁻¹) is the velocity vector of phase i ($\mathbf{v}_i = v_{ix} \hat{i} + v_{iy} \hat{j} + v_{iz} \hat{k}$) where \hat{i}, \hat{j} , and \hat{k}

are unit vectors in the x , y , and z directions, respectively, and v_{ix} , v_{iy} , v_{iz} are the respective components of the phase velocity), S_i ($M L^{-3} T^{-1}$) is the rate of mass loss or gain of phase i per unit volume due to chemical or biological processes. The rates of the mass loss of each phase per unit volume add up to the total mass loss rate per unit volume:

$$\sum_{i=1}^N S_i = S_v. \quad (8)$$

In order to develop a general equation of mass conservation for phase i , the method of *Mudd and Furbish* [2004] is used, in which equation (7) is first integrated over the control element and then depth integrated through the soil column. Kinematic boundary conditions are applied at $z = \zeta$ and $z = \eta$, and it is assumed that the velocity of phase i at the boundaries is the same as the average velocity of the bulk soil. This results in a general statement of mass conservation for phase i :

$$\frac{\partial}{\partial t} (\overline{h c_i \rho_s}) + \frac{\partial}{\partial x} (\overline{h v_{ix} c_i \rho_s}) + \frac{\partial}{\partial y} (\overline{h v_{iy} c_i \rho_s}) - h \overline{S_i} - c_{i\zeta} \rho_\zeta d_\zeta - c_{i\eta} \rho_r p_\eta = 0. \quad (9)$$

where the overbars represent a depth averaged quantity, $c_{i\zeta}$ is the concentration of phase i in material deposited at the surface of the soil (dimensionless), and $c_{i\eta}$ is the concentration of phase i at the soil-saprolite boundary (dimensionless). The first term in equation (9) is the change with respect to time of the mass of phase i in a column of soil. The second and third terms are the mass fluxes of phase i in the x and y directions, respectively. The fourth term is the rate of mass of phase i lost or gained due to chemical or biological processes (e.g., weathering of minerals, deposition of plant material). The last two terms are rate of mass of phase i lost or gained due to deposition of material on

the surface of the soil or production of soil at the soil-saprolite boundary.

Equations (1) and (9) are the most general form of equations of depth-integrated conservation of mass for the soil profile and for soil phase i , respectively. They have a number of independent variables and therefore must be closed with simplifying assumptions and additional constitutive equations before they can be solved analytically or using numerical models.

3. A 1-D, Two Phase Model of Hillslope Weathering and Transport

We now develop a two phase soil weathering model that consists of a chemically mobile phase with concentration c_m and a chemically immobile phase with concentration c_{im} . All mass lost due to chemical weathering is removed from the mobile phase:

$$\bar{S}_{im} = 0, \quad (10a)$$

$$\bar{S}_m = \bar{S}_v. \quad (10b)$$

For example, an immobile phase could be the mineral zircon, which is highly insoluble compared to other rock forming minerals [e.g., *Brimhall et al.*, 1992]. If an element (e.g., zirconium) only occurs in the immobile mineral (e.g., zircon), then the elemental concentration may be substituted for the mineral concentration. In this two phase system, if the concentration of the immobile phase is known, then the concentration of the mobile phase is also known (equation 5). Thus we only need a conservation statement for one of the soil phases. Here we solve the governing equations for the immobile phase. We conceptualize the system as having three layers (Figure 2): the soil, a saprolite layer from which the soil is produced, and a layer of unweathered bedrock. The concentration of the

immobile element in these three layers is denoted by c_{im} in the soil, c_η at the soil-saprolite boundary, and c_r in the unweathered bedrock.

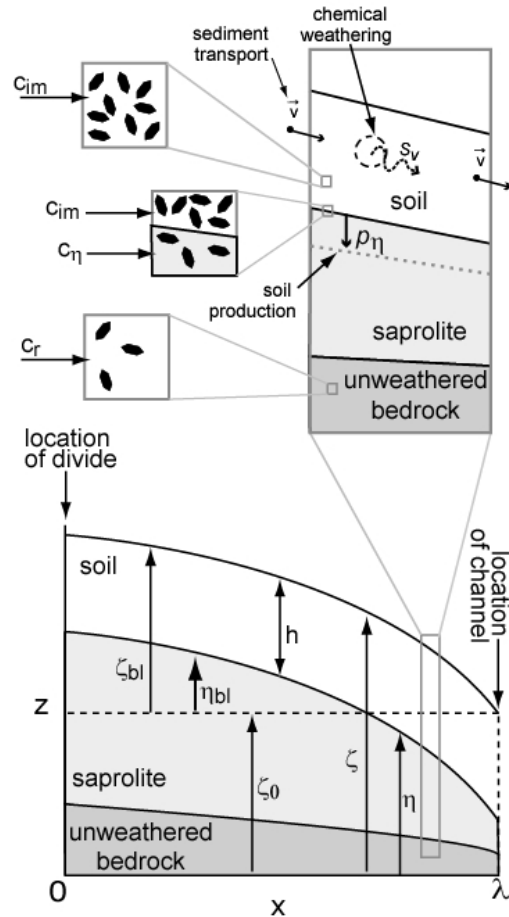


Figure 2. Schematic of the 1-D hillslope. The black particles represent the immobile phase in the bedrock, saprolite, and soil.

3.1. Simplifying assumptions

We begin by reducing the system to a one dimensional hillslope and assuming that deposition at the surface of the soil is zero ($d_c = 0$). We also assume that the soil is well mixed such that products that are depth integrated can be assumed to be the products of depth integrated quantities (e.g., $\overline{v_{ix} c_i \rho_s} \approx \bar{v}_{ix} \bar{c}_i \bar{\rho}_s$). Additionally, it is assumed that

there is no sorting, such that the velocity of any given phase is the same as the bulk soil velocity ($v_{ix} = v_x$ throughout the soil column). It is also assumed that sediment at the soil-saprolite interface does not have horizontal velocities ($v_x|_{z=\zeta} = v_y|_{z=\eta} = 0$).

The rate of production of mobile soil from saprolite has been found to decrease with soil thickness (h) at some field locations [e.g., *Heimsath et al.* 1997]:

$$p_\eta = W_0 e^{-\frac{h}{\gamma}}, \quad (11)$$

where W_0 ($L T^{-1}$) is the rate of soil production as the soil thickness approaches zero and γ (L) is a length scale that characterizes the rate of decline in the soil production rate with increasing soil thickness. We also assume that the depth integrated density of the soil is homogenous in the x and y directions. It has been suggested that the soil production function in many locations is peaked, with a maximum value at an intermediate soil depth [e.g., *Anderson, 2002; Carson and Kirkby, 1972; Gilbert, 1909*]. Here, however, we assume that the soil production rates of our modeled hillslopes are slow enough such that they lie on the portion of the soil production function where the production rate decreases with increasing soil thickness.

3.2. Flux Laws

A number of authors have presented constitutive equations for sediment flux [e.g., *Anderson, 2002; Culling, 1963; Gabet, 2000; Gabet et al., 2003; Kirkby, 1967; Roering et al., 1999; Roering, 2004*]. Here we use a generalized equation to describe sediment flux, φ :

$$\varphi = h \bar{v}_x \quad (12)$$

where φ has units $L^2 T^{-1}$. The form of φ may vary depending on the site. We present two common flux laws, the first where sediment flux is linearly proportional to slope, and the second where sediment flux increases nonlinearly as the soil surfaces approaches a critical gradient:

$$\varphi = -D \frac{\partial \zeta}{\partial x}, \quad (13a)$$

$$\varphi = -D \frac{\partial \zeta}{\partial x} \left(1 - \left[\frac{1}{S_c} \left| \frac{\partial \zeta}{\partial x} \right| \right]^2 \right)^{-1}, \quad (13b)$$

where D ($L^2 T^{-1}$) is a sediment diffusivity and S_c is a critical slope (dimensionless).

3.3. Lagrangian Coordinate System

Dynamic hillslope evolution is driven in part by incision at the base of the hillslope, and here we impose an external forcing on the modeled hillslope driven by channel incision at the base of the hillslope. We designate a coordinate system in which the elevation of the soil surface (ζ) and the elevation of the soil-saprolite boundary (η) are measured relative to the local base level, which is the elevation at the base of the hillslope:

$$\zeta_{bl} = \zeta - \zeta_0, \quad (14a)$$

$$\eta_{bl} = \eta - \zeta_0, \quad (14b)$$

where the subscript bl indicates an elevation relative to base level and ζ_0 is the elevation of local base level, taken here to be the absolute elevation at the base of the hillslope

(Figure 2). In the transient case, the time derivatives of both the elevation of the soil surface (ζ) and the elevation of the base of soil-saprolite boundary(η) will contain a base level lowering term ($\partial\zeta_0/\partial t$). This term is the incision or deposition rate at the lower boundary of the hillslope, which we call I ($L T^{-1}$). If there is a river that is incising through bedrock at the base of the hillslope, I will be negative. If the base of the hillslope is a colluvial hollow that is filling with sediment, I will be positive.

3.4. The Governing Equations for a Hillslope Soil Composed of Two Phases

Noting that the soil thickness $h = \zeta - \eta = \zeta_{bl} - \eta_{bl}$, the governing equations for a one-dimensional, two-phase hillslope may be stated as:

$$\frac{\partial \eta_{bl}}{\partial t} = - \left(W_0 e^{-\frac{h}{\gamma}} + I \right), \quad (15)$$

$$\frac{\partial \zeta_{bl}}{\partial t} + \frac{\partial \varphi}{\partial x} - \frac{h}{\rho_s} \bar{S}_v + \left(1 - \frac{\rho_\eta}{\rho_s} \right) W_0 e^{-\frac{h}{\gamma}} + I = 0, \quad (16)$$

and

$$\frac{\partial}{\partial t} (h \bar{c}_{im}) + \frac{\partial}{\partial x} (\varphi \bar{c}_{im}) - \frac{\rho_\eta}{\rho_s} c_{\eta im} W_0 e^{-\frac{h}{\gamma}} = 0. \quad (17)$$

Equation (15) describes the rate of lowering of the boundary between soil and saprolite relative to base level (Figure 3). Soil production (the first term to the right of the equality) will lower this boundary, whereas channel incision (the second term) will

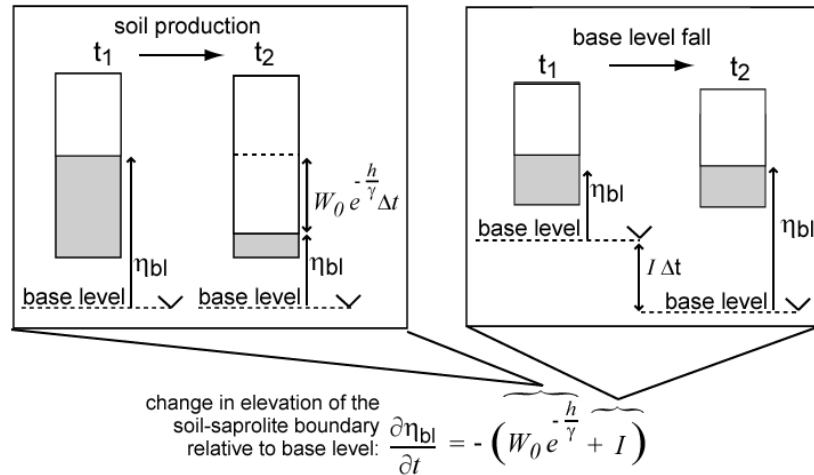


Figure 3. Schematic showing mechanisms for changing the elevation of the soil-saprolite boundary relative to base level.

increase the elevation of the boundary relative to base level (e.g., incision causes the difference between the elevation of the soil-saprolite boundary and the channel to grow). Equation (16) describes the evolution of the elevation of the soil surface through time (Figure 4). The second term in equation (16) is the rate of change of the elevation of the soil surface due to the divergence of sediment flux, the third term is the rate of change of the elevation of the soil surface due to chemical weathering, the third term is the rate of change of the elevation of the soil surface due to expansion or contraction of the soil when it is converted from saprolite to soil. The last term is the rate of change of the elevation of the soil surface due to incision, and appears because the elevation of the soil surface is measured relative to local base level. Equation (17) describes the change in time of the relative depth of the immobile phase (e.g., if a soil column is 1m thick, and the concentration of the immobile phase in this column is 0.1, then the relative depth of the immobile phase is 0.1m). The second term in equation (17) describes changes in the relative depth of the immobile phase due to sediment transport, and the third term

describes changes in the relative depth of the immobile phase due to soil production.

Equations (15), (16), and (17) may be combined to form an equation that describes the possible mechanisms for enriching or depleting the concentration of the immobile element in the soil (Figure 5):

$$h \frac{\partial \bar{c}_{im}}{\partial t} + \phi \frac{\partial \bar{c}_{im}}{\partial x} + \bar{c}_{im} \frac{h \bar{S}_v}{\bar{\rho}_s} + \frac{\rho_\eta}{\bar{\rho}_s} (\bar{c}_{im} - c_{\eta im}) W_0 e^{-\frac{h}{\gamma}}. \quad (18)$$

The concentration of the immobile phase at some point on the hillslope may be affected

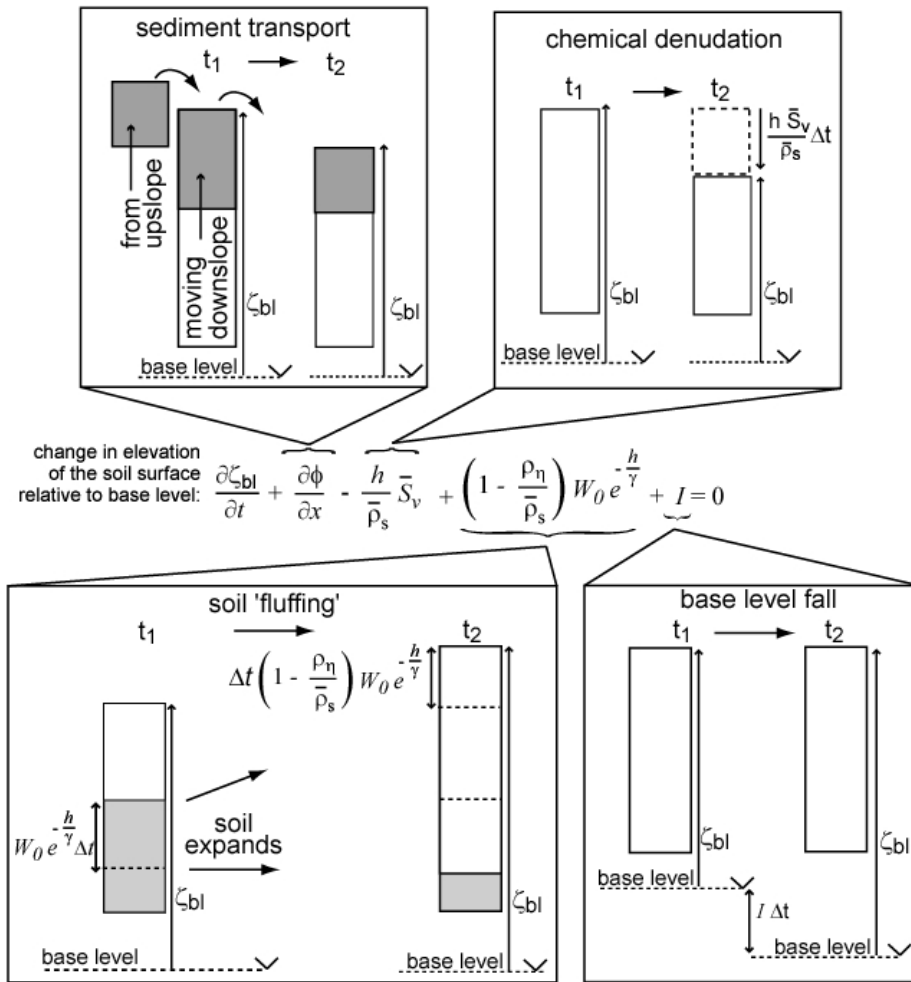


Figure 4. Schematic showing mechanisms for changing the elevation of the soil surface relative to base level.

by the transport of sediment in areas of spatial concentration gradients, which is described by the second term in equation (18). Thinning of soil by chemical dissolution will lead to an increase in the concentration of an immobile element (third term of equation 18). The fourth term of equation (18) describes the enrichment or dilution of the concentration of the immobile phase due to soil production.

3.5. Non-Dimensionalization and Scaling

The number of parameters in the system described by equations (15), (16) and (17) may be reduced by non-dimensionalizing the system. The length scales are non-dimensionalized with either the length of the hillslope, λ (L), or the decay depth of the soil production function γ (see equation 11):

$$\hat{x} = \frac{x}{\lambda}, \quad \hat{\zeta} = \frac{\zeta_{bl}}{\lambda}, \quad \hat{\eta} = \frac{\eta_{bl}}{\lambda}, \quad \hat{h} = \frac{h}{\gamma}, \quad (19a,b,c,d)$$

where dimensionless quantities are denoted with the carats. A lengthscale ratio (dimensionless) is defined as:

$$\theta_L = \frac{\lambda}{\gamma}. \quad (20)$$

We also define two timescales. The first timescale (T_D) is based on the relaxation time hillslope experiencing diffusion-like sediment transport [e.g., *Fernandes and Dietrich*, 1997; *Furbish and Fagherazzi*, 2001; *Jyotsna and Haff*, 1997; *Roering et al.*, 2001], and the second (T_P) is formed with soil production parameters:

$$T_D = \frac{\lambda^2}{D}, \quad T_P = \frac{\gamma}{W_0}, \quad (21a,b)$$

where we name T_D the diffusive timescale and T_P the production timescale. The diffusive timescale will range from tens of thousands to tens of millions of years [Mudd and Furbish, 2004]. Studies of soil or regolith production have found values of W_0 that range from approximately $1 \times 10^{-5} \text{ m yr}^{-1}$ to $2.5 \times 10^{-4} \text{ m yr}^{-1}$ and values of γ that range from approximately 0.25m to 0.5m [Heimsath et al. 1999; Heimsath et al., 2000; Heimsath et al., 2001; Small et al., 1999]. This gives production timescales ranging from thousands to tens of thousands of years. We scale time, the depth integrated mass loss due to chemical weathering per unit volume per unit time, and the base level lowering rate by the two timescales:

$$\hat{t} = \frac{t}{T_D}, \quad \hat{S} = \frac{T_P}{\rho_s} \bar{S}_v, \quad \hat{I} = \frac{T_P}{\gamma} I. \quad (22a,b,c)$$

Sediment flux is scaled by the diffusivity:

$$\hat{\phi} = -\frac{\Phi}{D}. \quad (23)$$

We define a diffusive to production timescale ratio (dimensionless) as

$$\theta_t = \frac{T_D}{T_P} = \frac{\lambda^2 W_0}{D \gamma} \quad (24)$$

and a soil to parent material density ratio (dimensionless) as

$$\tau_d = \frac{\rho_\eta}{\rho_s}. \quad (25)$$

The dimensionless concentration of the immobile phase is scaled by the concentration of

this phase in the bedrock:

$$\hat{c} = \frac{\bar{c}_{im}}{c_r}, \quad \hat{c}_\eta = \frac{c_{\eta im}}{c_r}. \quad (26a,b)$$

If chemical weathering is occurring on the hillslope, the concentration of the immobile phase in the soil will become enriched relative to the parent material (Figure 5), so the dimensionless concentration of the immobile phase in the soil (\hat{c}) and at the base of the soil (\hat{c}_η) represent enrichment ratios. The subscript *im* is dropped from the dimensionless concentrations because we are solving for the concentration of the immobile phase.

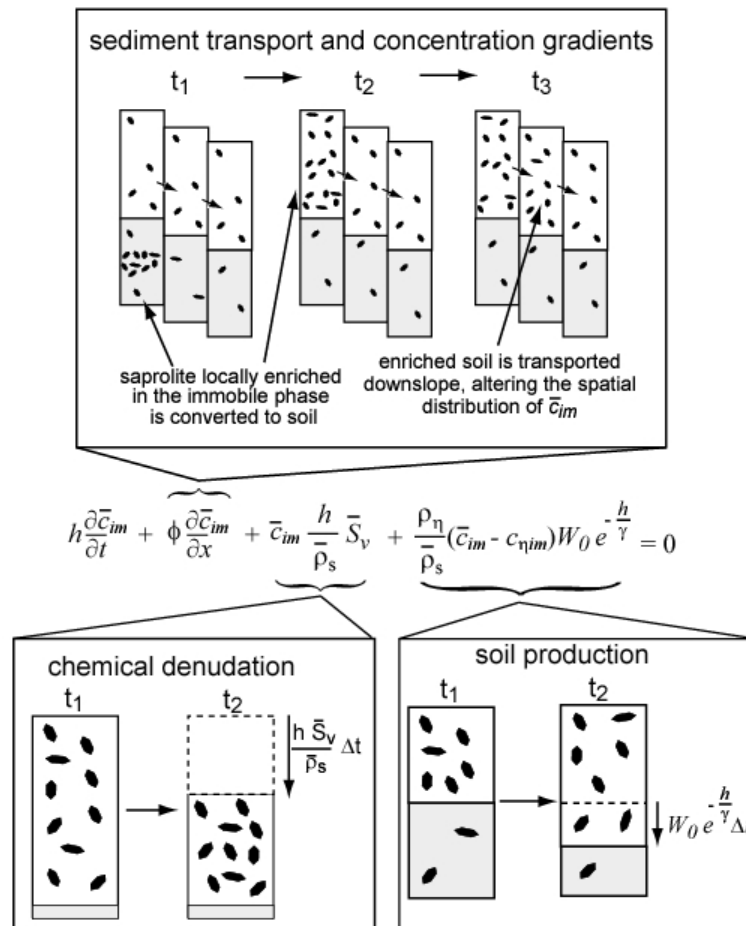


Figure 5. Schematic of the mechanisms that change the concentration of the chemically immobile phase within the soil layer.

Inserting equations (19)-(26) into equations (15), (16), and (17) results in:

$$\frac{\partial \hat{\eta}}{\partial \hat{t}} = -\frac{\theta_t}{\theta_L} (e^{-\hat{h}} + \hat{I}), \quad (27)$$

$$\frac{\partial \hat{\zeta}}{\partial \hat{t}} = \frac{\partial \hat{\phi}}{\partial \hat{x}} + \frac{\theta_t}{\theta_L} [\hat{h} \hat{S} - (1 - \tau_d) e^{-\hat{h}} - \hat{I}], \quad (28)$$

and

$$\frac{\partial}{\partial \hat{t}} (\hat{h} \hat{c}) = \theta_L \frac{\partial}{\partial \hat{x}} (\hat{\phi} \hat{c}) + \theta_t \hat{c}_\eta \tau_d e^{-\hat{h}}. \quad (29)$$

The large number of model parameters in equations (19)-(26), namely W_0 , γ , λ , D , $\bar{\rho}_s$, and ρ_η , are subsumed into three dimensionless groups (θ_t , θ_L , and τ_d) in the dimensionless equations (27)-(29). A single choice of a given value for any of the dimensionless groups can represent numerous hillslopes when the dimensionless governing equations are used.

4. On the Use of the Two Phase Hillslope System

Equations (27)-(29) may be used to explore the impact of the relative magnitude of chemical and mechanical denudation on hillslopes. Several recent studies [Riebe *et al.*, 2001; Riebe *et al.*, 2003; Riebe *et al.*, 2004a; Riebe *et al.*, 2004b] have suggested that if the enrichment of an immobile element and the total denudation rate (the sum of the chemical and mechanical denudation rates) are known, then the relative proportion of chemical to mechanical weathering may be determined using the relationship:

$$r_{ca} = r_T \left(1 - \frac{c_\eta}{c_{im}} \right), \quad (30)$$

where r_{ca} ($L T^{-1}$) is the apparent denudation rate due to chemical weathering measured by the technique of *Riebe et al.* [2001], and r_T ($L T^{-1}$) is the total denudation rate. The total denudation rate is the rate of conversion of saprolite to soil ($r_T = p_\eta$) and can be determined by using cosmogenic radionuclides collected at the soil-saprolite interface if the soil production rate is steady in time [e.g., *Heimsath et al.*, 1997, *Small et al.*, 1997]. The soil production is a function of the soil depth, so the assumption that the soil production rate is steady in time also implies that soil thickness is assumed to be steady in time. *Riebe et al.* [2001] also defined a chemical depletion fraction, or CDF, which can be directly related to the enrichment fraction:

$$CDF = \left(1 - \frac{\hat{c}_\eta}{\hat{c}} \right). \quad (31)$$

The CDF has been used by *Riebe et al.* [2001; 2003; 2004a; 2004b] to estimate the fraction of the total denudation that is occurring through chemical processes [which we call the denudation ratio, e.g., *Mudd and Furbish*, 2004], but this estimate matches the true fraction of denudation occurring through chemical processes only under certain conditions [*Riebe et al.*, 2001, appendix]. The first condition is in the case where soil experiences no sediment fluxes from upslope (e.g., a soil on a flat terrace or at a drainage divide). In that case, the apparent chemical denudation rate is equal to the actual chemical denudation rate, r_c , at that location. If there is downslope sediment transport, the chemical depletion fraction only yields the exact fraction of denudation occurring through chemical processes if the chemical composition of the parent material is homogenous and if the chemical denudation rate does not vary in space. Many hillslope soils, however, have chemical compositions that vary in space [e.g., *Birkeland*, 1999].

The spatial distribution of the chemical composition of the soil, including the immobile elements, depends on the spatial variation in chemical denudation rates in the soil, the transport of material with differing age and composition from upslope, and the spatial variation in parent material composition (Figure 5). To calculate the basin averaged chemical denudation rate, R_c , one must integrate the local denudation rate, r_c , over the entire basin (or over the one-dimensional transect used here, Figure 6).

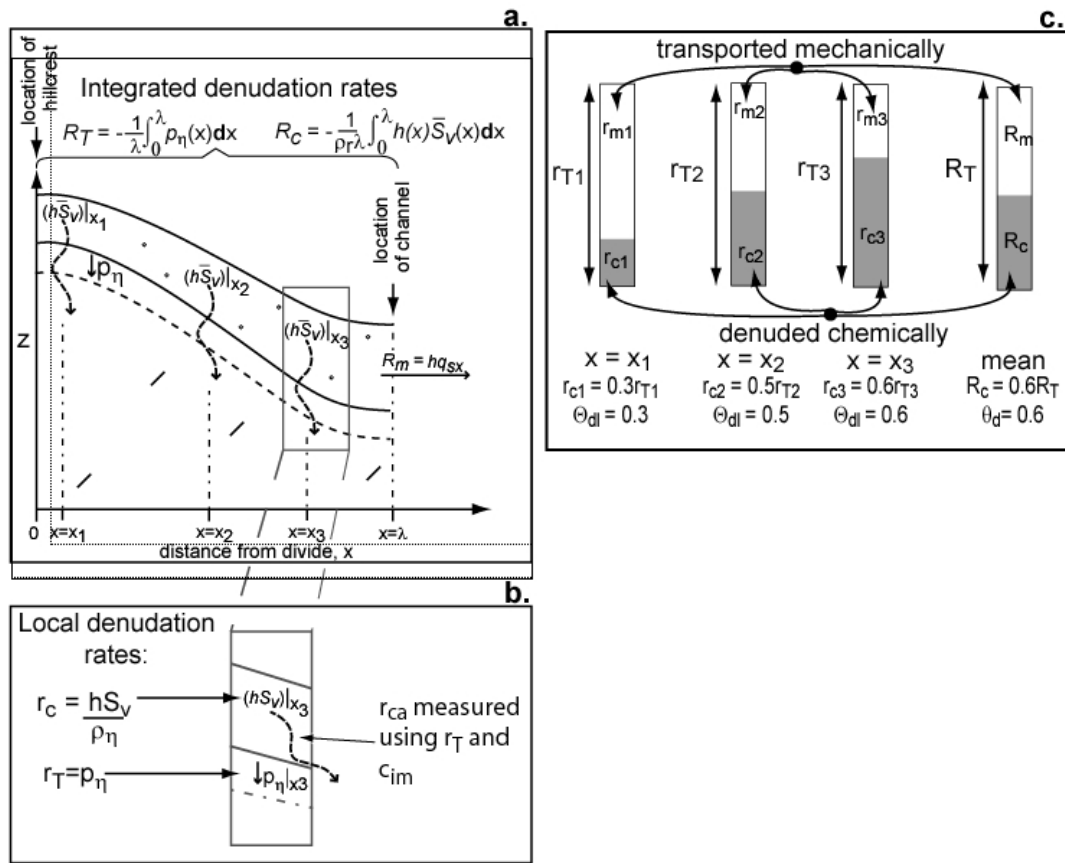


Figure 6. Schematic of the **a.** integrated denudation rates and **b.** local denudation rates. **c.** Spatial variations in the local denudation ratio and the integrated denudation ratio.

It should be noted that the denudation rates discussed here refer to denudation within the soil profile only, and does not include the mass lost to weathering processes within the saprolite. Also, all denudation rates in this contribution refer to rock equivalent units, for

example $r_c \cdot \Delta t$ is the thickness of rock lost in time Δt from within the soil, but the thickness of soil lost will be greater by the ratio of the density of the parent material to the density of the soil, τ_d . The local rate of chemical denudation is defined by:

$$r_c = - \frac{h \bar{S}_v}{\bar{\rho}_s \tau_d} . \quad (32)$$

We define both a local chemical denudation ratio, $\Theta_{dl} = r_c/r_T$, which is a function of position, and an integrated watershed denudation ratio $\theta_d = R_c/R_T$, that takes one value for a given hillslope (Figure 6c). These are the ratios of the chemical denudation rate to the total denudation rate. For example, if $\theta_d = 0.5$, then half of all the soil produced on a hillslope is denuded chemically, whereas if $\Theta_{dl} = 0.5$, then the local lowering rate due to chemical denudation in rock equivalent units ($h S_v / \rho_\eta = h S_v / \tau_d \bar{\rho}_s$) is half of the local rate of soil production.

The apparent local rate of chemical denudation, r_{ca} , diverges from the actual local rate of chemical denudation, r_c , for several reasons; we explore two important mechanisms that lead to apparent chemical denudation rates that differ from the actual chemical denudation rates. The reasons that we explore are spatial variations in the mass loss rate due to chemical weathering (S_v) and spatial variations in the enrichment of the immobile phase at the soil-saprolite boundary (c_η). These mechanisms are studied using the simple but illustrative case of a steady state hillslope, which allows for analytic solution of equations (27)-(29). The effect of transient incision or deposition rates are also explored using non-steady state models.

4.1. Steady State Solution of the Two Phase Hillslope Model

For a hillslope that is in steady state, the time derivatives in equations (27)-(29) vanish. The governing equations then become:

$$-e^{-\hat{h}} = \hat{I}, \quad (33)$$

$$\frac{\partial \hat{\phi}}{\partial \hat{x}} = \frac{\theta_t}{\theta_L} (\tau_d \hat{I} - \hat{h} \hat{S}), \quad (34)$$

$$\hat{c} \frac{\partial \hat{\phi}}{\partial \hat{x}} + \hat{\phi} \frac{\partial \hat{c}}{\partial \hat{x}} = \frac{\theta_t}{\theta_L} \hat{c}_\eta \tau_d \hat{I}. \quad (35)$$

The dimensionless incision rate, \hat{I} , is constant in time, such that the dimensionless soil depth is also constant in time and space by equation (33). To close the system, we define the spatial distribution of dimensionless mass loss rate due to chemical weathering, \hat{S} , and the spatial distribution of the enrichment of the immobile phase at the soil-saprolite boundary, \hat{c}_η . Although the sediment flux law influences the surface topography ($\hat{\zeta}$), slope ($\partial \hat{\zeta} / \partial \hat{x}$) and curvature ($\partial^2 \hat{\zeta} / \partial \hat{x}^2$), it does not influence the spatial distribution of the enrichment of the immobile phase on the hillslope (\hat{c}). This is shown in the solution to equation (35) presented later in this section. For the analysis of the steady state case, the simplest possible spatial variations of the dimensionless mass loss rate due to chemical weathering, \hat{S} , and the dimensionless concentration of the immobile phase at the base of the soil, \hat{c}_η , are assumed; they are approximated by linear functions (we consider more complex spatial variations in Appendix A):

$$\hat{S} = \chi (1 - \hat{x}) + \hat{S}_{divide}, \quad (36)$$

$$\hat{c}_\eta = \sigma (1 - \hat{x}) + \hat{c}_{\eta divide}, \quad (37)$$

where χ and σ (dimensionless) describe the variation of \hat{S} and \hat{c}_η as a function of space and the subscript *divide* indicates the value of the parameter at the hillslope divide. Recall that \hat{S} is negative if mass is lost to chemical weathering, so if χ is negative the dissolution rate increases downslope. If σ is positive, then the enrichment of the immobile phase at the soil-saprolite boundary increases downslope. No flux passes through the divide ($\hat{\phi}|_{\hat{x}=1} = 0$), whose location is at $\hat{x} = 1$. At the divide, the enrichment of the immobile phase in the soil is set by the ratio of chemical to total denudation at the divide and the enrichment of the immobile element at the soil-saprolite boundary at the divide:

$$\hat{c}|_{\hat{x}=1} = \hat{c}_{\eta divide} \left(1 - \frac{\hat{h} \hat{S}_{divide}}{\hat{I} \tau_d} \right)^{-1}. \quad (38)$$

Inserting equation (37) into equation (35) yields an ordinary differential equation whose solution, given the constant boundary condition described by equation (38) and the no flux condition at the divide, is:

$$\hat{c} = \frac{\theta_t \hat{I} \tau_d}{2 \theta_L} \frac{(\hat{x} - 1) \left[2 \hat{c}_{\eta divide} + \sigma (1 - \hat{x}) \right]}{2 \hat{\phi}}. \quad (39)$$

Similarly, the flux as a function of space may be solved by inserting equation (36) into equation (34) and integrating:

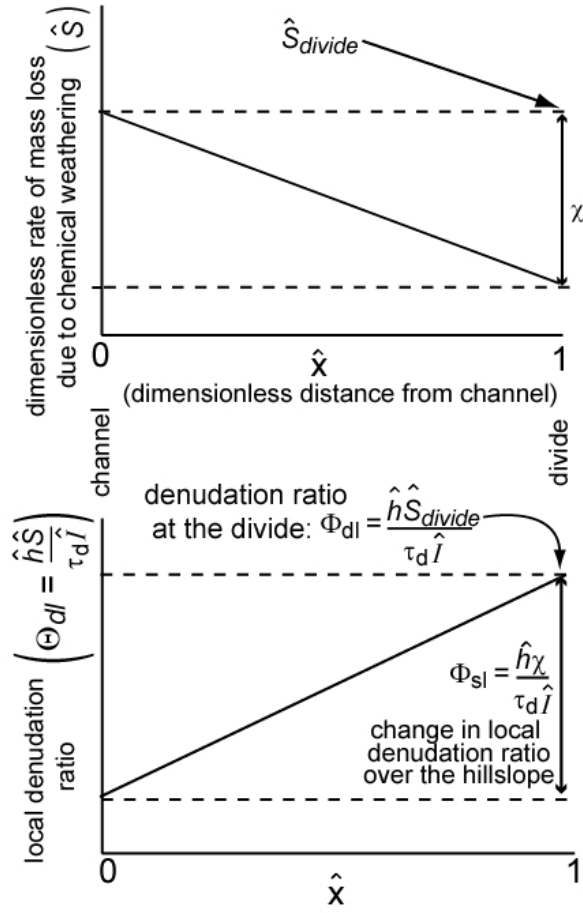


Figure 7. Schematic showing **a.** linear variation in space of the dimensionless mass loss rate due to chemical weathering (\hat{S}) and its relationship to the spatial variation in the local denudation ratio (Θ_{dl}).

$$\hat{\phi} = \frac{\theta_t}{2\theta_L} (\hat{x} - 1) \left[2\hat{I}\tau_d - \hat{h}(\chi(\hat{x} - 1) + 2\hat{S}_{divide}) \right]. \quad (40)$$

Equations (39) and (40) may be combined and simplified to yield the steady state solution for the enrichment of the immobile phase in the soil:

$$\hat{c} = \frac{\sigma(1 - \hat{x}) + 2\hat{c}_{\eta divide}}{2(1 - \Phi_{dl}) + \Phi_{sl}(\hat{x} - 1)} \quad (41)$$

where

$$\Phi_{dl} = \frac{\hat{h} \hat{S}_{divide}}{\hat{I} \tau_d}, \quad \Phi_{sl} = \frac{\hat{h} \chi}{\hat{I} \tau_d}. \quad (42a, b)$$

The ratios Φ_{dl} and Φ_{sl} represent the local denudation ratio at the divide and the change in the local denudation ratio over the length of the hillslope (Figure 7). In the steady state case where \hat{S} is described by equation (36) the local denudation ratio, Θ_{dl} , is:

$$\Theta_{dl} = \Phi_{sl} (1 - \hat{x}) + \Phi_{dl}. \quad (43)$$

If the chemical denudation rate increases downslope, then Φ_{sl} is positive. The chemical depletion fraction (CDF) may be calculated by inserting equations (37) and (41)

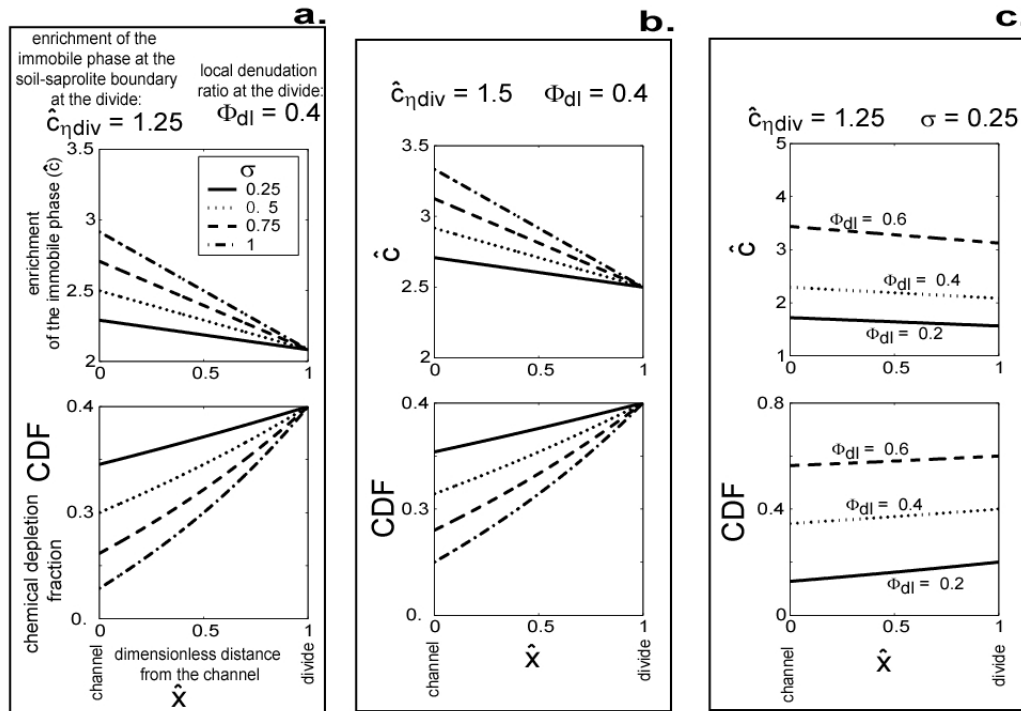


Figure 8. Plots of enrichment of the immobile phase in the soil (\hat{c}) and the chemical depletion fraction (CDF) for steady state solutions of the two phase hillslope system where there is no spatial variation in the local chemical denudation rate ($\Phi_{sl} = 0$). Legend in box **a.** applies to all plots in **a.** and **b.**

into equation (31). Several enrichment profiles and the corresponding CDF profiles are shown in Figures 8 and 9. In Figure 8, the enrichment of the immobile phase in the soil-saprolite interface increases downslope although the local denudation ratio does not vary in space. In Figures 9, the enrichment of the immobile phase at the base of the soil, \hat{c}_η , is constant in space and the local denudation ratio increases downslope (e.g., greater chemical weathering rates downslope). If $\sigma = 0$, the chemical depletion fraction is not a function of the enrichment of the immobile phase at the soil-saprolite boundary at the divide (the plots of the CDF in Figures 9a and 9b are identical). When the enrichment of the immobile phase at the base of the soil (\hat{c}_η) varies linearly in space, the downslope variation in the dimensionless concentration of the immobile phase in the soil (\hat{c}) is

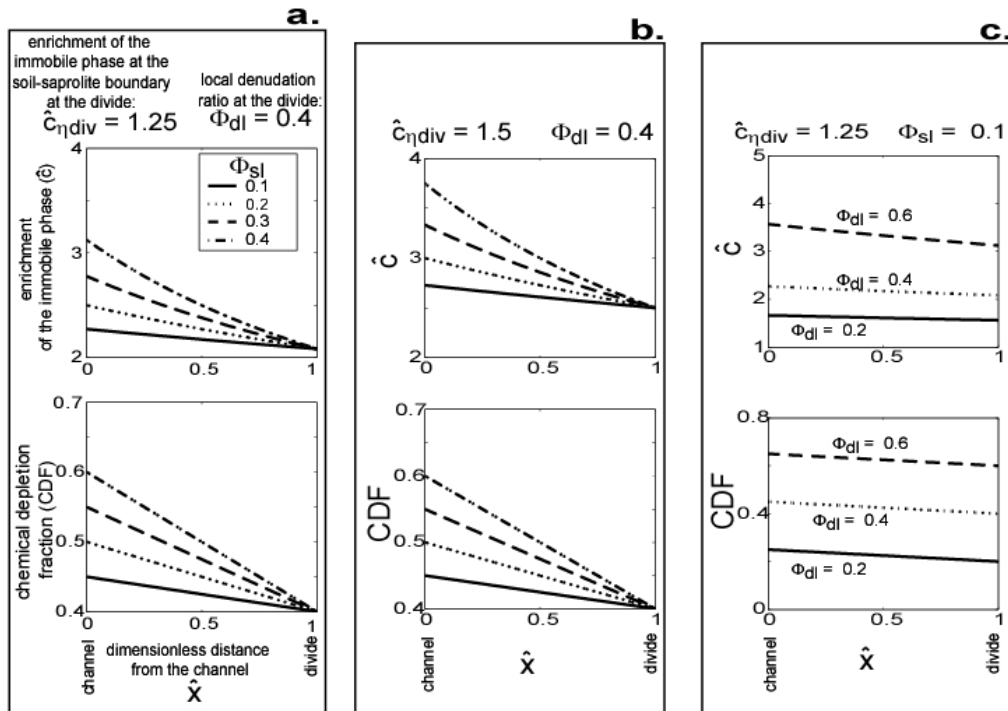


Figure 9. Plots of enrichment of the immobile phase in the soil (\hat{c}) and the chemical depletion fraction (CDF) for steady state solutions of the two phase hillslope system where there is no spatial variation in the enrichment of the immobile phase at the soil-saprolite boundary ($\sigma = 0$). Legend in box **a.** applies to all plots in **a.** and **b.**

linear, whereas when the local denudation ratio (Θ_{dl}) varies linearly, the downslope variation in the enrichment of the immobile phase, \hat{c} , is nonlinear.

While both of the sets of solutions represent an increase in chemical weathering downslope, with the first set having increased weathering in the saprolite, and the second having increased rate of chemical denudation in the soil, the resulting plots of the chemical depletion fraction (CDF) vary significantly. In the first set (Figure 8) the CDF decreases downslope, whereas in the second set the CDF increases downslope. The decrease in the chemical depletion fraction as one moves downslope in Figure 8 highlights the fact that on hillslopes with spatially varying enrichment ratios of the immobile phase at the soil-saprolite boundary, an estimate of the denudation ratio based on the CDF will not exactly match the true denudation ratio. In the case of Figure 8, the local denudation ratio is the same everywhere on the slope, but the CDF varies in space

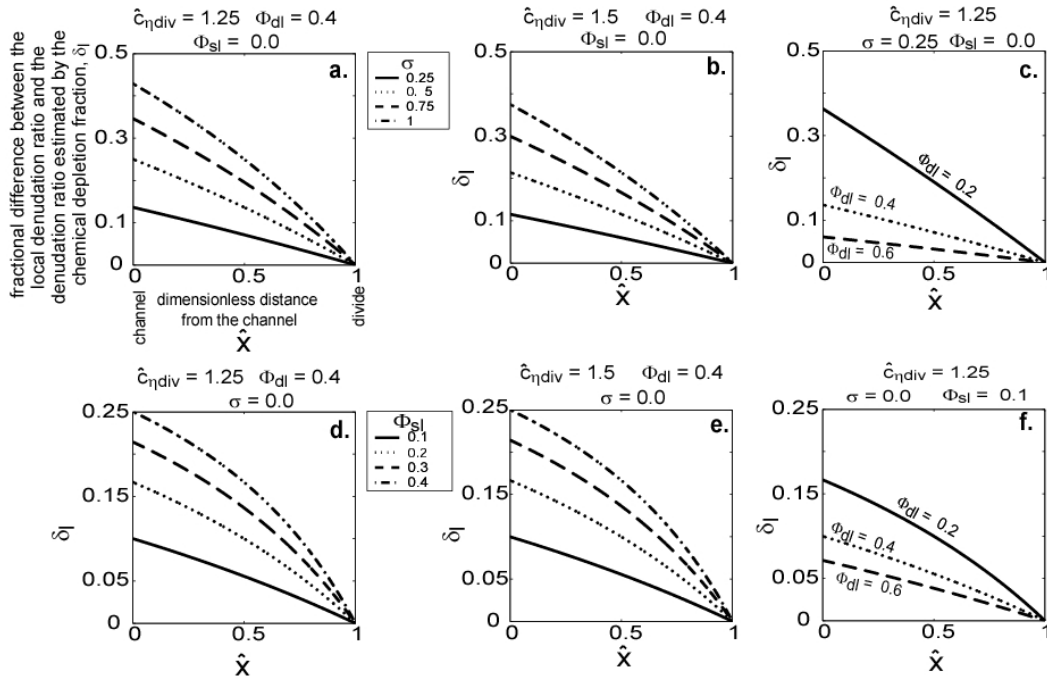


Figure 10. Normalized difference between the true local ratio of chemical to total denudation rate (Θ_{dl}) and this ratio estimated using the chemical depletion fraction (CDF).

because soil is being transported from upslope that is less enriched in the immobile phase due to the spatial variation in the enrichment of the saprolite.

The difference between the apparent denudation ratio (as quantified by the CDF) and the actual denudation ratio (set by the dimensionless mass loss rate due to chemical weathering, \hat{S}) may be quantified using equations (36) and (41). The fractional difference between the true local denudation ratio (Θ_{dl}) and the denudation ratio estimated by the CDF, which we call δ_l , is:

$$\delta_l = \frac{\Theta_{dl} - CDF}{\Theta_{dl}}. \quad (44)$$

Figure 10 plots δ_l for the scenarios plotted in Figures 8 and 9. If the rate of weathering is increasing downslope in either the soil-saprolite interface or in the soil itself, the chemical depletion fraction will underestimate the proportion of denudation caused by chemical weathering. Increasing either σ or χ , which increases the spatial variation in the enrichment of the immobile phase in the parent material (\hat{c}_η) and the dimensionless rate of mass loss due to chemical weathering (\hat{S}), respectively, increases the fractional difference in estimated and actual denudation ratios. In addition, hillslopes with lower overall denudation ratios (e.g., lower Φ_{dl}) will have larger discrepancies between the actual denudation ratio and the denudation ratio as estimated by the chemical depletion fraction. Thus, accounting for sediment transport and the spatial distribution of the immobile phase in the saprolite is especially important in regions with low rates of chemical denudation relative to mechanical denudation, for example in arid regions.

The integrated denudation ratio, θ_d , which is the ratio between the hillslope averaged chemical denudation rate and the total denudation rate, may be calculated by:

$$\theta_d = \frac{\hat{h}}{\hat{I}\tau_d} \int_0^1 \hat{S} d\hat{x} = \Phi_{dl} + \frac{\Phi_{sl}}{2} \quad (45)$$

If one is interested in calculating the ratio between chemical and total denudation averaged over a basin, use of the chemical depletion fraction is attractive because of its relative simplicity. Here we test the appropriateness of estimating the denudation ratio (θ_d) on hillslopes where soil is transported downslope and that have spatially heterogeneous parent material or chemical denudation rates the denudation rates. We consider three cases where the denudation ratio is estimated using the chemical depletion fraction measured i) at the hillslope base ($\hat{x} = 0$), ii) midway between the hillslope base and the divide ($\hat{x} = 0.5$), and at the divide ($\hat{x} = 1$). The fractional difference between the integrated denudation ratio and the denudation ratio estimated by the chemical depletion fraction, which we call δ_I , is

$$\delta_I = \frac{\theta_d - CDF}{\theta_d}. \quad (47)$$

A particular case of δ_I is when the enrichment at the soil-saprolite interface is spatially homogeneous ($\sigma = 0$). In this case, the error in the integrated denudation ratio estimated by the CDF is

$$\delta_I = \frac{\Phi_{sl} \hat{x}}{\Phi_{sl} + 2 \Phi_{dl}}. \quad (48)$$

Equation (48) demonstrates that if the parent material has a homogenous chemical composition, the chemical depletion fraction will accurately predict the denudation ratio

(θ_d , which is the ratio of the chemical denudation rate to the total denudation rate) at the

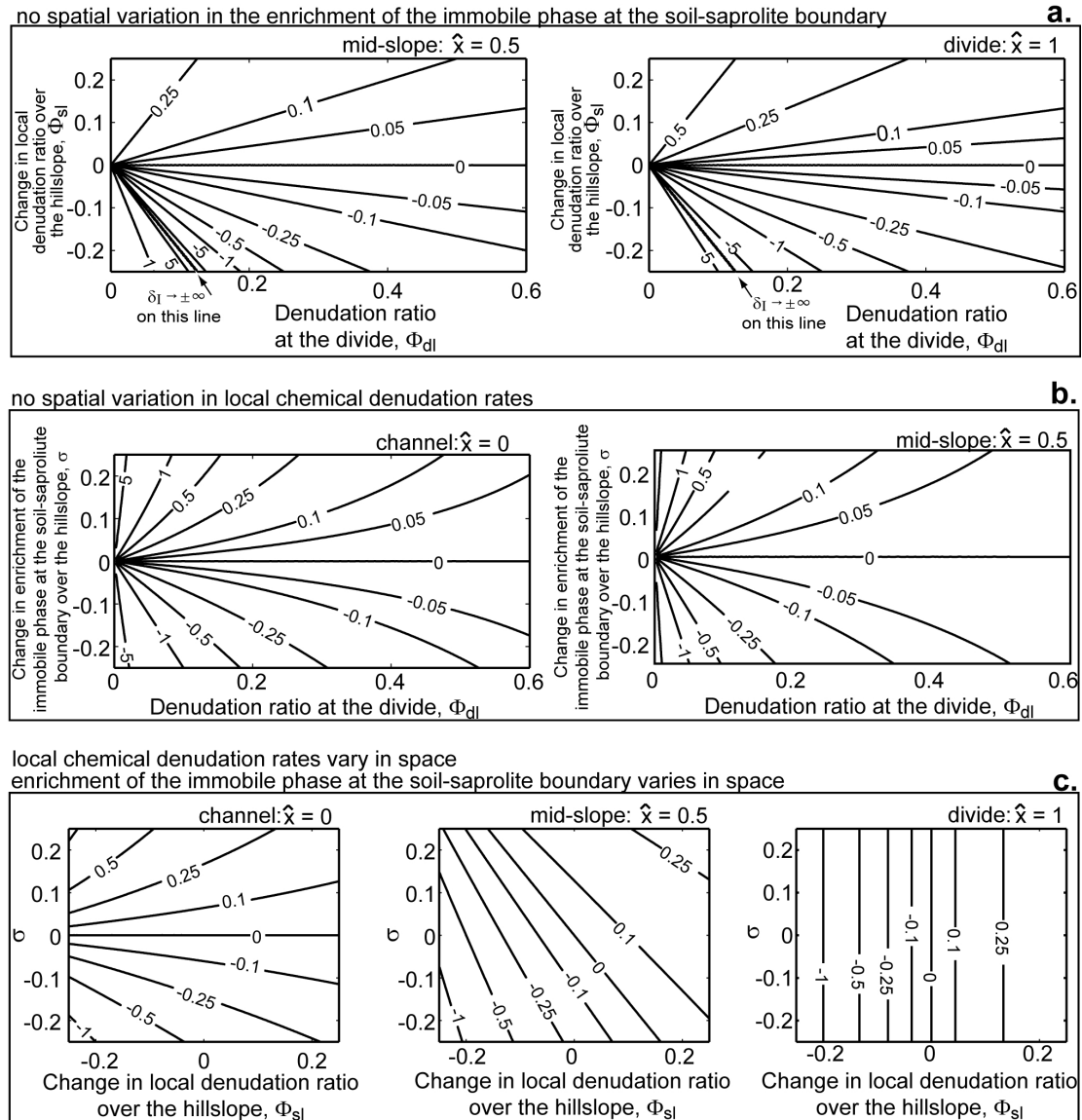


Figure 11. Contour plots of the fractional difference between the integrated denudation ratio and the denudation ratio estimated by the chemical depletion fraction (e.g., all plots show contours of $\delta_1 = (\theta_d - CDF)/\theta_d$). In all plots the enrichment of the immobile phase at the soil-saprolite boundary at the divide is equal to 1.25 ($\hat{c}_{ndiv} = 1.25$). Each individual plot shows contours of δ_1 at hillslope positions indicated above the plots (e.g., at the divide, mid-slope, or at the channel). **a.** Plots show hillslopes where the spatial variation in the enrichment of the immobile element at the soil-saprolite boundary does not vary in space ($\sigma=0$). **b.** Plots show hillslopes where the spatial variation in the local denudation ratio does not vary in space ($\Phi_{sl} = 0$). **c.** Plots show hillslopes where both the local denudation ratio and the enrichment of the immobile element at the soil-saprolite boundary vary in space. In these plots the denudation ratio at the divide, Φ_{dl} , is 0.2.

base of the hillslope. On the other hand, if chemical denudation rate does not vary in space (e.g., $\Phi_{sl} = 0$), the chemical depletion fraction will accurately predict the denudation ratio at the divide. The fractional difference between the integrated denudation ratio and the denudation ratio estimated by the chemical depletion fraction (δ_1) is plotted for a range of parameter values in Figure 11. For hillslopes that experience low chemical denudation rates as a proportion of the total denudation rate (e.g., low values of Φ_{dl}), the fractional difference between the denudation ratio estimated by the chemical depletion fraction and the true denudation ratio can exceed 25%. In landscapes where chemical denudation makes up a larger proportion of the total denudation, the denudation ratio estimated by the chemical depletion fraction is expected to differ from the true denudation ratio by less than 10% if spatial variations in the chemical denudation rate are small (Figure 11).

4.2. Quantifying the Changes in the Concentration of the Immobile Phase Related to Transient Incision or Deposition

If the lowering (or deposition) rate (\hat{I}) at the base of the hillslope changes, both the spatial distribution the chemical denudation rate and of the enrichment of the immobile phase may be affected. Consider a hillslope that is initially at steady state with a stream at its lower boundary incising at a rate of I_0 . The stream then experiences a step change in its incision rate, to a rate I . This causes soil to either be evacuated (if $I < I_0$, recall I takes a negative value for incision) or accumulate (if $I > I_0$) on the hillslope. How do chemical denudation rates respond? A simple example would be if the chemical denudation rates did not change when total denudation rates change. In this case, if the incision rate increased, then the soil would thin (see equation 15), and because the

chemical denudation rate is a product of the chemical weathering rate per unit volume and the soil thickness (see equation 32), the chemical denudation rate would decrease as well. Conversely, under a depositional regime, the soil depth would increase and the proportion of the total denudation accounted for by chemical weathering would increase.

Riebe et al. [2001] found that in catchments in the Sierra Nevada of California, the proportion of the total denudation rate due to chemical weathering did not change over a variety of total denudation rates. In hillslopes that have a constant denudation ratio, transient changes in incision rates will not lead to changes in the spatial distribution of the concentration of the chemically immobile phase, because any increase in the supply of fresh material, which is more susceptible to weathering [*White and Brantley* 2003], will be compensated by an increase in dissolution of the soluble phases in the soil.

White and Brantley [2003] noted that the age of minerals was of fundamental significance in determining the weathering rate, as fresh minerals weather many orders of magnitude faster than minerals that have been exposed to water for long periods of time. *Riebe et al.* [2001] argue that exposure of fresh mineral surfaces in faster eroding soils is one of the causes of the trend in which landscapes that are eroding more quickly have greater rates of chemical denudation, and as we will demonstrate below faster soil production is coupled to younger soil particles. Because soil age and chemical weathering rates may be linked, spatial variations in the age of soil particles may also influence the spatial distribution of weathering rates [e.g., *Green et al.* 2004].

Given the potential importance of soil particles ages in determining the rate of chemical weathering in the soil, we present here an analysis of both mean soil particle ages and the distribution of soil particle ages. We define soil particle age as the time

elapsed since the particle has been entrained into the mechanically active soil layer. For a “box” of hillslope soil with downslope dimension L , transverse dimension Y , and depth h , if the soil depth does not vary in time, then one way to define a mean residence time, T_R , of mass moving from bedrock into and through the soil is:

$$T_R = \frac{V}{I} = \frac{\bar{\rho}_s h L Y}{\rho_r p_\eta L Y} = \frac{h}{\tau_d p_\eta}. \quad (49)$$

Here, $V = hLY$ is the volume of the soil box, and $I = p_\eta LY$ is the steady (volumetric) rate of input of mass to the soil box at steady state. *Small et al.* [1999] noted this relationship between particle residence time and soil production, although in their treatment it was assumed that there was no density difference between the soil and the parent material. This mean residence time, T_R , may also be considered a “turnover time,” that is, the time required to replace the volume V at an input rate I .

The volumetric flux $Q(x)$ ($L^3 T^{-1}$) (equivalent to $h\phi$) through hY at a downslope distance x is

$$Q(x) = Y \tau_d p_\eta x, \quad (50)$$

so the flux density $q(x)$ ($M L T^{-1}$) is $q(x) = \bar{\rho}_s v(x) = \bar{\rho}_s Q(x)/hY = \rho_r p_\eta x/h$, where $v = p_\eta \tau_d x/h$ ($L T^{-1}$) is the particle velocity. Thus, T_R may also be defined

$$T_R = \frac{x}{v(x)}. \quad (51)$$

It can be seen that T_R increases with x ; but so does the particle velocity $v(x)$, such that T_R remains constant, as in equation (49).

The coordinate x above is Eulerian. Momentarily consider x from a Lagrangian

perspective, such that it denotes the position of a soil particle, in which case $v = dx/dt$, and

$$\frac{dx}{dt} = \frac{x}{T_R}. \quad (52)$$

Separating variables and integrating,

$$x = x_0 e^{\frac{t}{T_R}}, \quad (53)$$

where x_0 is the initial position of the particle, and $0 \leq x_0 \leq x$.

For the soil box with upslope and downslope sides at $x = 0$ and $x = \lambda$, respectively, particles “entering” the soil (from bedrock) are uniformly distributed between these limits. That is, at any instant, $0 \leq x_0 \leq \lambda$ with equal probability. The probability density function $f(x_0)$ of initial positions x_0 is thus

$$f(x_0) = \frac{1}{\lambda}. \quad (54)$$

Now, let τ denote the (travel) time that it takes a particle to move from its initial position x_0 to position $x = \lambda$, and let μ_τ denote the (ensemble) average time that particles reside in the soil box before reaching λ (whence they leave the box). With these definitions we rewrite equation (53) as

$$\lambda = x_0 e^{\frac{\tau}{T_R}} \quad (55)$$

and, for reference below, rearrange this to $x_0 = \lambda \exp(-\tau/T_R)$ noting that $\partial x_0 / \partial \tau = -(\lambda/T_R) \exp(-\tau/T_R)$. The probability density function $p(\tau)$ of travel times τ is defined by $p(\tau)$

$= f(x_0) | \partial x_0 / \partial \tau | :$

$$p(\tau) = \frac{1}{T_R} e^{-\frac{\tau}{T_R}}. \quad (56)$$

This is the exponential distribution with average $\mu_\tau = T_R$ and variance $\sigma^2 = T_R^2$. Thus, travel times τ are “mostly” short, with the probability decreasing exponentially with increasing travel time. Whereas the starting positions x_0 are uniformly distributed between 0 and λ , speeds increase with x , so travel times are disproportionately shortened.

In the steady state case, therefore, no spatial variation of the mean age of the particles occurs (equation 49), so if the age of the soil particles is the dominant factor in determining the chemical denudation rate, no spatial variation in the chemical denudation rate occurs. If, however, the incision at the base of the hillslope changes, then the age of the particles must adjust to the new conditions, leading to spatial variations in the soil age (Figure 12), and thus spatial variations in the chemical denudation rate. If the incision rate increases (Figure 12a), then in the time before the hillslope approaches its new steady state condition the soil will have lower mean soil ages near the base of the hillslope than at the divide. If the particle age drives the chemical denudation rate, this means that if the incision rate has recently increased, then the chemical denudation rate will increase downslope. Conversely, if the incision rate slows (Figure 12b), then soil near the base of the hillslope will be older than the soil upslope, and the chemical denudation rate will decrease downslope if soil age is the dominant factor controlling the chemical denudation rate.

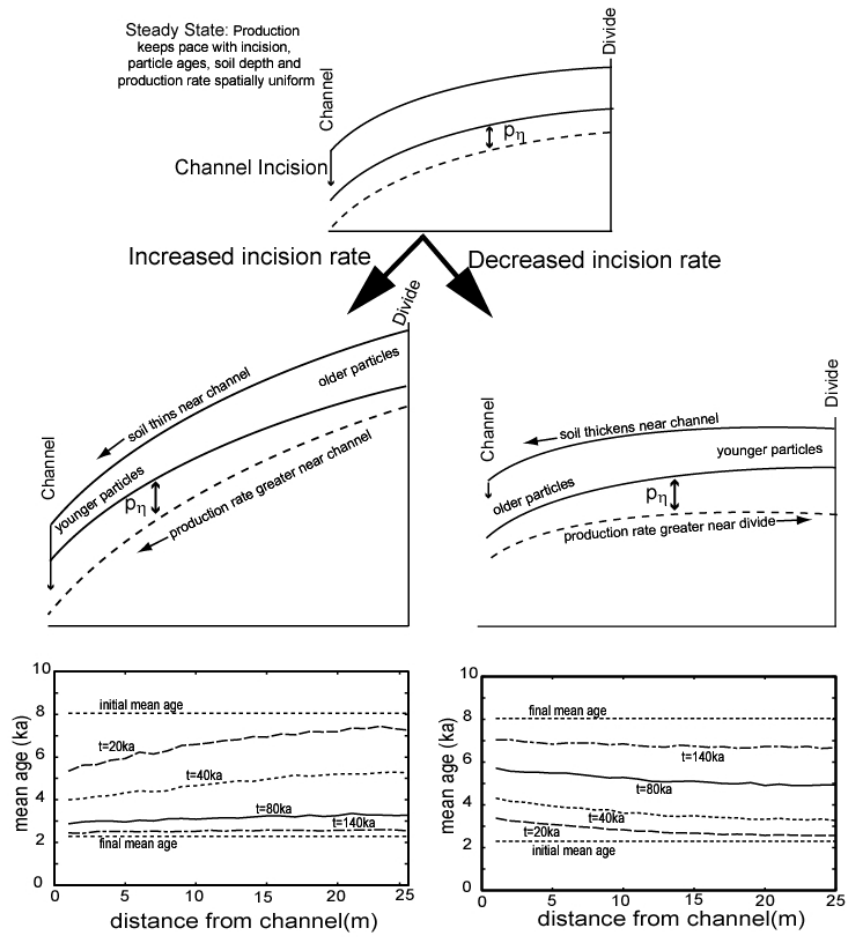


Figure 12. Diagram showing the response of a hillslope to increasing or decreasing incision rates. Bottom two figures show the calculated mean age of soil particles in thousands of years as a function of position. Parameter values are $W_0 = 2.5 \times 10^{-4} \text{ m yr}^{-1}$ and $\gamma = 0.5 \text{ m}$, $D = 0.01 \text{ m}^2 \text{ yr}^{-1}$. The hillslopes are at steady state for an initial incision rate I_0 at $t=0$, then the incision rate changes to incision rate I . The lines labeled ‘initial’ and ‘final’ mean age are theoretical values calculated with equation (49). Between the steady solutions are the mean age of the soil particles as a function of hillslope position, whose labels indicate the time elapsed after the change in incision rate. Particle ages are calculated by a stochastic numerical model that randomly selects discrete particles to move downslope each timestep; the number of particles moving is proportional to the sediment flux. The stochastic nature of the model causes the variance about the trend in the mean ages. The divide is at $x = 25 \text{ m}$. In the case of the increasing incision rate, $I_0 = 5.0 \times 10^{-5} \text{ m yr}^{-1}$ and $I = 1.0 \times 10^{-4} \text{ m yr}^{-1}$. In the case of the decreasing incision rate: $I_0 = 1.0 \times 10^{-4} \text{ m yr}^{-1}$ and $I = 5.0 \times 10^{-5} \text{ m yr}^{-1}$.

5. Conclusions

We have derived mass conservation equations that can be used to predict

concentrations of a chemically immobile phase in a hillslope soil. Under simplifying assumptions that are relevant to certain field situations, the spatial distribution of the enrichment of this immobile phase can be solved analytically. Chemical denudation rates in a hillslope soil can be measured using the concentration of immobile elements, but the enrichment of these immobile elements are influenced by spatial variations in chemical denudation rates and the chemical composition of the material from which the soil is derived. These considerations cloud the use of elemental depletion factors and cosmogenic nuclide-base total denudation rates [e.g. *Riebe et al.*, 2001] in identifying the relationship between physical erosion and chemical weathering. Although the method of *Riebe et al.* [2001] may be inadequate in regions where the chemical denudation rate is only a small fraction of the total denudation rate, it is still useful in locations where the chemical denudation rate is a significant portion of the total denudation rate (e.g., >50%) and where sediment transport and spatial variations in chemical denudation rates only introduce small (<10%) errors in the chemical denudation rates estimated using the chemical depletion fraction of *Riebe et al.* [2001]. In regions where the chemical denudation rate is a significant proportion of the total denudation rate, spatially distributed measurements of the enrichment of immobile soil phases are required to accurately quantify the relationship between physical erosion and chemical weathering.

We also present several possible responses of chemical weathering rates in the soil such as the expected distribution of particle ages, to unsteady channel incision rates. Depositional parts of a hillslope system have locally greater particle ages, which might be expected to reduce the local rate of chemical denudation. These areas of deposition would also coincide with topographic hollows, however, where there is an increased

likelihood of groundwater flow, which might be expected to increase weathering. Using immobile minerals to quantify weathering rates in such locations of transient deposition could allow researchers to assess the relative importance of hydrology and particle exposure ages on the rate of chemical weathering in hillslope soils.

Appendix 1

Here we offer several solutions to the steady state equations (34) and (35) based on a variety of descriptions of the spatial variation in \hat{S} and $\hat{c}_\eta = 0$. The enrichment of the immobile phase at the soil-saprolite interface may be measured in the field and then fitted. We have proposed a linear approximation in the text, here we propose three additional fits to the saprolite enrichment:

$$\hat{c}_\eta = \hat{c}_{\eta divide} e^{\frac{\hat{x}-1}{\alpha_{ce}}}, \quad (\text{A1})$$

$$\hat{c}_\eta = \alpha_{cq} (\hat{x} - 1) + \beta_{cq} (\hat{x} - 1)^2 + \hat{c}_{\eta divide}, \quad (\text{A2})$$

$$\hat{c}_\eta = \alpha_{cp} (\hat{x} - 1)^{\beta_{cp}} + \hat{c}_{\eta divide}, \quad (\text{A3})$$

where α and β are fitting parameters, the subscript c denotes a fitting parameter for \hat{c}_η , and the subscripts e , q , and p denote parameters for the exponential, quadratic, and power law fits, respectively. The solutions to equation (35) for the three approximations given by equations (A1), (A2) and (A3) are:

$$\hat{c} = \frac{\alpha_{ce} \theta_i \tau_d}{\theta_L \hat{\phi}} \left(e^{\frac{\hat{x}-1}{\alpha_{ce}}} - 1 \right) \hat{c}_{\eta divide}, \quad (\text{A4})$$

$$\hat{c} = \frac{\theta_t \hat{I} \tau_d (\hat{x} - 1)}{6 \theta_L \hat{\phi}} \left[6 \hat{c}_{\eta divide} + \alpha_{cq} (\hat{x} - 1) (2 [\hat{x} - 1] + 3 \beta_{cq}) \right], \quad (A5)$$

$$\hat{c} = \frac{\theta_t \hat{I} \tau_d (\hat{x} - 1)}{(1 + \beta_{cp}) \theta_L \hat{\phi}} \left[\hat{c}_{\eta divide} (1 + \beta_{cp}) + \alpha_{cp} (\hat{x} - 1)^{\beta_{cp}} \right]. \quad (A6)$$

To close equations (A4-A6), $\hat{\phi}$ must be evaluated. To do this, a functional form of \hat{S} must be proposed. Again, we provide three examples: an exponential function, a quadratic function, and a power law function:

$$\hat{S} = \hat{S}_{divide} e^{\frac{\hat{x}-1}{\alpha_{se}}}, \quad (A7)$$

$$\hat{S} = \alpha_{Sq} (\hat{x} - 1) + \beta_{Sq} (\hat{x} - 1) + \hat{S}_{divide}, \quad (A8)$$

$$\hat{S} = \alpha_{Sp} (\hat{x} - 1)^{\beta_{Sp}} + \hat{S}_{divide}, \quad (A9)$$

where again α and β are fitting parameters, the subscript S denotes a fitting parameter for \hat{S} , and the subscripts e , q , and p denote parameters for the exponential, quadratic, and power law functions, respectively. These fits lead to solutions for equation (35):

$$\hat{\phi} = \frac{\theta_t}{\theta_L} \left[\hat{S}_{divide} \left(1 - e^{-\frac{\hat{x}-1}{\alpha_{se}}} \right) \alpha_{se} \hat{h} + (\hat{x} - 1) \hat{I} \tau_d \right], \quad (A10)$$

$$\hat{\phi} = \frac{\theta_t}{6 \theta_L} [1 - \hat{x}] \left[\left(6 \hat{S}_{divide} + [\hat{x} - 1] [2 \alpha_{Sq} (\hat{x} - 1) + 3 \beta_{Sq}] \right) \hat{h} - 6 \hat{I} \tau_d \right], \quad (A11)$$

$$\hat{\phi} = \frac{(1 - \hat{x}) \theta_t}{(1 + \beta_{Sp}) \theta_L} \left[\hat{S}_{divide} \hat{h} \left(1 + \frac{\alpha_{Sp}}{\beta_{Sp}} [\hat{x} - 1]^{\beta_{Sp}} + \beta_{Sp} \right) - (1 + \beta_{Sp}) \hat{I} \tau_d \right]. \quad (A12)$$

6. List of Symbols

–	Overbars denote depth integrated quantities
^	Carats denote dimensionless quantities
α	Fitting parameter (see Appendix B)
β	Fitting parameter (see Appendix B)
c_i	Concentration of phase i (dimensionless)
c_m, c_{im}	Concentration of the chemically mobile and immobile phases (dimensionless)
c_η, c_r	Concentration of the immobile phase at the soil-saprolite interface and in the bedrock (dimensionless)
\hat{c}	Dimensionless enrichment relative to the unweathered parent material of the immobile phase in the soil
\hat{c}_η	Dimensionless enrichment relative to the unweathered parent material of the immobile phase in the saprolite
$\hat{c}_{\eta divide}$	Dimensionless enrichment relative to the unweathered parent material of the immobile phase in the saprolite at the divide
χ	Increase in \hat{c} as a function of position
CDF	chemical depletion fraction (dimensionless)
δ_l	Local error in the denudation ratio
δ_I	Integrated error in the denudation ratio

d_ζ	Deposition rate of sediment at soil surface ($L T^{-1}$)
D	Sediment diffusivity ($L^2 T^{-1}$)
η	Elevation of soil-bedrock interface (L)
η_0	Elevation of soil-bedrock interface at $x = 0$ (L)
η_{bl}	Elevation of soil-bedrock interface relative to base level (L)
$\hat{\eta}$	Dimensionless elevation of soil-bedrock interface relative to base level
$\phi, \hat{\phi}$	Dimensional ($L^2 T^{-1}$) and dimensionless sediment flux
Φ_{dl}	Local denudation ratio at the divide (dimensionless)
Φ_{sl}	Change in local denudation ratio over the hillslope (dimensionless)
γ	Soil production decay lengthscale (L)
h, \hat{h}	Soil depth (L) and dimensionless soil depth, respectively
I, \hat{I}	Dimensional ($L T^{-1}$) and dimensionless incision rate, respectively $I = \partial\zeta_0 / \partial t$
K	Sediment dispersion coefficient ($M L^{-1} T^{-1}$)
λ	Length of the hillslope (half the distance between channels) (L)
m_i, m_{tot}	mass of phase i and total mass of soil (M)
p_η	Soil production rate ($L T^{-1}$)
$\bar{\rho}_s$	Depth averaged dry bulk density of hillslope soil ($M L^{-3}$)
ρ_η	Dry bulk density of parent material ($M L^{-3}$)
r_{ca}, r_c	Apparent and actual local rate of chemical denudation ($L T^{-1}$)
R_{ca}, R_c	Apparent and actual integrated rate of chemical denudation ($L T^{-1}$)
r_T	Local rate of total denudation ($L T^{-1}$)
R_T	Integrated rate of total denudation ($L T^{-1}$)

S_v	Chemical denudation and deposition rate per unit volume ($M L^{-3} T^{-1}$)
\overline{S}_v	Depth averaged chemical denudation rate per unit volume ($M L^{-3} T^{-1}$)
\hat{S}	Dimensionless chemical denudation rate
\hat{S}_{divide}	Dimensionless chemical denudation rate at the divide
σ	Change in \hat{S} as a function of distance from the divide
S_c	Critical slope (dimensionless)
θ_L	Length ratio (dimensionless)
θ_t	Time ratio (dimensionless)
Θ_{dl}	Local denudation ratio
θ_d	Integrated denudation ratio
θ_{da}	Apparent integrated denudation ratio
τ_d	Density ratio (dimensionless)
T_p	Production timescale (T)
T_D	Diffusive (or relaxation) timescale (T)
T_R	Mean age of soil particles (T)
$\overline{v}_x, \overline{v}_y$	Depth averaged sediment velocity in the x and y direction ($L T^{-1}$)
W_0	Nominal rate of soil production ($L T^{-1}$)
x, \hat{x}	Dimensional (L) and dimensionless distance from the channel
ζ	Elevation of soil surface (L)
ζ_0	Elevation of soil surface at $x = 0$ (L)
ζ_{bl}	Elevation of soil surface relative to base level (L)
$\hat{\zeta}$	Dimensionless elevation of soil surface relative to base level

7. References

- Ahnert, F. (1976), Brief description of a comprehensive three-dimensional process-response model of landform development, *Z. Geomorph. Suppl. Bd.*, 25, 29-49.
- Anderson, S.P., W.E. Dietrich, and G.H. Brimhall (2002), Weathering Profiles, Mass-Balance Analysis, and Rates of Solute Loss: Linkages Between Weathering and Erosion in a Small, Steep Catchment, *Geological Society of America Bulletin*, 114 (9), 1143-1158.
- Anderson, R.S. (2002), Modeling the tor-dotted crests, bedrock edges, and parabolic profiles of high alpine surfaces of the Wind River Range, Wyoming, *Geomorphology*, 46 (1-2), 35-58.
- Andrews, D.J., and R.C. Bucknam (1987), Fitting Degradation of Shoreline Scarps by a Nonlinear Diffusion-Model, *Journal of Geophysical Research-Solid Earth and Planets*, 92 (B12), 12857-12867.
- April, R., R. Newton, and L.T. Coles (1986), Chemical-Weathering in 2 Adirondack Watersheds - Past and Present-Day Rates, *Geological Society of America Bulletin*, 97 (10), 1232-1238.
- Armstrong, A.C. (1976), A three-dimensional simulation of slope forms, *Z. Geomorph. Suppl. Bd.*, 25, 20-28.
- Berner, R.A., A.C. Lasaga, and R.M. Garrels (1983), The Carbonate-Silicate Geochemical Cycle and Its Effect on Atmospheric Carbon-Dioxide over the Past 100 Million Years, *American Journal of Science*, 283 (7), 641-683.
- Birkeland, P.W. (1999), *Soils and Geomorphology*, 430 pp., Oxford University Press, Oxford.
- Brimhall, G.H., and W.E. Dietrich (1987), Constitutive Mass Balance Relations Between Chemical- Composition, Volume, Density, Porosity, and Strain in Metasomatic Hydrochemical Systems - Results on Weathering and Pedogenesis, *Geochimica Et Cosmochimica Acta*, 51 (3), 567-587.
- Brimhall, G.H., O.A. Chadwick, C.J. Lewis, W. Compston, I.S. Williams, K.J. Danti, W.E. Dietrich, M.E. Power, D. Hendricks, and J. Bratt (1992), Deformational Mass-Transport and Invasive Processes in Soil Evolution, *Science*, 255 (5045), 695-702.
- Carson, M.A., and M.J. Kirkby (1972), *Hillslope Form and Process*, 475 p. pp., Cambridge University Press, Cambridge.
- Chadwick, O.A., G.H. Brimhall, and D.M. Hendricks (1990), From a black box to a gray

- box - a mass balance interpretation of pedogenesis, *Geomorphology*, 3, 369-390.
- Culling, W.E.H. (1960), Analytical Theory of Erosion, *Journal of Geology*, 68 (3), 336-344
- Culling, W.E.H. (1963), Soil Creep and the Development of Hillside Slopes, *Journal of Geology*, 71 (2), 127-161.
- Fernandes, N.F., and W.E. Dietrich (1997), Hillslope evolution by diffusive processes: The timescale for equilibrium adjustments, *Water Resources Research*, 33 (6), 1307-1318.
- Furbish, D.J., and S. Fagherazzi (2001), Stability of Creeping Soil and Implications for Hillslope Evolution, *Water Resources Research*, 37 (10), 2607-2618.
- Gabet, E.J. (2000), Gopher Bioturbation: Field Evidence for Non-Linear Hillslope Diffusion, *Earth Surface Processes and Landforms*, 25 (13), 1419-1428.
- Gabet, E.J., O.J. Reichman, and E.W. Seabloom (2003), The Effects of bioturbation on soil processes and sediment transport, *Annual Reviews of Earth and Planetary Science*, 31, 249-73.
- Gilbert, G.K. (1877), Report on the geology of the Henry Mountains: U.S. Geographical and Geological Survey of the Rocky Mountain Interior Region, pp. 160, U.S. Government Printing, Washington D.C.
- Gilbert, G.K. (1909), The convexity of hilltops, *Journal of Geology*, 17, 344-350.
- Green, E.G., W.E. Dietrich, and J.F. Banfield (2003), The Quantification of mass loss via geochemical weathering in hillslope processes, *Eos Trans. AGU, Fall Meet. Suppl.*, 84 (46), Abstract H51E-1128.
- Green, E.G., W.E. Dietrich, and J.F. Banfield (2004), Chemical weathering processes and mass losses on an actively eroding hill slope, *Eos Transactions*, 85 (47), H41H-04.
- Heimsath, A.M., W.E. Dietrich, K. Nishiizumi, and R.C. Finkel (1997), The Soil Production Function and Landscape Equilibrium, *Nature*, 388 (6640), 358-361.
- Heimsath, A.M., W.E. Dietrich, K. Nishiizumi, and R.C. Finkel (1999), Cosmogenic Nuclides, Topography, and the Spatial Variation of Soil Depth, *Geomorphology*, 27 (1-2), 151-172.
- Heimsath, A.M., J. Chappell, W.E. Dietrich, K. Nishiizumi, and R.C. Finkel (2000), Soil Production on a Retreating Escarpment in Southeastern Australia, *Geology*, 28 (9), 787-790.

- Heimsath, A.M., W.E. Dietrich, K. Nishiizumi, and R.C. Finkel (2001), Stochastic Processes of Soil Production and Transport: Erosion Rates, Topographic Variation and Cosmogenic Nuclides in the Oregon Coast Range, *Earth Surface Processes and Landforms*, 26 (5), 531-552.
- Jyotsna, R., and P.K. Haff (1997), Microtopography as an indicator of modern hillslope diffusivity in arid terrain, *Geology*, 25 (8), 695-698.
- Kirchner, J.W., R.C. Finkel, C.S. Riebe, D.E. Granger, J.L. Clayton, J.G. King, and W.F. Megahan (2001), Mountain erosion over 10 yr, 10 k.y., and 10 m.y. time scales, *Geology*, 29 (7), 591-594.
- Kirkby, M.J. (1967), Measurement and Theory of Soil Creep, *Journal of Geology*, 75 (4), 359-378.
- Kirkby, M.J. (1971), Hillslope process-response models based on the continuity equation, *Institute of British Geographers Special Publication*, 3, 15-30.
- Kirkby, M.J. (1977), Soil Development Models as a Component of Slope Models, *Earth Surface Processes and Landforms*, 2 (2-3), 203-230.
- Kirkby, M.J. (1985a), A Basis for Soil-Profile Modeling in a Geomorphic Context, *Journal of Soil Science*, 36 (1), 97-121.
- Kirkby, M.J. (1985b), A model for the evolution of regolith-mantled slopes, in *Models in Geomorphology*, edited by M.J. Woldenberg, pp. 213-237, Allen and Unwin.
- Merritts, D.J., O.A. Chadwick, D.M. Hendricks, G.H. Brimhall, and C.J. Lewis (1992), The Mass Balance of Soil Evolution on Late Quaternary Marine Terraces, Northern California, *Geological Society of America Bulletin*, 104 (11), 1456-1470.
- Mudd, S.M., and D.J. Furbish (2004), The Influence of chemical denudation on hillslope morphology, *Journal of Geophysical Research*, 109 (F02001), doi:10.1029/2003JF000087.
- Mudd, S.M., and D.J. Furbish (2005), Lateral migration of hillcrests in response to channel incision in soil mantled landscapes, *Journal of Geophysical Research-Earth Surface*, in Press.
- Nezat, C.A., J.D. Blum, A. Klaue, C.E. Johnson, and T.G. Siccama (2004), Influence of landscape position and vegetation on long-term weathering rates at the Hubbard Brook Experimental Forest, New Hampshire, USA, *Geochimica Et Cosmochimica Acta*, 68 (14), 3065-3078.
- Raymo, M.E., and W.F. Ruddiman (1992), Tectonic Forcing of Late Cenozoic Climate, *Nature*, 359 (6391), 117-122.

- Riebe, C.S., J.W. Kirchner, D.E. Granger, and R.C. Finkel (2001), Strong tectonic and weak climatic control of long-term chemical weathering rates, *Geology*, 29 (6), 511-514.
- Riebe, C.S., J.W. Kirchner, and R.C. Finkel (2003), Long-term rates of chemical weathering and physical erosion from cosmogenic nuclides and geochemical mass balance, *Geochimica Et Cosmochimica Acta*, 67 (22), 4411-4427.
- Riebe, C.S., J.W. Kirchner, and R.C. Finkel (2004a), Erosional and climatic effects on long-term chemical weathering rates in granitic landscapes spanning diverse climate regimes, *Earth and Planetary Science Letters*, 224 (3-4), 547-562.
- Riebe, C.S., J.W. Kirchner, and R.C. Finkel (2004b), Sharp decrease in long-term chemical weathering rates along an altitudinal transect, *Earth and Planetary Science Letters*, 218 (3-4), 421-434.
- Roering, J.J., J.W. Kirchner, and W.E. Dietrich (1999), Evidence for Nonlinear, Diffusive Sediment Transport on Hillslopes and Implications for Landscape Morphology, *Water Resources Research*, 35 (3), 853-870.
- Roering, J.J., J.W. Kirchner, and W.E. Dietrich (2001), Hillslope Evolution by Nonlinear, Slope-Dependent Transport: Steady State Morphology and Equilibrium Adjustment Timescales, *Journal of Geophysical Research-Solid Earth*, 106 (B8), 16499-16513.
- Roering, J.J. (2004), Soil creep and convex-upward velocity profiles: Theoretical and experimental investigation of disturbance-driven sediment transport on hillslopes, *Earth Surface Processes and Landforms*, 29 (13), 1597-1612.
- Small, E.E., R.S. Anderson, J.L. Repka, and R. Finkel (1997), Erosion rates of alpine bedrock summit surfaces deduced from in situ ^{10}Be and ^{26}Al , *Earth and Planetary Science Letters*, 150, 413-425.
- Small, E.E., R.S. Anderson, and G.S. Hancock (1999), Estimates of the Rate of Regolith Production Using Be-10 and Al-26 From an Alpine Hillslope, *Geomorphology*, 27 (1-2), 131-150.
- Stallard, R.F. (1995), Tectonic, Environmental, and Human Aspects of Weathering and Erosion - a Global Review Using a Steady-State Perspective, *Annual Review of Earth and Planetary Sciences*, 23, 11-39.
- Taylor, A., and J.D. Blum (1995), Relation between Soil Age and Silicate Weathering Rates Determined from the Chemical Evolution of a Glacial Chronosequence, *Geology*, 23 (11), 979-982.
- White, A.F., and S.L. Brantley (1995), Chemical weathering rates of silicate minerals: An overview, *Chemical Weathering Rates of Silicate Minerals*, 31, 1-22.

White, A., and S.L. Brantley (2003), The effect of time on the weathering of silicate minerals: why do weathering rates differ in the laboratory and field?, *Chemical Geology*, 202, 479-506.

Yoo, K., R. Amundson, A.M. Heimsath, W.E. Dietrich, and G.H. Brimhall (2004), The topographic control of chemical weathering in hillslope soils, *Eos Transactions*, 85 (47), H41H-05.

CHAPTER IV

LATERAL MIGRATION OF HILLCRESTS IN RESPONSE TO CHANNEL INCISION IN SOIL MANTLED LANDSCAPES

Abstract

We investigate lateral migration of hillcrests in response to vertical offsets or transient incision rates of channels bordering these hillcrests in soil mantled landscapes. For hillslopes undergoing sediment transport that is linearly proportional to the slope, the hillcrest offset distance is one quarter of the ratio of the vertical offset between the channels to the relief of the symmetric hillslope. If channels are downcutting at different rates, the speed of hillcrest migration will depend on the ratio of the downcutting rates and the density ratio, which is the ratio of the bulk density of the bedrock to the bulk density of the soil. The density ratio plays a fundamental role in determining the transient response of the hillcrest; lower density ratios lead to faster transient responses to changes in channel downcutting rates. Other parameters that affect the transient response of the hillcrest are the magnitude of transient differences in downcutting between the two channels, the time averaged incision rate, and a ratio of the elevation of the hillslope to a length that characterizes the decay in soil production with increasing soil thickness; different parameters will be important for different sediment flux laws. The profile of soil thickness reacts to transient changes in downcutting at a different rate than surface topography. Hillslopes experiencing transient channel downcutting may have surface topography that is symmetric about the hillcrest but will at the same time have a soil thickness profile that is asymmetric.

1. Introduction

Landscapes are dissected by drainage networks following periods of base level fall. It has been suggested [e.g., *Gilbert*, 1877; *Hack*, 1960] that after the landscape is fully dissected it will adjust to a condition in which the erosion rate averaged over the landscape will equal the rate of base level fall. There is field evidence that in areas of active tectonics, spatially averaged erosion rates equal the rock uplift rate [e.g., *Meigs et al.*, 1999; *Reneau and Dietrich*, 1991]. Field evidence also suggests that some drainage networks are stable over long periods of time in that the stream locations and profiles, and the locations of the drainage divides, do not vary significantly over time [*Bishop et al.*, 1985; *Young and McDougall*, 1993]. In some cases, however, there is evidence of drainage network change long after orogenesis. Postorogenic drainage network reorganization can occur through the migration of drainage divides [*Meyerhof*, 1972] or stream capture [*Harbor*, 1997; *Mather et al.*, 2000; *Zaprowski et al.*, 2001]. Drainage divide migration and stream capture may be due to transient changes in the rate of base level fall. Recent experimental results, however, suggest that even with a constant rate of base level fall drainage divides may migrate [*Hasbargen and Paola*, 2000]. This is in contrast to some numerical studies that have found that a constant rate of downcutting or uplift leads to stable channel and ridge networks [e.g., *Howard*, 1994; *Tucker and Bras*, 1998; *Willgoose et al.*, 1991]. *Pelletier* [2004], however, found that altering the flow routing algorithm of a landscape evolution model can lead to simulations that predict drainage divide migration, whereas *Densmore et al.* [1998] simulated migrating divides when stochastically driven landslides contributed to hillslope erosion..

In their experiments, *Hasbargen and Paola* [2000] found that while the basin

averaged erosion rate may be steady the local erosion rates of subbasins may be unsteady if not cyclic. Such locally transient erosion rates can lead to the migration of drainage divides (Figure 1). Channel incision rates that vary in space and time will lead to vertical offsets of the relative elevation of adjacent channels. The hillslopes that bound the drainage divide will react to the offsets over some delayed response time if the hillslope is undergoing creep [e.g., *Fernandes and Dietrich, 1997; Roering et al., 2001*], or nearly instantaneously if the hillslopes are at a critical slope; such hillslopes will respond to base

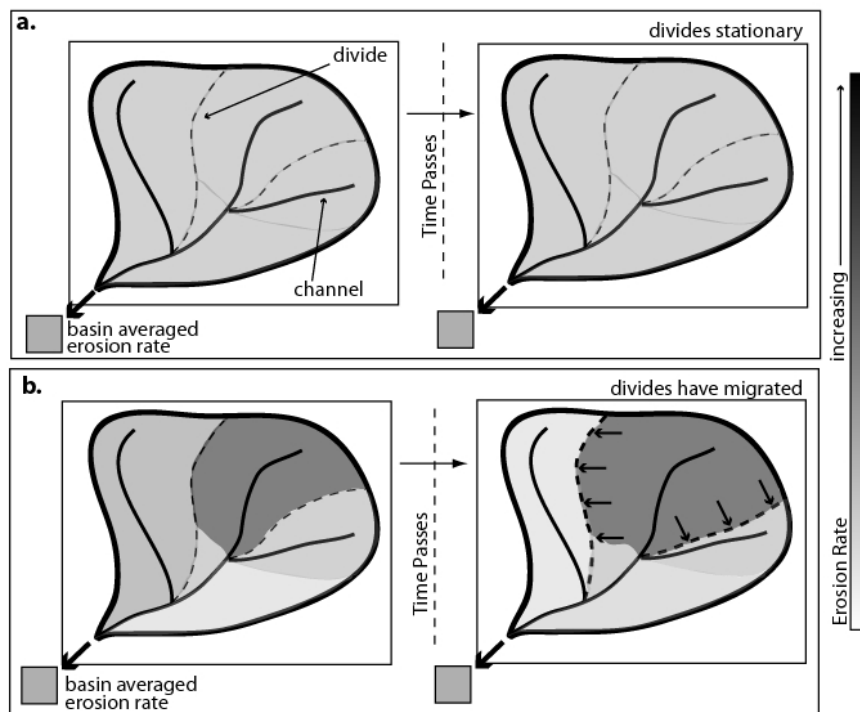


Figure 1. Two scenarios for erosion in a basin. The basin averaged erosion rate of both basins does not vary in time. In **a.**, the local erosion rates equal the basin averaged erosion rate, and the ridges are stationary. This is predicted by many numerical models for a case of constant downcutting at the basin outlet [e.g., *Howard, 1994*]. In **b.**, local erosion rates vary between subbasins, and divides can migrate, despite a constant rate of downcutting at the basin outlet. This has been observed in the laboratory setting [e.g., *Hasbargen and Paola, 2000*].

level fall with landsliding [e.g., *Burbank et al.*, 1996]. Whatever the response time, vertical offsets between adjacent channels will lead to the lateral migration of a drainage divide. If the drainage divide moves laterally, this will change the drainage area of the streams, thus changing the hydrology and sediment supply of the affected basins.

Field studies in tectonically quiescent regions have reported erosion rates in adjacent streams that vary by up to a factor of two [*Kirchner et al.*, 2001; *Matmon et al.*, 2003]. Others have used stream gradients and the stream power law to estimate spatially variable stream erosion rates in tectonically active regions. *Kobor and Roering* [2004] investigated stream gradients in the Oregon Coast Range and reported that local stream downcutting rates are spatially variable, although in the Oregon Coast Range it is thought that erosion rates are in equilibrium with uplift rates over large spatial scales [*Reneau and Dietrich*, 1991]. In addition, *Finlayson et al.* [2002] found that the erosion index, a metric that combines topographic and hydrologic data used to assess potential erosion rates, varies over several orders of magnitude across the Himalaya, despite the relatively uniform convergence of the Indian subcontinent.

Whereas a basin may be denuding at a constant rate averaged over geologic time, at shorter timescales stream incision is forced by various stochastic processes [e.g., *Benda and Dunne*, 1997; *Snyder et al.*, 2003; *Tucker*, 2004]. Because the stochastic forces (such as streamflow and sediment supply) controlling incision rates in bedrock channels may be nonlinear functions of drainage area, adjacent streams that have different drainage areas may experience time histories of downcutting events that are of different magnitude and frequency, causing local disequilibrium of erosion rates. Such local disequilibrium may force the migration of drainage divides if the signal of changing

incision rates can propagate up the hillslope and reach the divide. The likelihood that changes in channel downcutting rates will affect the divide in the case of a symmetric hillslope has been found to increase for variations in downcutting rates that have longer periods [*Furbish and Fagherazzi, 2001*].

Here we present analytical and numerical results of our investigations of the migration of drainage divides on 1-D hillslopes (which we refer to as hillcrests) under the conditions of vertical channel offsets and transient local incision rates. First, we develop and nondimensionalize the governing equations that describe conservation of mass on a hillslope. A numerical model is then used to solve these governing equations. We use the numerical model as a virtual laboratory [e.g., *Bras et al., 2003*] to explore the behavior of hillcrests in a number of different scenarios. These scenarios are selected to approximate natural conditions that have been hypothesized to lead to hillcrest migration [e.g., *Hasbargen and Paola, 2000; Mather et al., 2000; Smith and Bretherton, 1972*].

Analytical solutions are presented for specific instances of lateral hillcrest migration due to vertical channel offsets and differential channel downcutting rates. We then explore the nature of hillcrest migration on one-dimensional hillslopes that are subject to transient downcutting rates in the bounding streams, and which obey several different sediment flux laws. Two transient cases are investigated with a numerical model. The first set of model runs investigates the transient behavior of the hillcrest when knickpoints of an equal height pass through the two channels, separated by some time delay; a simplification of pulses of incision, manifested in knickpoints, that migrate through basins at different celerities [e.g., *Crosby and Whipple, 2005, in press*]. The second set of simulations tracks the migration of the hillcrest when the time averaged

downcutting rate is the same in both channels but the instantaneous rates vary in time with different amplitudes and frequencies.

2. A 1-D Model of Hillcrest Migration

2.1. Governing Equations

The basis for our hillcrest migration analysis is an equation for conservation of mass on a soil mantled hillslope, which is depth-averaged from the soil-bedrock interface to the soil surface. In one dimension, the equation is

$$\bar{\rho}_s \frac{\partial h}{\partial t} + \bar{\rho}_s \frac{\partial (h \bar{v}_x)}{\partial x} - \rho_\eta p_\eta = 0, \quad (1)$$

where h (L) is the soil thickness, ρ_s ($M L^{-3}$) is the dry bulk density of the soil, v_x ($L T^{-1}$) is the velocity of the sediment in the x -direction, ρ_η ($M L^{-3}$) is the density of the parent material, p_η ($L T^{-1}$) is the rate of bedrock lowering due to soil production, and the overbars denote depth-averaged quantities (Figure 2). Equation (1) is a version of the equation derived in *Mudd and Furbish* [2004] that contains the assumptions that there are no sources or sinks of mass in the soil (e.g., chemical denudation) and that the depth averaged dry bulk density is constant in time and spatially homogenous. The second assumption is reasonable for bioturbated soils, in which mechanical disturbances can loft soil to a constant porosity [*Brimhall et al.*, 1992]. We focus on hillslopes where diffusion-like sediment transport processes dominate (e.g., porous forested soils with little overland flow); we do not consider hillslopes where sediment flux due to overland flow plays a significant role.

The soil thickness, h , is defined as

$$h = \zeta - \eta, \quad (2)$$

where $\zeta(L)$ is the elevation of the soil surface and $\eta(L)$ is the elevation of the soil-bedrock boundary. The rate of soil production, p_η , has been found to be a function of the soil thickness,

$$p_\eta = W_0 e^{-\frac{h}{\gamma}}, \quad (3)$$

[e.g., *Heimsath et al.*, 1999] where W_0 ($L T^{-1}$) is the nominal rate of soil production when the soil thickness is zero and γ (L) is a length scale that characterizes the rate of decline in the soil production rate with increasing soil thickness.

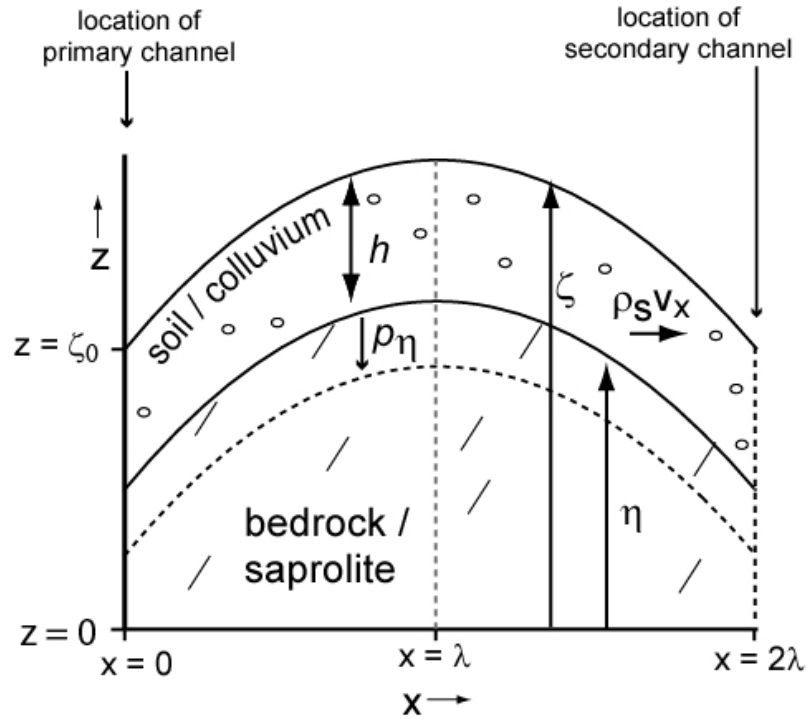


Figure 2. Schematic of the coordinate system. When incision rates in the primary and secondary equal and constant in time, the hillcrest is at $x = \lambda$.

Dynamic hillslope evolution is driven in part by incision at the base of the hillslope. We designate a coordinate system where the shape of the hillslope is measured relative to local base level (chosen as the elevation at the base of the hillslope):

$$\zeta_{bl} = \zeta - \zeta_0, \quad (4a)$$

$$\eta_{bl} = \eta - \zeta_0, \quad (4b)$$

where the subscript *bl* indicates elevation relative to base level and ζ_0 is the elevation of local base level (Figure 2). The lowering of the soil-bedrock interface relative to base level is then

$$\frac{\partial \eta_{bl}}{\partial t} = - \left(W_0 e^{-\frac{h}{\gamma}} + \frac{\partial \zeta_0}{\partial t} \right), \quad (5)$$

The second term on the right of equation (5), $\partial \zeta_0 / \partial t$, is the rate of base level lowering. If the channel at the base of the hillslope is incising into bedrock, $\partial \zeta_0 / \partial t$ will be negative. In the Lagrangian coordinate system, equation (1) becomes

$$\frac{\partial \zeta_{bl}}{\partial t} + \frac{\partial (h \bar{v}_x)}{\partial x} + \left(1 - \frac{\rho_\eta}{\rho_s} \right) W_0 e^{-\frac{h}{\gamma}} + \frac{\partial \zeta_0}{\partial t} = 0. \quad (6)$$

The second term in equation (6) describes the change in surface elevation of the hillslope relative to base level due to mechanical transport processes within the soil layer. The third term is a change in surface elevation due to soil production; it is nonzero when the dry bulk density of the soil is different from the dry bulk density of the bedrock.

Mechanical sediment transport processes in the absence of overland flow can include soil creep [e.g., *Culling*, 1963; *Heimsath et al.*, 2002; *Kirkby*, 1967; *Roering et*

al., 1999; *Young*, 1978], animal burrowing and disturbance [e.g., *Gabet*, 2000], frost heave processes [e.g., *Anderson*, 2002], and tree throw and root growth [e.g., *Gabet et al.*, 2003; *Roering et al.*, 2002]. In order to close equation (6), one must use a sediment flux law [e.g., *Dietrich et al.*, 2003] to describe the sediment transport processes. A number of flux laws have been proposed and tested using field data. There is evidence that on low relief hillslopes, sediment flux is linearly proportional to slope [*McKean et al.*, 1993; *Small et al.*, 1999]. The one dimensional linear sediment flux law can be stated as:

$$h \bar{v}_x = -D \frac{\partial \zeta_{bl}}{\partial x}, \quad (7)$$

where D ($L^2 T^{-1}$) is a sediment diffusivity. (Another coefficient occasionally reported in the literature, K , is in units of $M L^{-1} T^{-1}$ [e.g., *Fernandes and Dietrich*, 1997]. This coefficient is related to D by $K = \bar{\rho}_s D$. Some authors invert these two symbols [e.g., *Roering et al.*, 2001]; the quantities may be identified by their units). On steeper hillslopes, the interactions between disturbances, friction and gravity may lead to sediment flux that increases nonlinearly with slope [*Andrews and Bucknam*, 1987; *Roering et al.*, 1999]. This can be stated, in one dimensional form, as

$$h \bar{v}_x = -D \frac{\partial \zeta_{bl}}{\partial x} \left[1 - \left(\frac{1}{S_c} \frac{\partial \zeta_{bl}}{\partial x} \right)^2 \right]^{-1} \quad (8)$$

where S_c (dimensionless) is a critical slope. We refer to equation (8) as the linear-critical flux law.

2.2. Scaling and Nondimensionalization of the Governing Equations

The number of parameters in the system described by equations (5-8) can be reduced by nondimensionalizing the system. The variables of dimension length are nondimensionalized with:

$$\hat{x} = \frac{x}{\lambda}, \quad \hat{\zeta} = \frac{\zeta_{bl}}{\lambda}, \quad \hat{\eta} = \frac{\eta_{bl}}{\lambda}, \quad \hat{h} = \frac{h}{\gamma}, \quad (9)$$

where dimensionless quantities are denoted with carats and λ (L) is half the distance between adjacent channels (Figure 2). At both $x = 0$ and $x = 2\lambda$ there are channels that set the boundary condition of the hillslopes (the two hillslopes are separated by the hillcrest). We name the channel at $x = 0$ the primary channel and set its elevation to ζ_0 (the scaling of ζ_0 will be defined below). The channel at $x = 2\lambda$ is called the secondary channel.

A lengthscale ratio (dimensionless) is defined as:

$$\theta_L = \frac{\lambda}{\gamma}. \quad (10)$$

Note that $\hat{h} = \theta_L (\hat{\zeta} - \hat{\eta})$. A density ratio, τ_d , is defined as

$$\tau_d = \frac{\rho_\eta}{\rho_s}. \quad (11)$$

We form a timescale defined by the parameters of the soil production function, and name this the production timescale:

$$T_P = \frac{\gamma}{W_0}. \quad (12)$$

The rate of base level lowering ($\partial\zeta_0/\partial t = I$) is scaled by

$$\hat{I} = \frac{T_P}{\gamma} \frac{\partial\zeta_0}{\partial t} = \frac{1}{W_0} \frac{\partial\zeta_0}{\partial t}. \quad (13)$$

We also define a timescale based on the relaxation time of the hillslope [e.g., *Fernandes and Dietrich, 1997; Furbish and Fagherazzi, 2001; Jyotsna and Haff, 1997*].

The relaxation time is the time it takes for a hillslope to attain a new steady configuration after it has been perturbed. We define a diffusive timescale, T_D , as

$$T_D = \frac{\lambda^2}{D}. \quad (14)$$

This timescale is related to the relaxation time by a constant [e.g., *Fernandes and Dietrich, 1997; Furbish and Fagherazzi, 2001; Jyotsna and Haff, 1997*]. Time is scaled by T_D :

$$\hat{t} = \frac{t}{T_D}. \quad (15)$$

The production and diffusive timescales are used to define a timescale ratio, θ_t , (dimensionless):

$$\theta_t = \frac{T_D}{T_P} = \frac{\lambda^2 W_0}{D \gamma}. \quad (16)$$

A discussion of typical timescales and timescale ratios may be found in *Mudd and Furbish [2004]*. The linear and nonlinear flux laws described by equations (7) and (8) are scaled using equations (9) and (14). The resulting two equations can be written in the general

form:

$$h \bar{v}_x = \frac{\lambda^2}{T_D} \varphi, \quad (17)$$

where ϕ is a dimensionless function of slope with

$$\varphi = \frac{\partial \hat{\zeta}}{\partial \hat{x}} \quad (18)$$

in the case of the linear sediment flux law and

$$\varphi = \frac{\partial \hat{\zeta}}{\partial \hat{x}} \left[1 - \left(\frac{1}{S_c} \frac{\partial \hat{\zeta}}{\partial \hat{x}} \right)^2 \right]^{-1} \quad (19)$$

in the case of the linear-critical flux law.

2.3. Dimensionless Governing Equations

Inserting equations (9-19) into equations (5) and (6) gives the nondimensionalized governing equations for the hillslope system:

$$\frac{\partial \hat{\eta}}{\partial \hat{t}} + \frac{\theta_t}{\theta_L} \left(e^{-\hat{h}} + \hat{f} \right) = 0, \quad (20)$$

$$\frac{\partial \hat{\zeta}}{\partial \hat{t}} - \frac{\partial \varphi}{\partial \hat{x}} + \frac{\theta_t}{\theta_L} \left[(1 - \tau_d) e^{-\hat{h}} + \hat{f} \right] = 0. \quad (21)$$

Equations (20) and (21) allow the investigation, through both analytic and numerical techniques, of scenarios that will lead to hillcrest migration.

3. Analytical Solutions of Hillcrest Migration

Analytical solutions can be obtained for specific cases of hillcrest migration. We solve equations (20) and (21) for two cases: in the first case the channels are incising at the same rate but are offset vertically, and in the second case the adjacent channels are incising at constant but different rates.

3.1. Hillcrest Offset Due to Channel Elevation Differences at Topographic Steady State

Consider a one-dimensional hillslope between two channels that is at topographic steady state relative to local base level ($\partial \hat{\zeta} / \partial \hat{t} = \partial \hat{\eta} / \partial \hat{t} = 0$). The steady state condition implies that the production rate of soil is spatially uniform. If the channels that bound the ridge are at the same elevation, the hillslopes on either side of the ridge will be symmetric. If, however, the channels are at different elevations, the hillcrest will be offset toward the channel at a higher elevation. In this section we determine how the offset distance is affected by the dominant sediment flux law, the characteristics of the hillslope (e.g., hillslope relief) and the vertical offset of the two channels bounding the hillslope.

The horizontal offset of the hillcrest can be found analytically by solving equations (20) and (21) simplified for topographic steady state. Setting the time derivative in equation (20) to zero yields $\exp(\hat{h}) = -\hat{I}$. We assume sediment transport is linearly proportional to the slope (equations 7, 17 and 18) and set the time derivative in equation (21) to zero, giving an equation for the curvature of the hillslope:

$$\frac{\partial^2 \hat{\zeta}}{\partial \hat{x}^2} = \frac{\theta_t}{\theta_L} \tau_d \hat{I}. \quad (22)$$

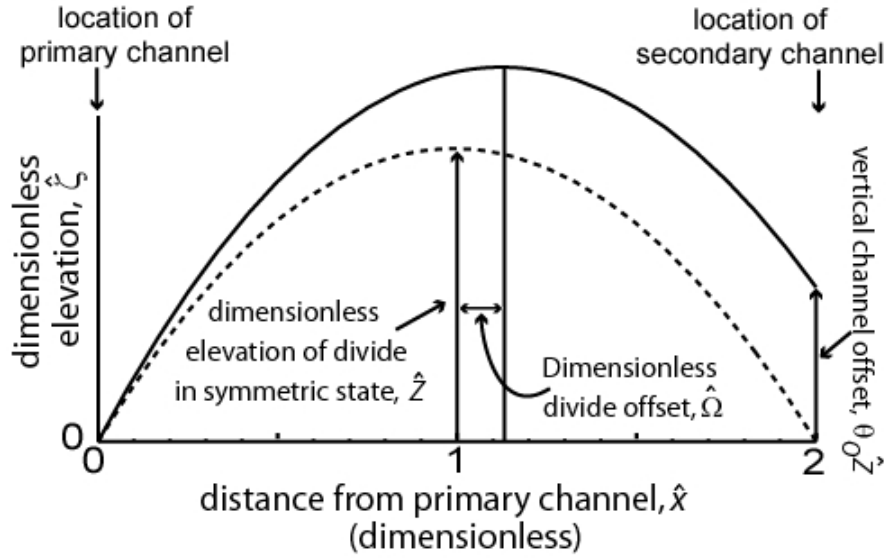


Figure 3. Dimensionless hillslope profiles: dashed line is a symmetric hillslope pair, solid line shows a profile where the secondary channel is offset vertically, the hillcrest in this profile is offset horizontally from the hillcrest of the symmetric profile.

The surface topography may be found by integrating equation (22) twice and applying the appropriate boundary conditions. The dimensionless surface elevation is set to zero at $\hat{x} = 0$. At $\hat{x} = 2$, which is the location of the secondary channel, the surface elevation is offset from the elevation of the channel at $\hat{x} = 0$. This vertical offset is measured as a fraction of the elevation of the hillcrest if both channels were incising at the same rate. The elevation at the hillcrest for a steady state hillslope when both channels are at the same elevation (\hat{Z}_{ls} , dimensionless) is

$$\hat{Z}_{ls} = -\frac{\tau_d \theta_t}{2 \theta_L} \hat{f}. \quad (23)$$

The offset ratio, θ_o , is defined as

$$\hat{\zeta}|_{\hat{x}=2} = \theta_o \hat{Z}_{ls} \quad (24)$$

where $\hat{\zeta}|_{\hat{x}=2}$ is the dimensionless elevation of the secondary channel (see Figure 3).

Using equations (23) and (24) as the second boundary condition for equation (22), the hillslope profile may be found:

$$\hat{\zeta} = \frac{\tau_d \theta_t}{\theta_L} \hat{f} \left[\frac{\hat{x}^2}{2} - \left(\frac{\theta_o}{4} + 1 \right) \hat{x} \right]. \quad (25)$$

The hillcrest offset, $\hat{\Omega}$ (dimensionless), is measured as the distance from $\hat{x} = 1$ (see Figure 3) and may be found by setting the slope of equation (25) to zero, solving for \hat{x} , and subtracting one:

$$\hat{\Omega} = \frac{\theta_o}{4}. \quad (26)$$

Equation (26) demonstrates that the hillcrest offset in the case of the linear sediment flux law is a simple function of geometry. That is, the hillcrest offset is one quarter of the offset ratio.

For comparison, we can calculate the hillcrest offset distance for the case of rapidly incising, steep topography. *Burbank et al.* [1996] found that in the Himalaya in a region of rapid incision, slope angles were independent of the incision rate, suggesting that a threshold slope had been attained. Imagine two rivers separated by hillslopes at a threshold slope, S_T [this slope was found to be ~ 0.8 ; *Burbank et al.*, 1996]. The dimensionless elevation of the hillcrest when both channels are at the same elevation is simply S_T , and if the river is offset by the product of θ_o and S_T , the hillcrest offset distance will be

$$\hat{\Omega} = \frac{\theta_o}{2}. \quad (27)$$

Recall that the linear sediment flux law applies to landscapes with gentle slopes. These two cases can be thought of as end member scenarios. In landscapes where slopes are gentle and incision rates are lower, vertical offsets in the elevations of adjacent channels will move the hillcrest a quarter of the offset ratio according to equation (26), whereas in rapidly eroding landscapes a vertical channel offset can cause twice the hillcrest offset as a fraction of the relief of the symmetric hillslope.

It should be noted, however, that landscapes where rivers are bounded by critical hillslope are generally high relief landscapes, such as the Himalaya [e.g., *Burbank et al.* 1996]. Suppose a knickpoint of some arbitrary height is generated due to a faulting or rapid sea level change. This knickpoint then migrates through a lower relief, soil mantled foreland and subsequently into a high relief mountainous area which has hillslopes at a threshold angle. In such a case the knickpoint would be a much smaller fraction of the relief in the high relief mountainous region than in the lower relief, soil mantled region. The ratio of the dimensional hillcrest offset distances in such a case is

$$\frac{\Omega_{ts}}{\Omega_{lr}} = - \frac{\lambda_{ts} \tau_d}{D S_T} \frac{\partial \zeta_0}{\partial t}, \quad (28)$$

where the subscript *ts* denotes the high relief, threshold slope landscape and the diffusivity, base level lowering rate, and bedrock to soil density ratio are all measured in the soil mantled landscape where sediment transport follows equation (18).

As an example, consider a knickpoint that is 10m in height (the 1996 Chichi earthquake in Taiwan had a vertical offset of 3-8m [*Chen et al.*, 2002]) that is generated on a landscape which has a background base level lowering rate of 0.01 mm yr⁻¹ in the foreland area. Suppose that in the hillslopes throughout this landscape are on average

500m long, there is no density contrast between the soil and the bedrock, the diffusivity in the soil mantled foreland is $0.025 \text{ m}^2 \text{ yr}^{-1}$, and the threshold slope is 0.8 in the mountainous area. Note that the base level lowering rate could be significantly higher in the mountainous area compared to the foreland area; background base level lowering plays no role in the amount of relief in landscapes with hillslopes at a threshold angle. Under these conditions, the knickpoint would cause the hillcrest in the foreland area to be offset by 25m, whereas the offset in the mountainous, threshold portion of the landscape from this same knickpoint would be 6.25m.

We may also compare the behavior of the above instances with the case of a hillslope where sediment transport follows a linear-critical sediment flux law (equation 8). The profile of a hillslope experiencing linear-critical sediment transport at steady state is described by:

$$\hat{\zeta} = S_c \sqrt{\frac{S_c^2}{16 Z_{ls}^2} + \hat{X}^2} - S_c \sqrt{\frac{S_c^2}{16 Z_{ls}^2} + (\hat{x} - \hat{X})^2} + \frac{S_c^2}{4 \hat{Z}_{ls}} \ln \left[1 + \sqrt{1 + \frac{16 (\hat{x} - \hat{X})^2 \hat{Z}_{ls}^2}{S_c^2}} \right] - \frac{S_c^2}{4 \hat{Z}_{ls}} \ln \left[1 + \sqrt{1 + \frac{16 \hat{X}^2 \hat{Z}_{ls}^2}{S_c^2}} \right], \quad (29)$$

where \hat{X} (dimensionless) is the location of the hillcrest. The symmetric case, where there is no hillcrest offset, is found by setting \hat{X} to one. We may solve for the elevation at the secondary channel by setting \hat{x} to two. This leads to a transient (nonalgebraic) equation in $\hat{\zeta}$; an analytic solution of the hillcrest offset as a function of S_c , \hat{Z}_{ls} , and θ_0 has not been

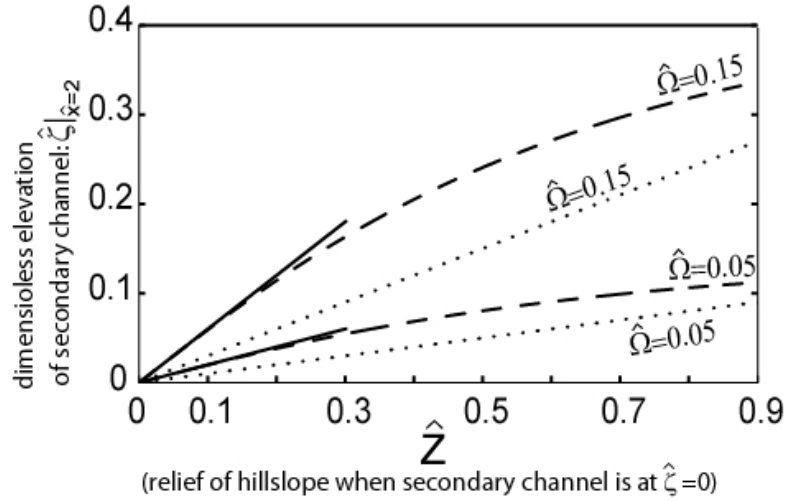


Figure 4. Contours of the dimensionless hillcrest offset ($\hat{\Omega}$) as a function of hillslope relief and vertical channel offset. The solid line is for hillslopes experiencing a linear sediment flux law, the dashed line is for linear-critical slopes, and the dotted line is for threshold slopes.

found. We may solve for the vertical channel offset for various values of the hillcrest offset and the elevation of the hillcrest in the symmetric case and compare these offsets with the linear and critical hillslope cases. Figure 4 plots contours of the dimensionless hillcrest offset ($\hat{\Omega}$) as functions of the relief of the hillslope when it is in symmetric state (\hat{Z}) and the elevation of the secondary channel (recall the primary channel is always at an elevation of $\hat{\zeta} = 0$). We have plotted the hillcrest offset as a function of the relief of the hillslopes in the symmetric state because it is not a function of the elevation of the secondary channel. For low relief hillslopes (low values of \hat{Z}), the behavior of the hillslopes obeying a linear-critical flux law approaches the behavior of the hillslopes obeying the linear sediment flux law. As the relief of the hillslopes increase, the linear-critical slopes behave more like the threshold slopes. If two hillslopes experience a vertical offset of the same dimensionless height, the hillslope with less relief will experience the greater hillcrest offset. For hillslopes with the same vertical offset and the

same relief, the hillcrest offset will be greatest for the threshold slopes, followed by the linear-critical slopes, with the hillslopes where sediment flux goes linearly with slope having the lowest hillcrest offset.

3.2. Migrating Hillcrest Due to Steady But Unequal Channel Incision Rates

To examine the possibility of stream capture associated with hillcrest migration, we consider the case in which two adjacent channels are incising at steady, but different, rates. The incision rate of the channel at $\hat{x} = 0$ is \hat{I} , and at $\hat{x} = 2$ the incision rate is set to a fraction of \hat{I} , which we call θ_I (dimensionless). If the channel at $\hat{x} = 2$ is incising at a different rate than the channel at $\hat{x} = 0$, then the relative elevation of the channel at $\hat{x} = 2$ will change:

$$\left. \frac{\partial \hat{\zeta}}{\partial \hat{t}} \right|_{\hat{x}=2} = \frac{\theta_I}{\theta_L} \hat{I} (\theta_I - 1). \quad (30)$$

Numerical solutions have demonstrated that from arbitrary initial conditions and steady but unequal downcutting rates at $\hat{x} = 0$ and $\hat{x} = 2$, the soil thickness reaches a steady state after some finite period of time ($\partial \hat{h} / \partial \hat{t} = 0$). We call this a pseudo steady state because while the soil thickness does not change in time, the surface topography is transient, and the pseudo steady-state condition only exists until the channel that is incising at a slower rate is captured by the fast-eroding channel. When the dimensionless soil production rate, $\exp(\hat{h})$, reaches its steady state condition it is a linear function of \hat{x} . This linear function is:

$$e^{-\hat{h}} = \frac{\hat{I}(1 - \theta_I)}{2} \hat{x} - \hat{I}. \quad (31)$$

Equation (31), combined with the dimensionless equation for soil thickness using the linear flux law, results in an equation for the curvature of the pseudo steady state hillslope:

$$\frac{\partial^2 \hat{\zeta}}{\partial \hat{x}^2} = \frac{\theta_t \tau_d}{\theta_L} \hat{f} - \frac{\theta_t \tau_d}{\theta_L} \frac{\hat{f}(1 - \theta_I)}{2} \hat{x}. \quad (32)$$

At $\hat{x} = 0$, the boundary condition is $\hat{\zeta} = 0$. At $\hat{x} = 2$, the boundary condition may be found by integrating with respect to time and letting $\hat{\zeta}$ at $\hat{t} = 0$ be equal to zero:

$$\hat{\zeta} \Big|_{\hat{x}=2} = \frac{\theta_t}{\theta_L} \hat{f} (\theta_I - 1) \hat{t}. \quad (33)$$

These two boundary conditions may be used to solve for the pseudo steady state topography:

$$\begin{aligned} \hat{\zeta} = & -\frac{\tau_d \theta_t \hat{f} (1 - \theta_I)}{12 \theta_L} \hat{x}^3 + \frac{\tau_d \theta_t \hat{f}}{2 \theta_L} \hat{x}^2 \\ & + \frac{\theta_t \hat{f}}{2 \theta_L} (1 - \theta_I) \hat{t} \hat{x} - \left(\frac{\tau_d \theta_t \hat{f}}{\theta_L} - \frac{\tau_d \theta_t \hat{f} [1 - \theta_I]}{3 \theta_L} \right) \hat{x}. \end{aligned} \quad (34)$$

The dimensionless elevation of the hillslope ($\hat{\zeta}$) is a function of both \hat{x} and \hat{t} . The hillcrest is located where the slope of the soil surface equals zero. The location of the

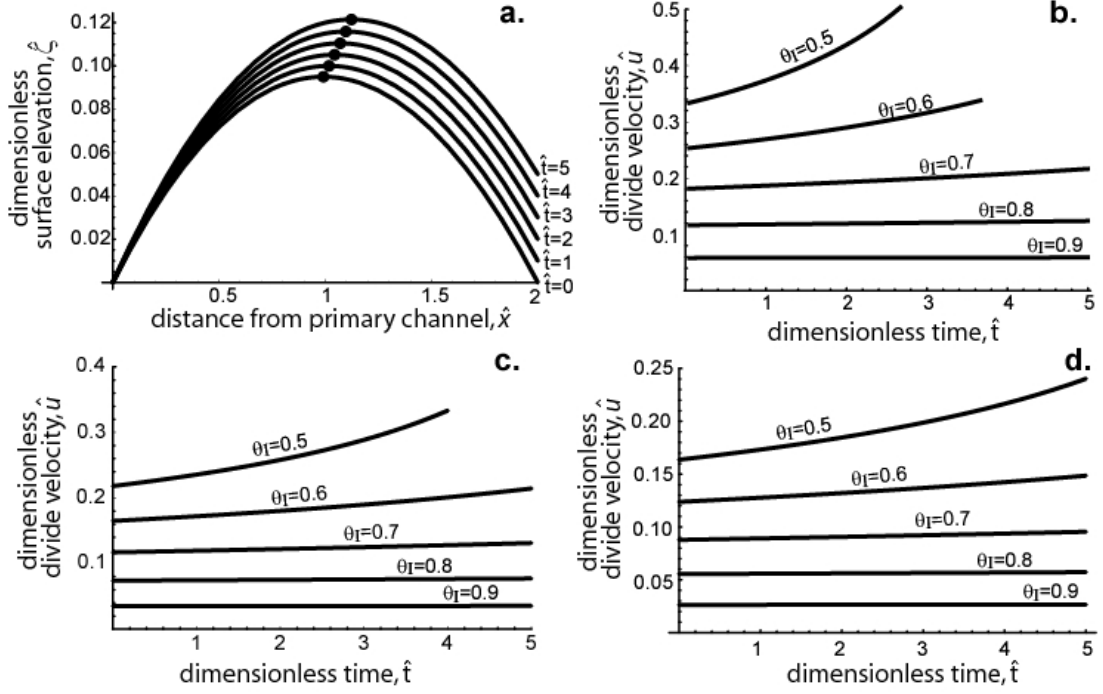


Figure 5. Pseudo steady state hillcrest migration. The parameter θ_I is the ratio of the rate of incision in the secondary channel to the rate of incision in the primary channel. **a.** Profile of a hillslope where the secondary channel is incising at a slower rate than the primary channel. Black dots denote the location of the hillcrest. Parameters are: $\tau_d = 2$, $\theta_I = 10$, $\theta_D = 100$, $I = -0.1$, and $\theta_I = 0.9$. **b.** Dimensionless velocity of the hillcrest for $\tau_d = 1$. **c.** Dimensionless velocity of the hillcrest for $\tau_d = 1.5$. **d.** Dimensionless velocity of the hillcrest for $\tau_d = 2$. In **b.** for $\theta_I = 0.5$, $\theta_I = 0.6$ and in **c.** for $\theta_I = 0.5$ the plots end where the location of the hillcrest is $x = 1$. Note the change in vertical scale in **b.-c.**

hillcrest, \hat{x}_d , is found to be:

$$\hat{x}_d = \frac{\sqrt{6\tau_d(2\tau_d + 2\theta_I[3\hat{t} + \tau_d] + \theta_I^2[2\tau_d - 3\hat{t}] - 3\hat{t})} - 6\tau_d}{3(\theta_I - 1)\tau_d}. \quad (35)$$

The dimensionless lateral migration speed of the hillcrest, \hat{u}_d , is found by differentiating equation (35) with respect to dimensionless time:

$$\hat{u}_d = \frac{3(1 - \theta_I)}{\sqrt{6\tau_d(2\tau_d - 3\hat{t} + 2\theta_I[3\hat{t} + \tau_d] + \theta_I^2[2\tau_d - 3\hat{t}])}}. \quad (36)$$

The dimensionless incision rate (\hat{I}) of the primary channel and the time and length ratios (θ_l and θ_D) are important in determining the curvature, slope, and relief of the pseudo steady state hillslope, but they play no role in determining the location and migration speed of the hillcrest. The behavior of the hillcrest is solely a function of θ_l , τ_d , and \hat{t} . Figure 5 shows some of the behavior of the pseudo steady state hillslope. As the secondary channel incises at a slower rate than the primary channel, the relative elevation of the secondary channel increases, and the hillcrest migrates away from the primary channel (Figure 5a). In all cases the migration speed of the hillcrest increases with time. As θ_l approaches one, the relationship between \hat{u}_d and \hat{t} may be approximated as linear, but at smaller values of θ_l (when the secondary channel is being offset from the primary channel at a faster rate), \hat{u}_d increases nonlinearly with time (Figures 5b-d). The density ratio (τ_d) is inversely related to \hat{u}_d (equation 36), and \hat{u}_d also decreases with increasing θ_l . Lower values of θ_l mean that the vertical offset distance between channels will increase more rapidly (equation 34), and the faster this relief between channels is generated, the faster the hillcrest migrates.

Stream capture occurs when the location of the hillcrest equals the location of the secondary channel ($\hat{x}_d = 2$). The dimensionless time to stream capture (\hat{t}_{sc}) is found by setting the hillcrest location equal to the location of the secondary channel in equation (35) and solving for time:

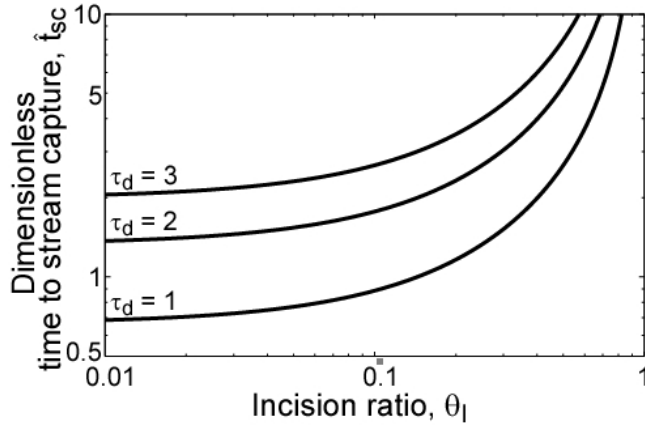


Figure 6. The dimensionless time to stream capture (\hat{t}_{sc}) as a function of the incision ratio θ_I and the density ratio τ_d . As θ_I approaches 1, \hat{t}_{sc} asymptotically approaches infinity.

$$\hat{t}_{sc} = -\frac{2\tau_d(1+2\theta_I)}{3(\theta_I-1)} \quad (37)$$

Figure 6 shows how \hat{t}_{sc} varies with variations in θ_I . For small values of θ_I , meaning that the vertical offset elevation between the primary and secondary channel grows rapidly, \hat{t}_{sc} can approach or be less than one (the time to stream capture approaches the relaxation time of the hillslope). As θ_I moves to values of 0.3-0.4, the time to stream capture begins to increase rapidly, and as θ_I approaches one the time to stream capture approaches infinity.

Both *Matmon et al.* [2003] and *Kirchner et al.* [2001] have measured θ_I values approaching 0.5 in the field (see Table 1). In the drainage basins measured for these two studies, the channel spacing is large enough ($O(10^3-10^4\text{m})$) that the imbalance in erosion rates over adjacent basins would need to persist for tens of millions of years for a basin to

Table 1. Measured incision ratios of adjacent basins. ^aBasin references are the location names used in *Kirchner et al.* [2001] (Source = 1), *Matmon et al.* [2003] (Source = 2), and *Riebe et al.* [2000] (source = 3) of the adjacent basins used to calculate θ_l . The data from *Riebe et al.* [2000] were derived from their Figure 1.

basin reference ^a	θ_l	Source
25,27	0.68±0.18	1
26,27	0.69±0.19	1
14,15	0.71±0.21	1
1,2	0.55±0.14	1
GSCS-1, GSCS-2	0.49±0.12	2
GSBC-1, GSCA-1	0.59±0.15	2
GSCO-4, GSRF-11	0.57±0.14	2
Fall River	0.50±0.11	3
Fort Sage	0.16±0.07	3

capture the adjacent stream via this mechanism. For example, with $\lambda = 500\text{m}$ (the approximate spacing between basins one and two in *Kirchner et al.* [2001]), $D = 0.025\text{ m}^2\text{ yr}^{-1}$, no density difference between the soil and bedrock ($\tau_d = 1$), and $\theta_l = 0.5$, the time to stream capture from a symmetrical state (the two channels are at the same elevation) would be 2.66×10^7 years. The hillcrest migration speed in such a case would be on the order of 0.01mm yr^{-1} . This rate may seem negligible, but consider a situation in which $\lambda = 100\text{m}$, a scale at which the basin averaged erosion rates in adjacent basins have yet to be measured using detrital cosmogenic radionuclides. With all other parameters the same as above excluding the channel spacing, the time to stream capture decreases to $\sim 1 \times 10^6$ years. This time would reduce to five hundred thousand years if θ_l were 0.2, which is the ratio of erosion rates between adjacent catchments reported by *Riebe et al.* [2000] at Fort

Sage, California. The cosmogenic isotope method used to calculate the spatially varying erosion rates by both *Matmon et al.* [2003] and *Kirchner et al.* [2001] averages rates over this timescale; such a duration of an average imbalance in erosion rates between adjacent basins is reasonable. To dimensionalize the hillcrest migration velocity, the dimensionless velocity is multiplied by the factor λ/D , so shorter slopes with higher diffusivities will have faster hillcrest migration velocities. More field studies quantifying spatially varying rates of erosion in adjacent basins at the $\lambda \leq 100\text{m}$ scale could better constrain the likelihood of stream capture through a mechanism of differential downcutting rates in adjacent basins.

Consider also the problem of escarpment retreat. A number of authors have suggested that escarpments can retreat at rates of 1mm yr^{-1} if the escarpment has retreated at a constant rate since the time of rifting, whereas others have suggested that the recent retreat rates are considerably slower, and that a majority of the retreat occurred shortly after rifting (for an overview, see *van der Beek et al.* [2002] and references therein). On the southeastern Australian escarpment *Heimsath et al.* [2000] found that on the coastal side of the escarpment the basin averaged erosion rate (measured using ^{10}Be concentration in river sand) was $51.49 \times 10^{-6} \text{ m yr}^{-1}$, whereas the basin averaged erosion rate on the upland side of the escarpment was $15.47 \times 10^{-6} \text{ m yr}^{-1}$. This difference in erosion rates could lead to migration of the hillcrest, contributing to escarpment retreat; the difference in erosion rates gives a θ_1 value of 0.3 between the coastal and upland side of the escarpment. *Heimsath et al.* [2001] also found the diffusivity to be $0.004 \text{ m}^2 \text{ yr}^{-1}$. We consider the hillslope length in this case the distance from the hillcrest to the channel head. For hillslopes with lengths on the order of 10-100m and with a density ratio (τ_d) of

1.5, the hillcrest retreat rates would be on the order of 10^{-4} to 10^{-5} meters per year. This should be considered only a rough estimate of escarpment retreat rates due to the fact that as the hillslope on the fast-eroding side of the escarpment grows in length as the hillcrest migrates toward the upland, the location of the fluvial network is likely to change.

For hillcrests that migrate rapidly, the diffusivities would have to be extremely high, the hillslopes short, density differences between soil and bedrock low, and the difference in erosion rates on either side of the escarpment pronounced. For example, with no difference in the densities of soil and bedrock ($\tau_d = 1$), hillslopes that are 20m long, a difference in erosion rates of a factor of 20 ($\theta_1 = 0.05$), and a diffusivity at the upper range of any measured ($D = 0.03 \text{ m}^2 \text{ yr}^{-1}$, see *Fernandes and Dietrich* [1997] for a range of diffusivities) the hillcrest would migrate at a rate on the order of 1mm per year.

4. Numerical Simulations of Transient Hillcrest Migration

To investigate the transient response of the hillslope hillcrest to unsteady downcutting in the primary and secondary channels we solve equations (20) and (21) numerically. We focus the numerical investigation on two scenarios of transient channel incision. The first scenario models knickpoints propagating through a drainage basin. Two knickpoints of identical elevation travel through the primary and secondary channel, but there is a delay between the time these knickpoints pass the base of the hillslope. This delay is a natural feature of knickpoint propagation because the celerity of the knickpoint varies between basins if they have different sediment supplies or water discharges [*Crosby and Whipple, in press; Whipple and Tucker, 1999*]. The second scenario models the effect of having incision rates that vary with different frequency and amplitude in the

primary and secondary channels. This variation is an approximation of downcutting of streams that have different thresholds for channel incision and flood distributions that cause temporal variations in downcutting rates [e.g., *Snyder et al.*, 2003; *Tucker*, 2004]. For these two cases, the long term average erosion rate is set to be the same in both the primary and secondary channel.

4.1. The Effect of Delayed Knickpoint Migration

In the first set of simulations the two channels bounding a 1-D hillslope pair are incising at a background rate \hat{I} . A knickpoint passes through the primary channel at $\hat{t} = 0$. It incises a fraction of the total relief of the hillslope θ_{kp} . After a delay time of \hat{t}_{kpd} , a knickpoint of the same elevation passes through the secondary channel. A finite difference model is used to track the transient response of the hillslopes separating the channels to the passage of these knickpoints. The response of a hillslope with a linear flux law (equation 7) has been explored by *Fernandes and Dietrich* [1997] and *Roering et al.* [2001], but the simulations presented here differ in both the forcing (in the form of incision rates) and the incorporation of soil production. Additionally we allow asymmetry of the hillslope, which leads to hillcrest migration.

Inclusion of soil production in modeling the transient response of a hillslope is significant in two important ways. First, as will be shown later in this section, the expansion (or contraction) of the material on the hillslope as it is converted from bedrock to soil (encapsulated in the parameter τ_d) acts as a first order control on the transient response of the hillslope. Second, the response of the soil thickness can lag behind the response of the surface topography.

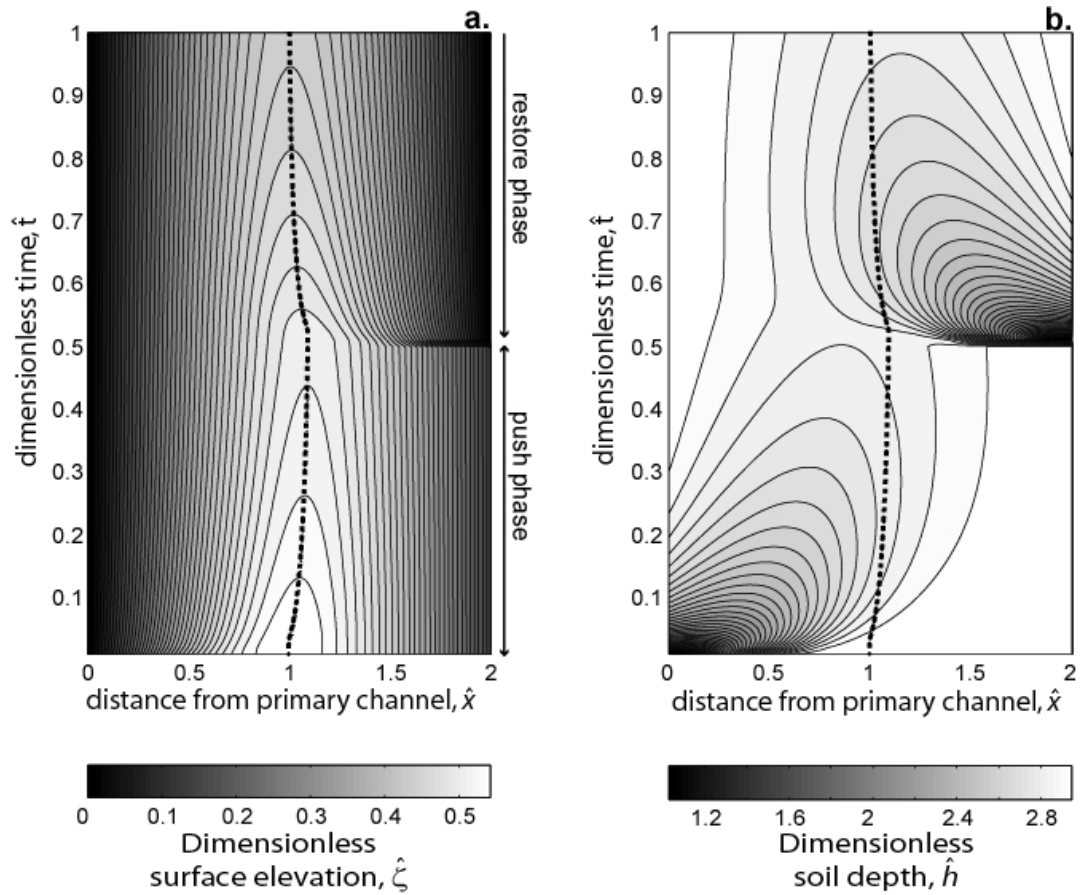


Figure 7. Transient behavior of a hillslope subjected to two knickpoints of the same elevation. Figures are read from bottom to top for advancing dimensionless time (t); a horizontal slice through the figures would represent a profile at a given t . **a.** Contours represent surface elevation. **b.** Contours represent soil thickness. The dotted lines in **a.** and **b.** show the location of the hillcrest.

4.1.1. Linear Flux Law

In the first set of delayed knickpoint migration simulations, a linear sediment flux law is used (equation 7). When a knickpoint in the primary channel reaches the base of the modeled hillslope, the hillslope is steepened near the channel and responds with increased sediment flux. The increased sediment flux from the disturbance causes soil to be evacuated (Figure 7). Evacuation of soil causes a reduction in the soil thickness, thus

causing an increase in soil production (see equation 3). After the initial wave of increased sediment flux and the corresponding decrease in soil thickness, the soil recovers back to its steady thickness, but at a rate different from the rate of return to steady surface topography. Figure 7a shows the response of the surface topography to the passage of the two knickpoints and Figure 7b shows the response of the soil thickness. After the passage of each knickpoint the disturbances in soil thickness move away from the disturbed channel, widen, and decay (Figure 7b). The disturbance to the surface topography propagates upslope until it reaches the hillcrest, at which point it begins to “push” the hillcrest away from the disturbed channel. As the disturbance in topography and soil depth moves away from the primary channel and approaches the hillcrest, soil is evacuated toward the disturbed channel, and the sediment flux toward the undisturbed channel is reduced. This reduces the soil depth downslope of the hillcrest away from the disturbed channel. We call the period during which the hillcrest moves away from the primary channel the push phase. As the hillcrest moves toward the secondary channel a wave of increased erosion propagates away from the secondary channel. At some time after the second channel has been disturbed the hillcrest begins to migrate back toward its equilibrium position at $\hat{x} = 1$. We refer the period of time between the time the hillcrest begins to migrate back toward the primary channel due to the passage of the second knickpoint and the time when the hillcrest returns to the equilibrium position the restore phase.

The motion of the hillcrest has a characteristic shape (e.g., the dotted lines in Figure 7) determined by the processes described in the previous section. Numerical simulations have shown this motion to be a function of the knickpoint delay \hat{t}_{kpd} , the

density ratio τ_d , the knickpoint ratio θ_{kp} , and a ratio θ_z :

$$\theta_z = \frac{1}{2} \frac{\lambda^2}{D\gamma} \frac{\partial \zeta_0}{\partial t}. \quad (38)$$

The quantity θ_z is the ratio between the time it takes soil eroding at the background rate

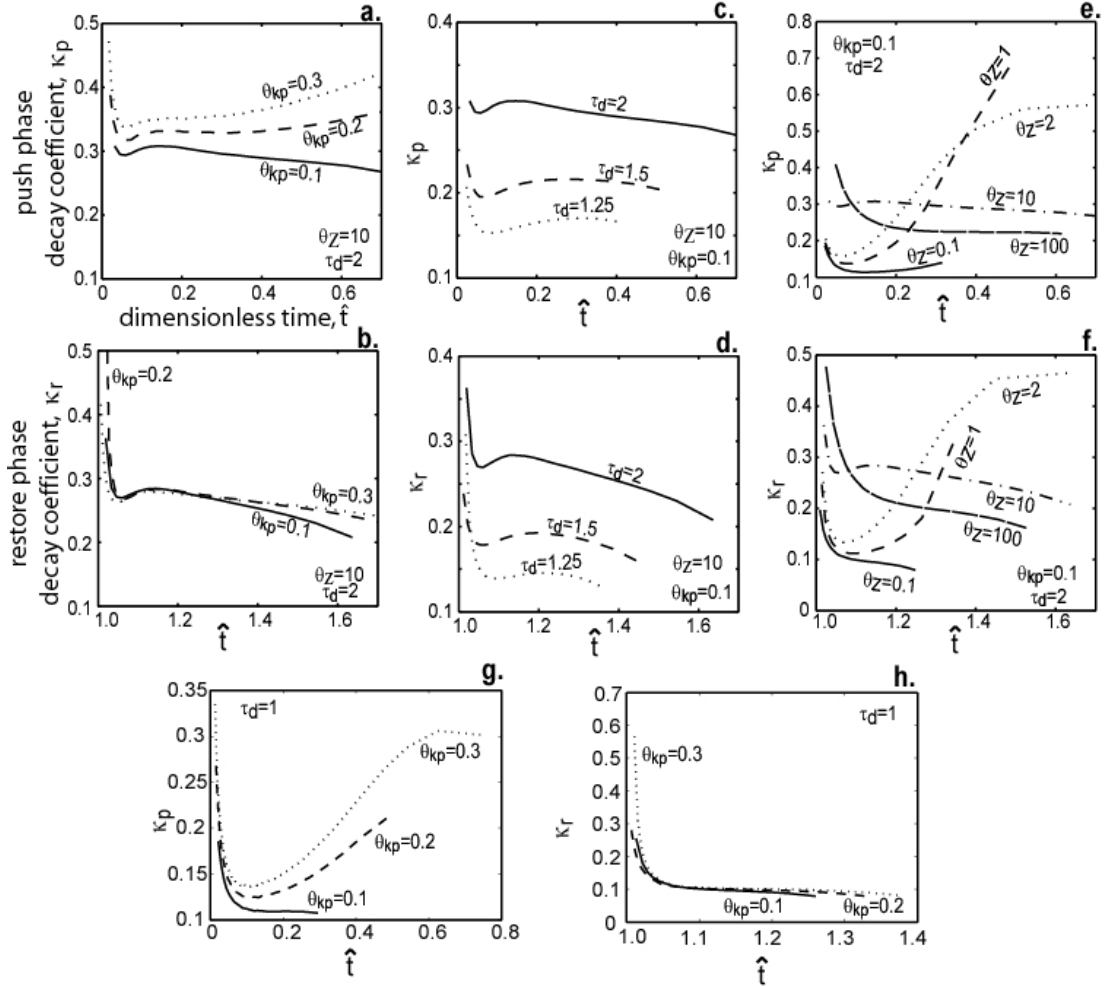


Figure 8. Relaxation time of hillcrest migration as a fraction of hillslope relaxation time (κ). All runs have a t_{kpd} of 1. **a.** and **b.** show variation in θ_{kp} with other parameters held constant for push (**a.**) and restore (**b.**) phases. **c.** and **d.** show variation in τ_d with other parameters held constant for push (**c.**) and restore (**d.**) phases. **e.** and **f.** show variation in θ_z with other parameters held constant for push (**e.**) and restore (**f.**) phases. **g.** and **h.** show variation in θ_{kp} with $\tau_d=1$ for push (**e.**) and restore (**f.**) phases. In **g.** and **h.** there is no sensitivity to θ_z . Note the change in vertical scale.

$\partial\zeta_0/\partial t$ to erode through soil of thickness 2γ and the relaxation time of the hillslope. For example, a hillslope with a background incision rate of $2.5 \times 10^{-5} \text{ m yr}^{-1}$ (similar to the erosion rates measured with Be^{10} in the Smokey Mountains [Matmon *et al.*, 2003] and southeast Australia [Heimsath *et al.*, 2001]), a soil production length scale (γ) of 0.5m, a diffusivity of $0.01 \text{ m}^2 \text{ yr}^{-1}$, and a hillslope length (λ) of 100m would have a θ_z value of 25.

At an approximation, both the push phase and the restore phase may be described by an exponential decay function of the form:

$$F(\hat{t}) = F_e + (F_s - F_e) e^{-\frac{\hat{t}}{\kappa}}, \quad (39)$$

[e.g., Howard, 1988; Roering *et al.*, 2001] where $F(t)$ is some function of time (in this case the location of the hillcrest) F_s is the value of the function at the start time (and perturbed from equilibrium), and F_e is the value at the function at equilibrium. In the case of the push phase F_e is the theoretical maximum push distance (equation 26) and in the case of the restore phase F_e is $\hat{x} = 1$. The decay constant, κ , is a dimensionless parameter that determines how quickly the system will adjust to perturbations. It is a response time that is scaled, like \hat{t} , by the relaxation time of the hillslope. The decay constant, κ , represents the time it takes the hillcrest to respond to perturbation as a fraction of the hillslope relaxation time. For example, if $\kappa = 0.1$, the disturbed hillcrest will have migrated ninety percent of the distance to the maximum theoretical offset after a period of 0.23 times the hillslope diffusive timescale ($T_D = \lambda^2/D$), whereas if $\kappa = 1$ the hillcrest will have migrated back to a tenth of the original disturbance after period of 2.3 times T_D .

In some cases, the exponential approximation may be relatively poor. Closer

examination of the motion of the hillcrest reveals that the exponential fit of the hillcrest relaxation time varies in dimensionless time. To illustrate this more complex behavior, we linearize equation (39) with respect to \hat{t} :

$$X = \frac{\hat{t}}{\kappa}, \quad (40a)$$

where

$$X = -\ln \left[\frac{F(\hat{t}) - F_e}{F_s - F_e} \right]. \quad (40b)$$

The slope of the line that defines X as a function of \hat{t} is related to the hillcrest relaxation time as a fraction of the hillslope relaxation time:

$$\frac{dX}{d\hat{t}} = \frac{1}{\kappa}. \quad (41)$$

We define two decay coefficients, $\kappa_p(\hat{t})$ for the push phase and $\kappa_a(\hat{t})$ for the restore phase. This approach allows us to examine the adjustment rate of the hillcrest as a function of time. This approach is necessary because the hillslope-soil system is responding on two different timescales which lead to a complex response of the system to transient perturbations. The two timescales are related to the adjustment of topography from sediment fluxes (which respond to changes in slope), and the adjustment of soil production (which respond to changes in soil depth). A time varying κ measures the changing rate of adjustment of the hillcrest to the equilibrium state as the coupled system responds to transient changes in channel incision rates. Greater hillcrest relaxation times (e.g., greater κ values) represent slower adjustment of the hillcrest to channel

perturbations, whereas smaller hillcrest relaxation times (e.g., smaller κ values) represent faster adjustment of the hillcrest to channel perturbations.

Variations in the density ratio τ_d and the offset ratio θ_{kp} lead to systematic variations in the hillcrest relaxation time throughout the duration of the push phase. Increasing θ_{kp} leads to increasing hillcrest relaxation times in both the push and restore phases (κ_p and κ_r , e.g., Figure 8a). Increasing θ_{kp} increases the disturbance of the surface topography relative to the relief of the hillslope, which would presumably lead to faster response times, but the hillcrest also must move farther from equilibrium, increasing the response time. The numerical results imply that the increased distance the hillcrest must migrate to reach equilibrium is more significant in determining the adjustment rate than the perturbation in surface topography caused by the knickpoint.

Increasing τ_d (greater soil lofting) increases the relaxation time of the hillcrest (Figure 8c, d), except in some cases shortly after the passage of the second knickpoint (Figure 8d). The relaxation time of the hillcrest is more sensitive to changes in τ_d than to changes in θ_{kp} early in the push phase and throughout the restore phase (compare Figures 8a to 8c and 8b to 8d). For example, consider a hillslope with a diffusivity (D) of $0.02\text{m}^2\text{yr}^{-1}$ and a length (λ) of 40m, and all other parameters the same as those used to generate Figure 8b. The diffusive timescale of this hillslope is then 80ka. Such a hillslope whose soil is half as dense as the bedrock ($\tau_d = 2$) will have its hillcrest migrate ninety percent of the distance to its maximum theoretical offset (determined by equation 26) within approximately 50ka. If the soil density ratio is lowered to 1.25, however, this time becomes approximately 30ka.

The relaxation time of hillcrest migration responds in a complex way to changes

in θ_z (Figure 8e, 8f). When the disturbance caused by a knickpoint first reaches the hillcrest the rate of response is greater for hillslopes with smaller values of θ_z (with smaller values of κ corresponding to faster response rates, Figure 8e, f). As time passes however, the response rates adjust, and for larger values of time the response rate increases with increasing values of θ_z . The physics of this complex response can be further elucidated by examining the special case of $\tau_d=1$. Examination of equation (21) reveals that if $\tau_d=1$, then the first term in the brackets goes to zero. This term is the transient response of the surface due to the lofting of the soil as it is converted from its parent material. When $\tau_d=1$, the response of the hillcrest has no dependence on θ_z . The changes in the relaxation time of the hillcrest through time for $\tau_d=1$ are shown in Figure 8g and 8h. Changes in the relaxation time of the hillcrest due to lofting processes can be found by subtracting the lines in Figures 8g and 8h from the lines in Figure 8e and 8f. The difference in these trends demonstrates that lofting process can have a significant effect on the transient behavior of the hillslope.

Figure 9 shows dimensionless hillcrest offset distances for runs with different values of θ_z and \hat{t}_{kpd} . These curves show that the trend in faster response times (lower κ values) for lower values of θ_z shortly after the passage of the knickpoint dominates the behavior of the hillcrest. Specifically, for lower values of θ_z the initial response of the hillcrest to perturbations is faster than for lower values of θ_z , and most of the divides motion occurs in these early stages. Recall that lower values of θ_z would result from shorter hillslopes, lower background incision rates, greater diffusivities, and greater soil production length scales.

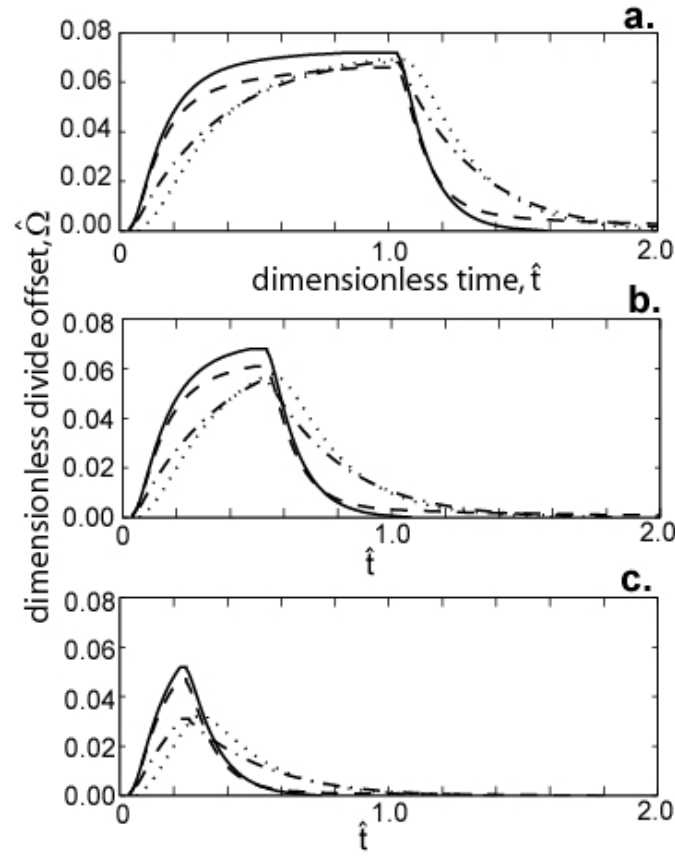


Figure 9. Hillcrest offset through dimensionless time for hillslopes with linear sediment transport, $\tau_d=2$, and $\theta_{kp}=0.3$. The solid lines have $\theta_z = 0.1$, the dashed lines have $\theta_z = 1.0$, the dash-dot lines have $\theta_z = 10$, and the dotted lines have $\theta_z = 100$. **a.** $t_{kpd} = 1$, **b.** $t_{kpd} = 0.5$, **c.** $t_{kpd} = 0.2$.

4.1.2. Linear-Critical Flux Law

When hillslope sediment transport follows the linear-critical sediment flux law (equation 8), we define θ_{kp} to be the ratio of the height of the knickpoints to \hat{Z}_{ls} . Unlike the linear case, linear-critical hillslopes with the same value of θ_z do not lead to identical hillcrest migration behavior if τ_d and θ_{kp} are the same. Because we do not have an analytical solution for the maximum offset distance as a function of the other model parameters, using equation (40) to calculate the decay rates is difficult because the final

state of the hillcrest may only be calculated by iterative numerical means. We have chosen instead to directly compare the motion of the hillcrest for various parameter values (Figure 10). For low relief slopes, the behavior of hillslopes with linear-critical sediment transport approximates the behavior of slopes with linear sediment transport for reasons discussed in section 3.1. As the relief increases, however, the nonlinear flux terms begin to dominate transport [Roering *et al.*, 2001], and the behavior of the hillcrest departs from the behavior of hillslopes with a linear sediment flux law.

Figure 10a compares the migration of the hillcrest for linear-critical slopes with varying dimensionless relief but identical values of θ_z . As the relief increases, the

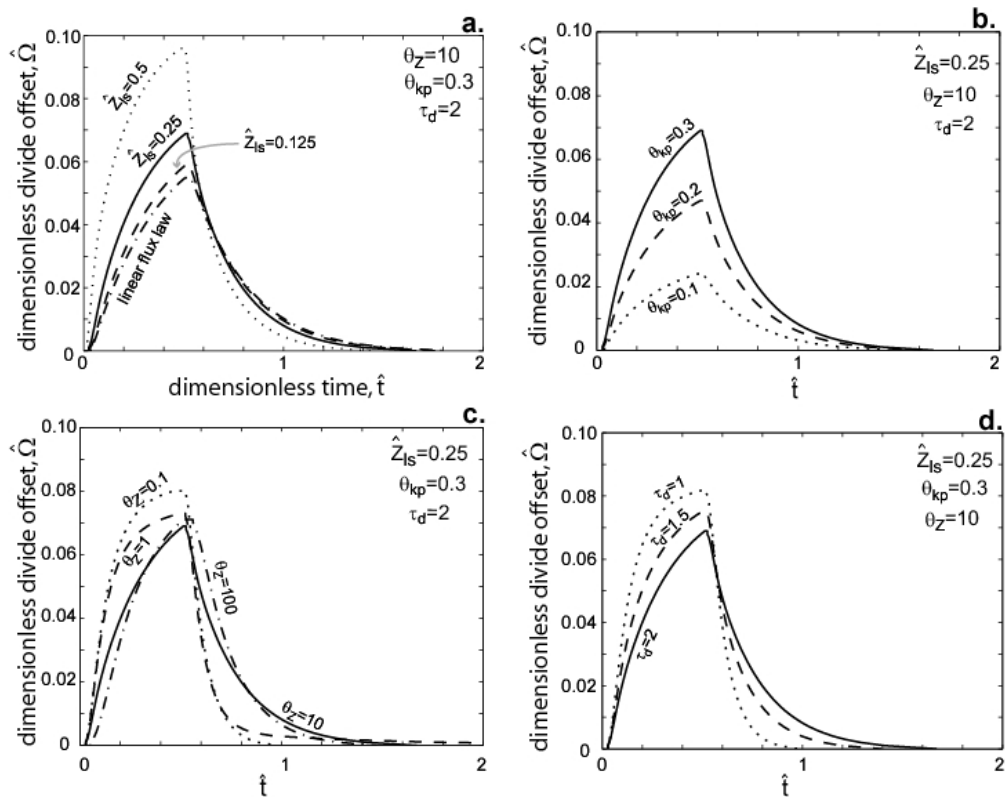


Figure 10. Hillcrest offset as a function of dimensionless time. All runs use a linear-critical sediment flux law unless where labeled. The knickpoint delay (t_{kpd}) is 0.5. **a.** Variations in Z_{ls} . **b.** Variations in θ_{kp} . **c.** Variations in θ_z . **d.** Variations in τ_d . The solid line in all four plots is from the same model run.

distance that the hillcrest migrates also increases. Although the hillcrest migrates further for the hillslopes with higher relief, the adjustment rate is faster such that they spend less time out of the symmetry after the second knickpoint has migrated past the base of the hillslope (Figure 10a). If the relief is held constant, varying the knickpoint ratio θ_{kp} affects the distance the hillcrest travels but has only a negligible effect on how long the hillcrest spends away from $\hat{x} = 1$ after the passage of the second knickpoint (Figure 10b). This implies that the adjustment rate for hillslopes with variations in θ_{kp} is approximately the same during the restore phase, a result that mirrors the behavior of the linear case (see Figure 8b). Similarly, the response of the hillcrest mirrors the linear case for variations in θ_z (Figure 10c) and τ_d (Figure 10d). As noted in section 4.1.1., the richest variation in the behavior of the hillcrest occurs when θ_z is varied. Variations in the dimensionless relief, the density ratio, and the knickpoint ratio lead to systematic variations in the response rate in that varying these parameters will either increase or decrease the response rate in the same manner regardless of the knickpoint delay.

4.1.3. Soil Storage and Thickness Effects

To track soil storage, we measure the ratio of the total storage of sediment on the hillslope at dimensionless time \hat{t} to the total soil storage at steady state. We name this ratio the soil storage ratio θ_{ss} . For both flux laws, the soil thickness, \hat{h} , reacts more slowly than the surface topography (Figure 7b) such that when the hillcrest returns to the symmetric position at $\hat{x} = 1$, the soil has not returned to a steady state (where $\partial\hat{h}/\partial\hat{t} = 0$ and $\theta_{ss} = 1$). Typical plots of the time evolution of soil storage after perturbations by knickpoints are shown in Figure 11. The lines in Figure 11 end when the hillcrest in the simulation has returned to the equilibrium position at $\hat{x} = 1$. The reduction in soil storage

on the hillslopes caused by the evacuation of sediment due to the knickpoints will be greater for increasing τ_d and θ_{kp} . Hillslopes with faster background incision rates \hat{l} have smaller changes in soil storage on the hillslope because slower incision rates lead to thicker soils, and the amount of sediment evacuated from the hillslope will be a smaller percentage of the total soil storage in thicker soils. We restrict our description of the dynamic behavior of soil storage following perturbation to this simple summary, as a detailed analysis is beyond the scope of this contribution.

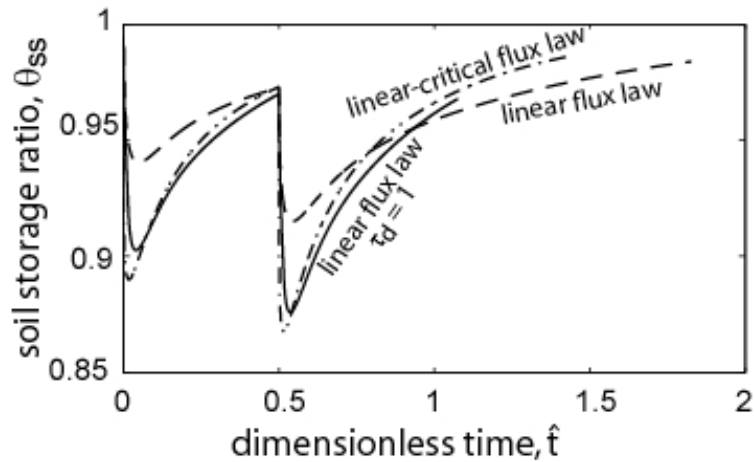


Figure 11. Change in soil storage ratio through time. All runs have $\theta_z=10$, $\hat{t}_{kpd} = 0.5$, and $\theta_{kp} = 0.3$. All plots have $\tau_d=2$ unless noted. Hillslope with linear-critical flux law has a Z_{ls} value of 0.5.

4.2. The Effect of Variations in Amplitude and Frequency of Incision Rates

The incision rate of a channel is related to water discharge and sediment flux [e.g., Howard et al., 1994; Sklar and Dietrich, 2004; Whipple and Tucker, 1999], both of which are likely to be stochastic in time [e.g., Snyder et al., 2003; Tucker, 2004]. The probability distribution of discharge and sediment flux will vary depending on the size of

the basin, so, for example, if two adjacent basins are of different size and are eroding at the same rate averaged over a time far greater than the time of individual events, one basin may be incising with frequent but low magnitude incision events while the other may be incising in infrequent but high magnitude events. This discrepancy in the frequency and magnitude of incision events in adjacent basins with the same long term lowering rate can perturb the location of the hillcrest separating these basins.

Here we approximate the time varying nature of stream incision by modeling the incision rate in the primary and secondary channels with sine waves of different amplitudes and frequencies. We make this simplification because the computational time required to run the large number of simulations that would need to be performed to quantify hillcrest migration based on a stochastic distribution is prohibitive. The approach of modeling erosion rate variability using sinusoidal functions has been taken by *Furbish and Fagherazzi* [2001] in investigating the transient response of a hillslope with a fixed hillcrest and a linear sediment flux law. Here we expand this analysis to investigate the behavior of the hillcrest as the two channels incise with the same average incision rate but with different frequencies and amplitudes.

We model adjacent channels that, on a long term average, incise at the same rate \hat{I}_{avg} . The incision rate of the primary channel has a dimensionless amplitude \hat{A}_p and a dimensionless period \hat{P}_p such that the incision rate of the primary channel (\hat{I}_p) through time is:

$$\hat{I}_p = \hat{I}_{avg} - \hat{A}_p \sin\left(\frac{2\pi}{\hat{P}_p} \hat{t}\right). \quad (42)$$

All dimensionless amplitudes and incision rates are scaled analogously to \hat{I} (see equation

13) and all dimensionless periods are scaled analogously to dimensionless time (see equation 15). The incision in the secondary channel has an amplitude and period that are related to the amplitude and period of the primary channel by

$$\hat{A}_s = \theta_A \hat{A}_p, \quad (43a)$$

$$\hat{P}_s = \theta_P \hat{P}_p. \quad (43b)$$

We call θ_A and θ_P the amplitude and period ratios, respectively. The downcutting rate of the secondary channel is then

$$\hat{I}_s = \hat{I}_{avg} - \theta_A \hat{A}_p \sin\left(\frac{2\pi}{\theta_P \hat{P}_p} \hat{t}\right). \quad (44)$$

We present here a general overview of the behavior of the hillslopes and hillcrests subject to sinusoidal variations in the downcutting rates of the bordering channels, rather than perform a complete study of parameter space. Our numerical experiments focus on hillslopes on which sediment transport can be described by the linear-critical sediment flux law. We illustrate typical behavior of the hillcrest for hillslopes where $\theta_z = 10$, $\hat{Z}_{ls} = 0.5$ (this means the relief of the linear-critical hillslope will be ~ 0.4 because the linear critical flux law limits the steepness of the hillslope gradient on high relief hillslopes), and $\tau_d = 2$. From the results in section 4.1.2., it should be noted that the hillcrest will move greater distances than the runs presented here if τ_d were reduced, and the hillcrest would move more slowly and move a shorter distance if \hat{Z}_{ls} were decreased.

If the two channels have different instantaneous incision rates (e.g., θ_A and θ_P are not equal to one), vertical channel offsets will be generated though time. Greater channel

offsets will lead to greater distances of hillcrest migration. The migration of the hillcrest is similar to the temporal pattern of channel offset, but the oscillation of the hillcrest will be damped and shifted in phase compared to the oscillations in the vertical channel offset. The phase shift is significant because it means that when vertical channel offsets are nil, the divide will still be offset.

Furbish and Fagherazzi [2001] found that higher frequency oscillations (e.g.,

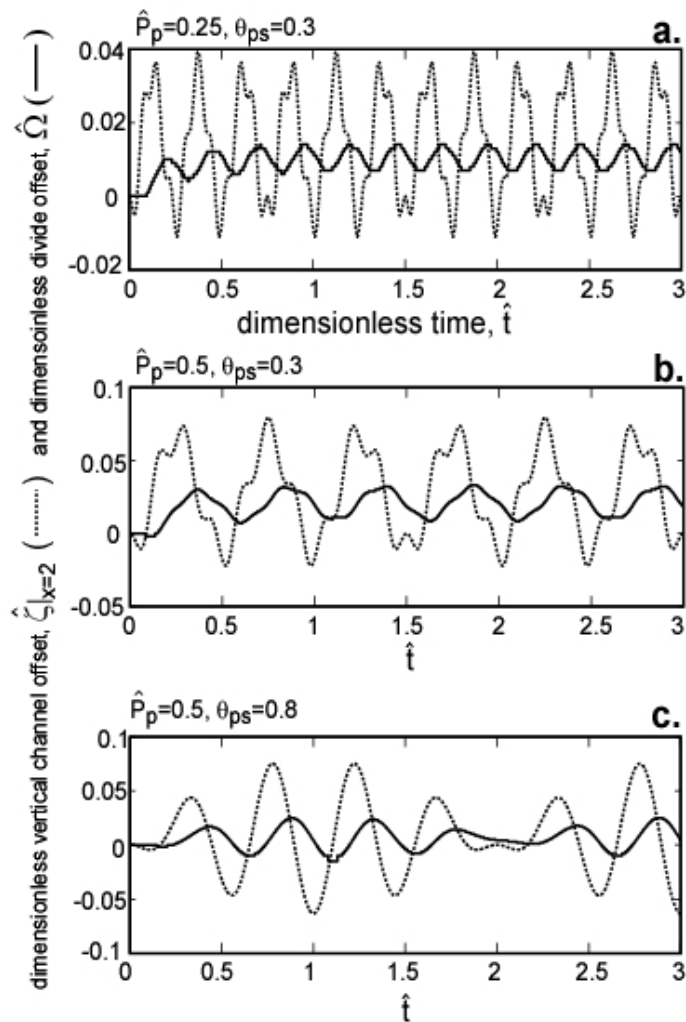


Figure 12. Vertical channel offset and hillcrest offset for hillslopes bounded by channels with oscillating incision rates. All runs use a linear-critical flux law and have $\theta_z=10$, $\tau_d=2$, $Z_{ls}=0.5$, $I_{avg}=-0.2$, $A_p=0.2$, and $\theta_A=1$. The dotted lines are the vertical channel offset and the solid lines are the hillcrest offset. The P_p and θ_p values are listed above each plot.

lower values of \hat{P}_p , more cycles of the incision rate in a given time period) in the channel incision rate are less likely to reach the drainage hillcrest than lower frequency oscillations (e.g., higher values of \hat{P}_p , fewer cycles of the incision rate in a given time period). We find this to be true in the case where the hillcrest is free to migrate and break the symmetry of the hillslope. The average offset over time may be solved analytically; this average offset will increase linearly with \hat{A}_p , increase monotonically with θ_A and \hat{P}_p , and decrease monotonically with θ_p .

Three examples of vertical channel offsets and hillcrest offsets as a function of time are plotted in Figure 12a,b, and c. The high frequency oscillations in Figure 12a result in smaller hillcrest offsets than the lower frequency examples of Figures 12b and 12c. The oscillations in the incision rate of the bounding channels will lead to oscillations in the vertical channel offset, and higher frequency oscillations in the vertical offset will be less likely to influence the migration of the hillcrest than lower frequency oscillations. Figure 12 demonstrates that the response of the hillcrest reflects the vertical channel offset, but this signal is damped and delayed. We point out that the dimensionless time \hat{t} is scaled by the diffusive timescale T_D , which ranges from 10^4 to 10^6 years [Mudd and Furbish, 2004]. Variations in downcutting on the human timescale (e.g., a 10 year cycle of incision rates caused by, for example, El Nino climate cycles, gives a \hat{P}_p of 10^{-5} for a 100m long hillslope with a diffusivity of $0.01 \text{ m}^2 \text{ yr}^{-1}$) will likely not be reflected in the hillcrest, whereas variations caused by long term climate change will be reflected in the motion of the hillcrest. In Figures 12a and b all parameters are the same except for the periods of the incision rate fluctuations. Note that in Figure 12a, which has a shorter period (lower \hat{P}_p), the hillcrest offset is a smaller fraction of the channel offset than in the

case of Figure 12b.

Consider a dimensional realization of figure 12 where the hillslope has a length of 20m and a diffusivity of $0.01 \text{ m}^2 \text{ yr}^{-1}$. This gives a T_D value of 40ka. The relief of the hillslope is $\sim 8\text{m}$. In the case of Figure 13a, where $\hat{P}_p = 0.25$, the incision rate of the primary channel varies over a period of 10ka, whereas the secondary channel varies over a period of 3ka ($\theta_p = 0.3$). These periods change to 20ka and 6.67ka for the hillslope modeled in Figure 12b ($\hat{P}_p = 0.5$, $\theta_p = 0.3$). In both these cases, the hillcrest will migrate with a period that is approximately the period of the primary (low frequency) channel (10ka and 20ka for Figures 12a and b, respectively). Dimensional vertical offsets between the two channels would be 0.8m in the case of Figure 12a and 1.6m, in the case of Figure 12b. The maximum hillcrest offsets would be 0.28m for the case of Figure 12a and 0.66m for the case of Figure 12b.

The damping of high frequency variations is also reflected in the soil storage and soil thickness. Figure 13 shows the spatial variation in soil thickness as a function of time. The secondary channel has higher frequency oscillations; these oscillations in soil thickness are not transmitted from the secondary channel to the hillcrest, rather the soil thickness at the hillcrest is dominated by the signal from the primary channel with a lower frequency of oscillation. In summary, the transient behavior of the surface topography, the location of the hillcrest, and the soil thickness will be dominated by channels whose incision rate varies with low frequency.

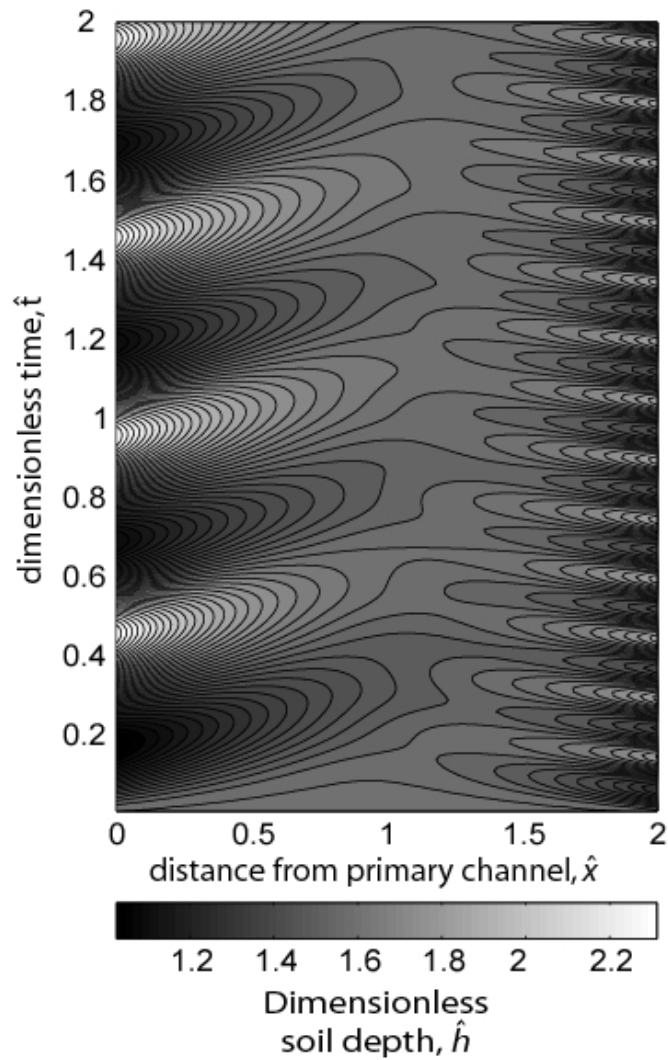


Figure 13. Soil thickness as a function of time and space for a hillslope bounded by channels with oscillating incision rates. A linear-critical flux law is used. Parameter values are $\theta_z=10$, $\tau_d=2$, $Z_{ls} = 0.5$, $I_{avg}=-0.2$, $A_p=0.2$, and $\theta_A=1$, $P_p=0.5$, and $\theta_p=0.3$.

5. Conclusions

We have investigated the behavior of lateral hillcrest offset and migration under conditions of vertical offsets in the elevation of channels bounding a hillcrest and locally varying incision rates in the bounding channels. For hillslopes on which sediment transport takes on specific transport relations (linear or linear-critical flux laws), the

offset from symmetry of the hillcrest is a geometric function of the vertical channel offset. The transient response of the hillcrest is faster for knickpoints with greater relief (larger θ_{kp} , the ratio between the relief of the knickpoint and the relief of the hillslope) and slower for increasing density ratios on the hillslope (the ratio of the dry bulk density of the rock to the dry bulk density of the soil, τ_d). The rate of hillcrest migration is sensitive to the ratio between the diffusive timescale of the hillslope and the time it takes to erode through a fixed thickness of soil (2γ) at the background incision rate; we name this ratio θ_z . Although the response rate of the hillcrest varies in time, most of the divide migration take place early after disturbance of a channel; the divide will migrate faster for lower values of θ_z . All else being equal, shorter hillslopes, lower background incision rates, greater diffusivities, and greater soil production length scales will lead to faster hillcrest migration. Within a reasonable range of parameter values (e.g, $\theta_z = 1-100$, $\tau_d = 1-2$, $\theta_{kp} = 0.1-0.3$), the divide offset will reach a significant portion (e.g., $\exp[-1]$) of its theoretical maximum offset within a fraction (e.g., <0.5) of the diffusive timescale ($T_D = \lambda^2/D$) of the hillslope. For hillslopes where sediment transport follows a linear-critical flux law, increasing hillslope relief will also lead to faster responses of the hillcrest to channel perturbations.

The hillcrests of hillslopes that are bounded by channels whose incision rates vary in time migrate in a manner that reflects the vertical channel offset generated by the transient channel downcutting rates. Higher frequency oscillations in the channel downcutting rate are less likely to influence the position of the hillcrest than low frequency oscillations. While we have not performed an exhaustive study of the effect of incision rate oscillations, we have found that for incision rates that vary periodically over

a time that is less than one quarter of the diffusive timescale ($T_D = \lambda^2/D$, for typical hillslopes $T_D = 10^3 - 10^7$ years), the migration of the hillcrest in our simulations was less than 2% of the hillslope length. If the incision rates of the two channels bounding a hillslope are periodic through time, then the horizontal offset of the hillcrest is also periodic in time. The oscillation of the hillcrest will be out of phase with the oscillation of the vertical offset of the channels, and we have found that the hillcrest can be in an asymmetric position when there is no difference in the elevation in the channels. If channels bounding a hillcrest are at the same elevation, but the hillcrest is not equidistant from the two channels, then this could be a indication of an imbalance in the erosion rates of the two channels bounding the hillslope.

We have focused primarily on situations in which the long term average incision rates in the two channels are the same. This situation leads to hillcrests that oscillate about a central location, but we do not invoke a feedback that can fix a hillcrest in a new location after a transient disturbance in the channel downcutting rates or permanently change the spatial distribution of the hillcrests. The presence of features such as stream capture in the field and the experiments of *Hasbargen and Paola* [2000] indicate that there may be positive feedbacks between divide migration, channel offsets, and local incision rates. It is generally agreed that the longitudinal profiles and incision rates of fluvial channels are nonlinearly related to both drainage area and sediment supply [e.g., *Sklar and Dietrich* 2004; *Whipple* 2004]. A migrating divide will change both the drainage area and sediment supply to the two channels bounding it. If a transient change in channel downcutting persists long enough and is great enough to change the drainage area or sediment supply in a manner that affects the incision rate and profile of the

channel, the position of the hillcrest may become ‘fixed’ such that the hillcrest does not move back to its original position, and the drainage basin configuration may change to reflect a new equilibrium configuration.

6. List of Symbols

\hat{A}_p, \hat{A}_s	Amplitude of the incision rate in the primary and secondary channel, respectively (dimensionless)
D	Sediment diffusivity ($L^2 T^{-1}$)
η	Elevation of soil-bedrock boundary (L)
η_0	Elevation of soil-bedrock boundary at $x = 0$ (L)
η_{bl}	Elevation of soil-bedrock boundary relative to base level (L)
$\hat{\eta}$	Dimensionless elevation of soil-bedrock boundary relative to base level
ϕ	Dimensionless function of slope that varies with the sediment flux law
γ	Soil production decay lengthscale (L)
h, \hat{h}	Soil thickness (L) and dimensionless soil thickness, respectively
I, \hat{I}	Dimensional ($L T^{-1}$) and dimensionless incision rate, respectively
\hat{I}_p	Incision rate of secondary channel (dimensionless)
\hat{I}_s	Incision rate of primary channel (dimensionless)
\hat{I}_{avg}	Long term average incision rate (dimensionless)
K	Sediment dispersion coefficient ($M L^{-1} T^{-1}$)
κ_p	Decay coefficient for the push phase of hillcrest migration (dimensionless)
κ_r	Decay coefficient for the restore phase of hillcrest migration (dimensionless)

λ	Length of the hillslope (half the distance between channels) (L)
$\hat{\Omega}$	Dimensionless hillcrest offset
$\hat{\Omega}_{lr}, \hat{\Omega}_{cs}$	Dimensionless hillcrest offset of a low relief and critical slope hillslope, respectively
p_{η}	Soil production rate (L T ⁻¹)
\hat{P}_p, \hat{P}_s	Period of the variation in incision rate in the primary and secondary channel, respectively (dimensionless)
$\bar{\rho}_s$	Depth averaged dry bulk density of hillslope soil (M L ⁻³)
ρ_{η}	Dry bulk density of parent material (M L ⁻³)
S_c	Critical slope for linear-critical flux law (dimensionless)
S_T	Threshold slope (dimensionless)
θ_L	Length ratio (dimensionless)
θ_t	Time ratio (dimensionless)
θ_{kp}	Knickpoint ratio (dimensionless)
θ_I	Incision ratio (dimensionless)
θ_O	Offset ratio (dimensionless)
θ_A	Amplitude ratio (dimensionless)
θ_P	Period ratio (dimensionless)
θ_{ss}	Soil storage ratio (dimensionless)
θ_Z	Ratio of erosion timescale to diffusive timescale (dimensionless)
τ_d	Density ratio (dimensionless)
t, \hat{t}	Dimensional (T) and dimensionless time
\hat{t}_{sc}	Dimensionless time to stream capture

\hat{t}_{kpd}	Dimensionless time of knickpoint delay
T_p	Production timescale (T)
T_D	Diffusive (or relaxation) timescale (T)
\hat{u}_d	Dimensionless velocity of the hillcrest
\bar{v}_x	Depth averaged sediment velocity in the x direction (L T ⁻¹)
W_0	Nominal rate of soil production (L T ⁻¹)
x, \hat{x}	Dimensional (L) and dimensionless distance from the primary channel
\hat{x}_d	Dimensionless location of the hillcrest
\hat{Z}	Dimensionless elevation of the hillcrest
\hat{Z}_{ls}	Dimensionless elevation of the hillcrest for a symmetric hillslope with a linear sediment flux law
ζ	Elevation of soil-bedrock boundary (L)
ζ_0	Elevation of soil-bedrock boundary at $x = 0$ (L)
ζ_{bl}	Elevation of soil-bedrock boundary relative to base level (L)
$\hat{\zeta}$	Dimensionless elevation of soil-bedrock boundary relative to base level

7. References

- Ahnert, F. (1967), The role of the equilibrium concept in the interpretation of landforms of fluvial erosion and deposition, in *L'evolution des Versants*, edited by P. Macar, pp. 23-41, Univ. of Liege, Liege, France.
- Anderson, R.S. (2002), Modeling the tor-dotted crests, bedrock edges, and parabolic profiles of high alpine surfaces of the Wind River Range, Wyoming, *Geomorphology*, 46 (1-2), 35-58.

- Andrews, D.J., and R.C. Bucknam (1987), Fitting degradation of shoreline scarps by a nonlinear diffusion-model, *Journal of Geophysical Research-Solid Earth and Planets*, 92 (B12), 12857-12867.
- Benda, L., and T. Dunne (1997), Stochastic forcing of sediment routing and storage in channel networks, *Water Resources Research*, 33 (12), 2865-2880.
- Bishop, P., R.W. Young, and I. Mcdougall (1985), Steam profile change and longterm landscape evolution - early Miocene and modern rivers of the East Australian Highland Crest, central New-South-Wales, Australia, *Journal of Geology*, 93 (4), 455-474.
- Bras, R.L., G.E. Tucker, and V. Teles (2003), Six myths about mathematical modeling in geomorphology, in *Prediction in Geomorphology*, edited by P.R. Wilcock, and R.M. Iverson, pp. 63-79, American Geophysical Union, Washington, D. C.
- Brimhall, G.H., O.A. Chadwick, C.J. Lewis, W. Compston, I.S. Williams, K.J. Danti, W.E. Dietrich, M.E. Power, D. Hendricks, and J. Bratt (1992), Deformational mass-transport and invasive processes in soil evolution, *Science*, 255 (5045), 695-702.
- Burbank, D.W., J. Leland, E. Fielding, R.S. Anderson, N. Brozoic, M.R. Reid, and C. Duncan (1996), Bedrock incision, rock uplift and threshold hillslopes in the northwestern Himalayas, *Nature*, 379 (8), 505-510.
- Chen, Y.G., W.S. Chen, Y. Wang, P.W. Lo, T.K. Liu, and J.C. Lee (2002), Geomorphic evidence for prior earthquakes: lessons from the 1999 Chichi earthquake in central Taiwan, *Geology*, 30 (2), 171-174.
- Crosby, B.T., and K.X. Whipple (2005), Knickpoint initiation and distribution within fluvial networks: 236 waterfalls in the Waipaoa River, North Island, New Zealand, *Geomorphology*, in press.
- Culling, W.E.H. (1963), Soil creep and the development of hillside slopes, *Journal of Geology*, 71 (2), 127-161.
- Densmore, A. L., M. A. Ellis, and R. S. Anderson (1998), Landsliding and the evolution of fault bounded mountains, *Journal of Geophysical Research*, 103, 15,203–15,219.
- Dietrich, W.E., D.G. Bellugi, L.S. Sklar, and J.D. Stock (2003), Geomorphic transport laws for predicting landscape form and dynamics, in *Prediction in Geomorphology*, edited by P.R. Wilcock, and R.M. Iverson, American Geophysical Union, Washington, D. C.
- Fernandes, N.F., and W.E. Dietrich (1997), Hillslope evolution by diffusive processes: The timescale for equilibrium adjustments, *Water Resources Research*, 33 (6),

1307-1318.

- Finlayson, D.P., D.R. Montgomery, and B. Hallet (2002), Spatial coincidence of rapid inferred erosion with young metamorphic massifs in the Himalayas, *Geology*, 30 (3), 219-222.
- Furbish, D.J. (2003), Using the dynamically coupled behavior of the land-surface geometry and soil thickness in developing and testing hillslope evolution models, in *Prediction in Geomorphology*, edited by P.R. Wilcock, and R.M. Iverson, American Geophysical Union, Washington, D. C.
- Furbish, D.J., and S. Fagherazzi (2001), Stability of creeping soil and implications for hillslope evolution, *Water Resources Research*, 37 (10), 2607-2618.
- Gabet, E.J. (2000), Gopher Bioturbation: Field evidence for non-linear hillslope diffusion, *Earth Surface Processes and Landforms*, 25 (13), 1419-1428.
- Gabet, E.J., O.J. Reichman, and E.W. Seabloom (2003), The Effects of bioturbation on soil processes and sediment transport, *Annual Reviews of Earth and Planetary Science*, 31, 249-73.
- Gilbert, G.K. (1877), Report on the geology of the Henry Mountains: U.S. Geographical and Geological Survey of the Rocky Mountain Interior Region, pp. 160, U.S. Government Printing, Washington D.C.
- Hack, J.T. (1960), Interpretation of erosional topography in humid temperate region, *American Journal of Science*, 258-A, 80-97.
- Harbor, D.J. (1997), Landscape evolution at the margin of the Basin and range, *Geology*, 25 (12), 1111-1114.
- Hasbargen, L.E., and C. Paola (2000), Landscape instability in an experimental drainage basin, *Geology*, 28 (12), 1067-1070.
- Heimsath, A.M., W.E. Dietrich, K. Nishiizumi, and R.C. Finkel (1999), Cosmogenic nuclides, topography, and the spatial variation of soil depth, *Geomorphology*, 27 (1-2), 151-172.
- Heimsath, A.M., J. Chappell, W.E. Dietrich, K. Nishiizumi, and R.C. Finkel (2000), Soil Production on a Retreating Escarpment in Southeastern Australia, *Geology*, 28 (9), 787-790.
- Heimsath, A.M., J. Chappell, W.E. Dietrich, K. Nishiizumi, and R.C. Finkel (2001), Late Quaternary Erosion in Southeastern Australia: a Field Example Using Cosmogenic Nuclides, *Quaternary International*, 83-5, 169-185.

- Heimsath, A.M., J. Chappell, N.A. Spooner, and D.G. Questiaux (2002), Creeping soil, *Geology*, 30 (2), 111-114.
- Howard, A.D. (1988), Equilibrium models in geomorphology, in *Modeling in Geomorphic Systems*, edited by M.G. Anderson, pp. 49-72, John Wiley, New York.
- Howard, A.D. (1994), A Detachment-limited model of drainage-basin evolution, *Water Resources Research*, 30 (7), 2261-2285.
- Howard, A.D., W.E. Dietrich, and M.A. Siedl (1994), Modeling fluvial erosion on regional to continental scales, *Journal of Geophysical Research*, 99, 13971-13986.
- Jyotsna, R., and P.K. Haff (1997), Microtopography as an indicator of modern hillslope diffusivity in arid terrain, *Geology*, 25 (8), 695-698.
- Kirchner, J.W., R.C. Finkel, C.S. Riebe, D.E. Granger, J.L. Clayton, J.G. King, and W.F. Megahan (2001), Mountain erosion over 10 yr, 10 k.y., and 10 m.y. time scales, *Geology*, 29 (7), 591-594.
- Kirkby, M.J. (1967), Measurement and theory of soil creep, *Journal of Geology*, 75 (4), 359-378.
- Kobor, J.S., and J.J. Roering (2004), Systematic variation of bedrock channel gradients in the central Oregon Coast Range: implications for rock uplift and shallow landsliding, *Geomorphology*, 62 (3-4), 239-256.
- Mather, A.E., A.M. Harvey, and M. Stokes (2000), Quantifying long-term catchment changes of alluvial fan systems, *Geological Society of America Bulletin*, 112 (12), 1825-1833.
- Matmon, A., P.R. Bierman, J. Larsen, S. Southworth, M. Pavich, R. Finkel, and M. Caffee (2003), Erosion of an ancient mountain range, the Great Smoky Mountains, North Carolina and Tennessee, *American Journal of Science*, 303 (9), 817-855.
- McKean, J.A., W.E. Dietrich, R.C. Finkel, J.R. Southon, and M.W. Caffee (1993), Quantification of soil production and downslope creep rates from cosmogenic Be-10 accumulations on a hillslope profile, *Geology*, 21 (4), 343-346
- Meigs, A., N. Brozovic, and M.L. Johnson (1999), Steady, balanced rates of uplift and erosion of the Santa Monica Mountains, California, *Basin Research*, 11 (1), 59-73.
- Meyerhof, H.A. (1972), Postorogenic development of Appalachians, *Geological Society of America Bulletin*, 83 (6), 1709-1727.
- Mudd, S.M., and D.J. Furbish (2004), The Influence of chemical denudation on hillslope morphology, *Journal of Geophysical Research*, 109 (F02001),

doi:10.1029/2003JF000087.

- Pelletier, J.D. (2004), Persistent drainage migration in a numerical landscape evolution model, *Geophysical Research Letters*, 31 (20), doi: 10.1029/2004GL020802.
- Reneau, S.L., and W.E. Dietrich (1991), Erosion rates in the southern Oregon Coast Range - evidence for an equilibrium between hillslope erosion and sediment yield, *Earth Surface Processes and Landforms*, 16 (4), 307-322.
- Riebe, C.S., J.W. Kirchner, D.E. Granger, and R.C. Finkel (2000), Erosional equilibrium and disequilibrium in the Sierra Nevada, inferred from cosmogenic Al-26 and Be-10 in alluvial sediment, *Geology*, 28 (9), 803-806.
- Roering, J.J., P. Almond, P. Tonkin, and J. McKean (2002), Soil transport driven by biological processes over millennial time scales, *Geology*, 30 (12), 1115-1118.
- Roering, J.J., J.W. Kirchner, and W.E. Dietrich (1999), Evidence for nonlinear, diffusive sediment transport on hillslopes and implications for landscape morphology, *Water Resources Research*, 35 (3), 853-870.
- Roering, J.J., J.W. Kirchner, and W.E. Dietrich (2001), Hillslope evolution by nonlinear, slope-dependent transport: steady state morphology and equilibrium adjustment timescales, *Journal of Geophysical Research-Solid Earth*, 106 (B8), 16499-16513.
- Sklar, L.S., and W.E. Dietrich (2004), A mechanistic model for river incision into bedrock by saltating bed load, *Water Resources Research*, 40, W06301, doi:10.1029/2003WR002496.
- Small, E.E., R.S. Anderson, and G.S. Hancock (1999), Estimates of the rate of regolith production using Be-10 and Al-26 from an alpine hillslope, *Geomorphology*, 27 (1-2), 131-150.
- Smith, T.R., and F.P. Bretherton (1972), Stability and the conservation of mass in drainage basin evolution, *Water Resources Research*, 8 (6), 1506-1528.
- Snyder, N.P., K.X. Whipple, G.E. Tucker, and D.J. Merritts (2003), Importance of a stochastic distribution of floods and erosion thresholds in the bedrock river incision problem, *Journal of Geophysical Research-Solid Earth*, 108 (B2), 2117, doi:10.1029/2001JB001655.
- Tucker, G.E. (2004), Drainage basin sensitivity to tectonic and climatic forcing: implications of a stochastic model for the role of entrainment and erosion thresholds, *Earth Surface Processes and Landforms*, 29, 185-205.
- Tucker, G.E., and R.L. Bras (1998), Hillslope processes, drainage density, and landscape morphology, *Water Resources Research*, 34 (10), 2751-2764.

- van der Beek, P., M.A. Summerfield, J. Braun, R.W. Brown, and A. Fleming (2002), Modeling postbreakup landscape development and denudational history across the southeast African (Drakensberg Escarpment) margin, *Journal of Geophysical Research*, 107 (B12), 2351, doi:10.1029/2001JB000744.
- Whipple, K.X., and G.E. Tucker (1999), Dynamics of the stream-power river incision model: Implications for height limits of mountain ranges, landscape response timescales, and research needs, *Journal of Geophysical Research-Solid Earth*, 104 (B8), 17661-17674.
- Whipple, K.X. (2004), Bedrock rivers and the geomorphology of active orogens, *Annual Review of Earth and Planetary Sciences*, 32, 151-185.
- Willgoose, G., R.L. Bras, and I. Rodriguez-Iturbe (1991), A coupled channel network growth and hillslope evolution model .1. Theory, *Water Resources Research*, 27 (7), 1671-1684.
- Young, A. (1978), A twelve-year record of soil movement on a slope, *Z. Geomorph. Suppl. Bd.*, 29, 104-110.
- Young, R., and I. McDougall (1993), Long-term landscape evolution - early Miocene and modern rivers in southern New South Wales, Australia, *Journal of Geology*, 101 (1), 35-49.
- Zaprowski, B.J., E.B. Evenson, F.J. Pazzaglia, and J.B. Epstein (2001), Knickzone propagation in the Black Hills and northern High Plains: A different perspective on the late Cenozoic exhumation of the Laramide Rocky Mountains, *Geology*, 29 (6), 547-550.

CHAPTER V

RESPONSES OF SOIL MANTLED HILLSLOPES TO TRANSIENT CHANNEL INCISION RATES

Abstract

Channel incision drives hillslope morphology in soil mantled hillslopes. When channel incision rates change, numerous hillslope soil properties (e.g., surface topography, erosion rates, soil thickness, soil production) adjust as a response to this change in the lower boundary of the hillslope. Here we investigate the timescales of adjustment of the properties of soil mantled hillslopes when channel incision rates change in time. An idealized soil mantled hillslope (linear sediment flux law, soil density equal to bedrock density) is first investigated and the transient evolution of this hillslope is determined analytically. This analysis reveals two dominant timescales of adjustment. The longer of these two timescale determines at what rate the entire hillslope adjusts to a change in channel incision rates, and is proportional to $4\lambda^2/(\pi^2 D)$ where λ is the length of the hillslope and D is the sediment diffusivity. Numerical simulations are then performed that examine responses of hillslopes that incorporate non-linear responses to transient channel incision (e.g., hillslopes that experience non-linear sediment transport, have soil thickness that responds to the soil production function). Using these numerical models we show that the ratio between the density of the soil (ρ_s) and the density of the soils' parent material (ρ_η) can alter the long term response of the hillslope to changes in channel incision rates such that the characteristic timescale becomes $4\rho_\eta\lambda^2/(\pi^2 D\rho_s)$. In addition, we show that the adjustment of the soil erosion rate, the soil production rate, and the soil thickness have different characteristic timescales.

1. Introduction

The evolution of soil mantled landscapes is driven, in part, by channels at the base of hillslopes that erode through the landscape and remove the sediment that is delivered to them by the hillslopes. The relationship between channel erosion rates and hillslope evolution has been a focus of geomorphic research for over a century [e.g., *Davis* 1899; *Gilbert* 1877; *Hack* 1960; *King* 1953, *Penck* 1972]. Modern understanding of the response of hillslope soils to changes in channel incision rates has followed the work of *W. E. H. Culling* [1960], who first applied a rigorous statement of mass conservation to an eroding hillslope soil.

Gibert [1909] suggested that the erosion rate of a hillslope soil is proportional to the topographic gradient, an observation that has been confirmed by a number of studies [e.g., *Dietrich et al.* 2003 and references therein]. When channel incision rates change, several properties of the soil adjust in response. If, for example, the channel incision rate increases, the hillslope responds by steepening near the channel. As a result, soil thins near the channel. The steeping of soil near the channel removes sediment slightly upslope, thus steepening and removing soil at that location. In this way changes in channel incision rates result in changes in soil properties that propagate away from the channel [e.g., *Furbish and Fagherrazzi* 2001; *Mudd and Furbish*, 2005; *Roering et al.*, 2001].

The adjustments of the soil to changes in channel incision rates exhibit characteristic timescales [e.g., *Ahnert*, 1987; *Fernandes and Dietrich*, 1997; *Furbish and Fagherrazi* 2001; *Jyotsna and Haff*, 1997; *Roering et al.* 2001]. These timescales include

the time it takes hillslopes to adjust to a new channel incision rate (the hillslope relaxation time, *e.g.*, *Ahnert*, [1987]), and the time needed for signals to propagate a certain distance upslope [*e.g.*, *Furbish and Fagherrazzi* 2001].

It is useful to quantify these timescales for studies of both hillslope and fluvial geomorphology for two reasons. First, the timescale of transient hillslope response to changes in the channel incision rate provides an estimate the period over which the resulting changes in soil properties are likely to be stored on the hillslope. Second, the adjustment timescale of a hillslope soil responding to a change in channel incision rate must be known in order to evaluate whether it is appropriate to assume that a landscape has achieved a steady state or equilibrium condition. An equilibrium condition may be defined as the condition achieved when hillslopes have adjusted to match channel incision rates such that the surface topography of the landscape does not change in time [*e.g.*, *Carson and Kirkby*, 1972; *Gilbert* 1909; *Hack*, 1960; *Howard*, 1988].

Here we extend the work of *Fernandes and Dietrich* [1997] and *Roering et al.* [2001], who examined the timescales over which hillslope soils respond to changes in channel incision rates, by including not only the response of hillslope erosion rates and surface topography but also the soil thickness. For sufficiently simple conditions, the equations that govern the evolution of hillslope soils may be solved analytically. These solutions can then be used to elucidate how hillslope soils respond to changes in channel incision rates. Namely, these solutions allow for extraction of two timescales: one that can be used to estimate the adjustment rate of the entire hillslope to changes in channel incision rates and another that can be used to estimate the rate of propagation of the transient channel incision signal away from the channel. In addition, we use numerical

simulations to demonstrate that if channel incision rates are perturbed the response of different hillslope properties, such as the erosion rate, the soil thickness, and the soil production rate, will respond on different characteristic timescales such that although, for example, if the erosion rate of the hillslope has equilibrated to a change in channel incision rate the soil thickness may still be experiencing transient behavior.

2. Mass Conservation of Eroding Hillslope Soils

We begin by considering soil mantled landscapes in which the transport of soil due to landsliding and overland flow is insignificant. We define the soil layer as the near surface material that is being mechanically disturbed by processes such as soil creep [e.g., *Culling*, 1963; *Heimsath et al.*, 2002; *Kirkby*, 1967; *Roering et al.*, 1999; *Young*, 1978], animal burrowing and disturbance [e.g., *Gabet*, 2000; *Yoo et al.* 2005], frost heave processes [e.g., *Anderson*, 2002], and tree throw and root growth [e.g., *Gabet et al.*, 2003; *Roering et al.*, 2002]. In the presence of topographic gradients, this mechanically active layer is transported downslope. Underlying this mechanically active soil layer is a mechanically undisturbed saprolite layer. Material is entrained from the mechanically inactive saprolite into the mechanically active soil layer through soil production [e.g., *Carson and Kirkby*, 1972, *Heimsath*, 1997]. Once soil is produced, it can either accumulate on the land surface or be removed through either mechanical or chemical denudation processes.

Consider a one dimensional hillslope that has a mantle of soil with a thickness h (L), a surface elevation ζ (L) (Figure 1), and a soil-saprolite boundary that is at an

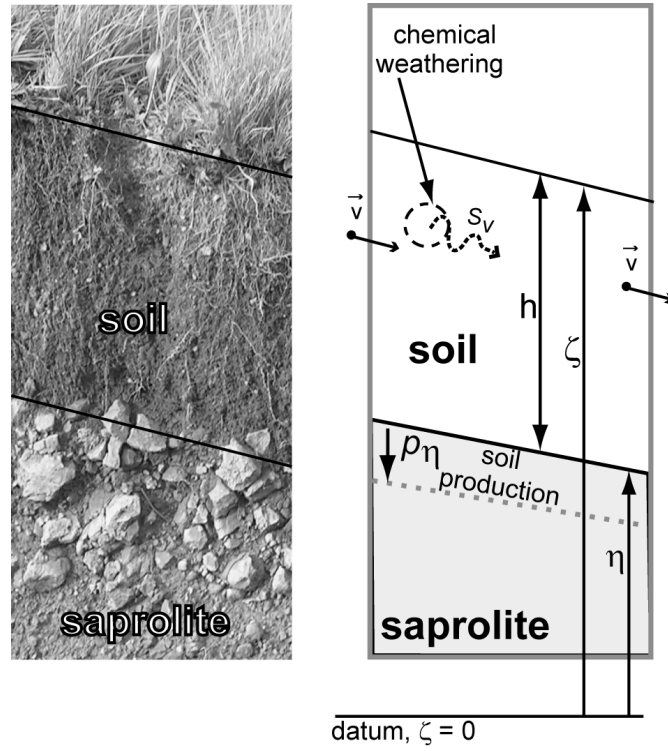


Figure 1. Schematic of the soil profile.

elevation η (L) (Figure 1), such that the soil thickness is equal to:

$$h = \zeta - \eta. \quad (1)$$

A depth integrated [e.g., *Mudd and Furbish, 2004; Paola and Voller, 2005*] statement of mass conservation for the hillslope soil is

$$\frac{\partial h}{\partial t} = -\frac{\partial(h\bar{v}_x)}{\partial x} + \frac{\rho_\eta}{\rho_s} p_\eta, \quad (2)$$

where ρ_s ($M L^{-3}$) is the dry bulk density of the soil, v_x ($L T^{-1}$) is the bulk velocity of the sediment in the x -direction, ρ_η ($M L^{-3}$) is the density of the parent material, p_η ($L T^{-1}$) is the rate of bedrock lowering due to soil production, and the overbars denote depth-averaged quantities. All terms in equation (2) represent rates of change in the soil

thickness, in units of length per time. The first term on the right of the equality is the rate of change in the soil thickness due to mechanical sediment transport processes and the last term is the rate of change in the soil thickness due to soil production. Equation (2) assumes that there is no deposition or erosion at the surface of the soil (i.e., all sediment transport occurs as movement within the mechanically active soil layer), no denudation occurs by chemical processes, and that soil bulk density does not vary in space or time.

The lowering of the soil-saprolite boundary is determined by the soil production rate

$$\frac{\partial \eta}{\partial t} = -p_{\eta}. \quad (3)$$

Note that by convention, the production rate is defined as positive down. Combining equations (1-3), the change in the surface elevation with respect to time is

$$\frac{\partial \zeta}{\partial t} = -\frac{\partial (h \bar{v}_x)}{\partial x} + \left(\frac{\rho_{\eta}}{\rho_s} - 1 \right) p_{\eta}. \quad (4)$$

3. Timescales of Adjustment to Transient Channel Incision for a Simplified Soil Mantled Hillslope

A simplified version of equation (4) can be solved analytically in order to examine the basic behavior of soil mantled landscapes as they respond to changes in channel incision rates. The value of this analysis is that it provides a way to concisely define both short and long timescales that characterize the transient response of a hillslope to a change in the channel incision rate, including how these timescales vary

with hillslope position, and which are not readily accessible from direct numerical solutions of the governing equations. In addition, the analytical analysis clarifies key points introduced in the seminal work of *Culling* [1965], as will be described later in this section. Analytical solutions also provide an important benchmark for understanding numerical solutions and results of others [e.g. *Fernandes and Dietrich, 1997; Roering et al. 2001*] aimed at defining characteristic timescales of response.

We first assume that the density of the saprolite is the same as the density of the soil ($\rho_s = \rho_n$), and that sediment transport is linearly proportional to slope:

$$h \bar{v}_x = -D \frac{\partial \zeta}{\partial x} \quad (5)$$

where D [$L^2 T^{-1}$] is a sediment diffusivity. It is assumed that the diffusivity is not a function of space. With these assumptions, equation (4) reduces to

$$\frac{\partial \zeta}{\partial t} = D \frac{\partial^2 \zeta}{\partial x^2}. \quad (6)$$

Culling [1965] recognized that equation (6) was analogous to the equation describing the conduction of heat in a solid, and that this equation may be solved analytically using the finite Fourier transform method [e.g., *Carslaw and Jeager, 1960; Deen 1998*].

In order to solve equation (6), both boundary and initial conditions must be assigned. We consider a hillslope with a divide at the location $x = 0$ (Figure 2). No sediment passes across the divide such that the divide serves as a no flux boundary condition for the one dimensional hillslope (i.e., $\partial \zeta / \partial x = 0$ at $x = 0$). A channel is at the location $x = \lambda$ (Figure 2). The channel, as it erodes through bedrock or sediment and

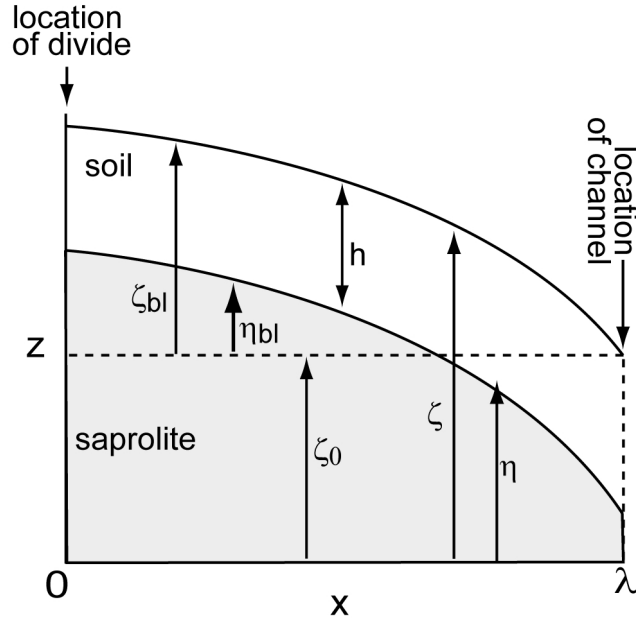


Figure 2. Schematic of the 1-D hillslope.

removes soil delivered to it by the hillslope, serves as the second boundary condition.

The initial condition is selected such that the hillslope topography is in equilibrium with an initial channel incision rate of I_0 ($L T^{-1}$) such that the entire hillslope is eroding at that rate. The incision rate then changes to a different rate I ($L T^{-1}$). If a coordinate system is selected such that the channel at $x = \lambda$ is always at $\zeta = 0$, the solution to equation (6), with the above boundary and initial conditions, is:

$$\zeta_{bl}(x, t) = \frac{16 \lambda^2}{D \pi^3} \sum_{n=0}^{\infty} \frac{(-1)^n}{(1+2n)^3} \left[(I_0 - I) e^{-\frac{D \pi^2 (1+2n)^2 t}{4 \lambda^2}} + I \right] \cos \left[\frac{\pi (1+2n) x}{2 \lambda} \right], \quad (7)$$

where the subscript bl indicates that the surface topography is measured relative to the elevation of the channel (Figure 2). Equation (7) differs from the solution presented in *Culling* [1965] in that the channel is eroding through the bed and equation (7) explicitly includes the initial hillslope adjusted to a downcutting rate of I_0 . In contrast, *Culling*

[1965] presented solutions for both a hillslope whose channel stayed at a constant elevation and that eroded to a plane, and also a hillslope bounded at both sides by channels that incised at a constant rate.

The erosion rate of the hillslope soil as a function of time and space can be found by differentiating equation (7):

$$\frac{\partial \zeta}{\partial t} = -I - \frac{4}{\pi} (I_0 - I) \sum_{n=0}^{\infty} \frac{(-1)^n}{(1+2n)} e^{-\frac{D\pi^2(1+2n)^2 t}{4\lambda^2}} \cos\left[\frac{\pi(1+2n)x}{2\lambda}\right]. \quad (8)$$

Note that the erosion rate in equation (8) is measured relative to a fixed datum (i.e., not relative to the incision rate of the channel). An example of a hillslope responding to a change in the rate of channel incision at its base as described by equations (7) and (8) is shown in Figure 3.

Howard [1988] suggested that the adjustment of a hillslope to a step change in the channel incision rate can be approximated by an exponential decay function of the form

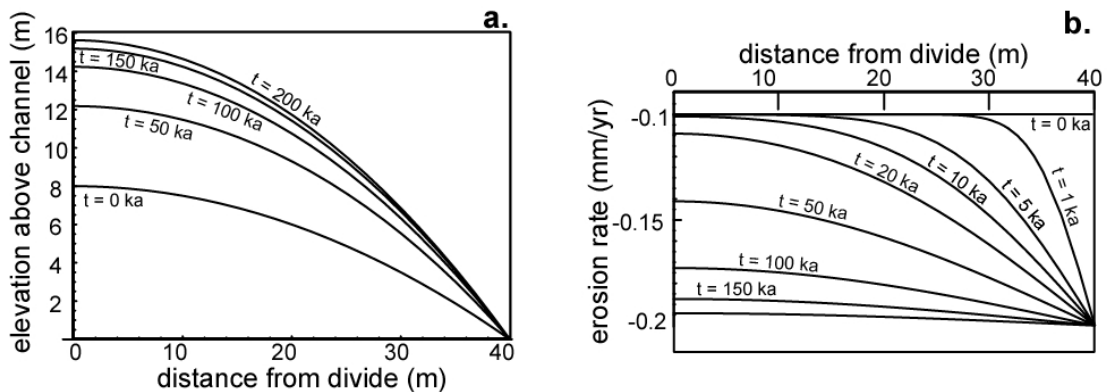


Figure 3. Analytical solutions of equation (6) for surface topography (a.) and erosion rate (b.). The hillslope is 40m long ($\lambda=40\text{m}$) and has a diffusivity (D) of $0.01 \text{ m}^2 \text{ yr}^{-1}$. Initially, the hillslope topography reflects a steady condition adjusted to a channel incision rate (I_0) of 0.0001 m yr^{-1} . At time $t = 0$ the channel incision rate is increased to 0.0002 m/yr^{-1} .

$$F(t) = F_f + (F_i - F_f) e^{-\frac{t}{\tau}}, \quad (9)$$

where F is a time dependant function, F_f is the value of the function at its final equilibrium value, F_i is the initial value of the function, and τ (T) is a timescale that characterizes the rate at which the transient signal decays (e.g., if $t = 3\tau$ the function is within 5% of the final equilibrium value). Both *Roering et al.* [2001] and *Mudd and Furbish* [2005] used equation (9) to estimate hillslope response timescales, but as observed by *Mudd and Furbish* [2005], this approach may not be adequate to fully characterize the response timescales of soil mantled hillslopes.

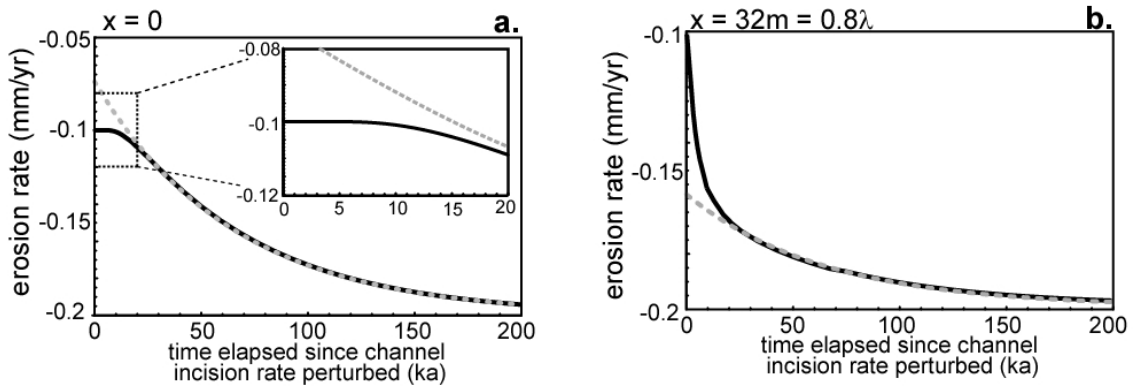


Figure 4. The true erosion rate (solid lines) and erosion rate predicted by fitting equation (11) (dashed grey lines) as a function of time at the divide (**a.**, $x = 0$) and a point near the channel (**b.** $x = 32\text{m} = 0.8\lambda$). The hillslope is the same as that described in Figure 3.

Equation (9) may be used to fit values of the timescale of the hillslope response to changes in the channel incision rate (τ) at different points on the hillslope, and this fit may be compared with the precise timescale of response extracted from equation (8).

Figure 4 shows a comparison of the precise erosion rate predicted by equation (8) and the

erosion rate based on the simple exponential response described by equation (9) as a function of time. Near the channel, the hillslope responds rapidly to the perturbation in the channel incision rate (Figure 4b), whereas at points near the divide (Figure 4a) the perturbation is only felt after some delay (as identified by *Roering et al.* [2001] in their Figure 8). As time increases, equation (9) can approximate the response of the hillslope, but it does not capture the shorter timescale behavior that causes a fast response near the channel and a delayed response near the divide (Figure 4).

As observed by *Culling* [1965] and embodied in equation (7) and equation (8), the response of the hillslope can be described by a sum of harmonic functions. Each wavenumber (i.e., $n = 0, 1, 2, 3, \dots$) in the series of harmonic functions has a different characteristic timescale, analogous to τ in equation (9). The timescale for each harmonic function, τ_n (T), is

$$\tau_n = \frac{4\lambda^2}{D\pi^2(1+2n)^2}. \quad (10)$$

As the wavenumber increases, the characteristic timescale decreases, such that the long-term behavior of the hillslope is dominated by the wavenumber $n = 0$, or in other words, $\tau_0 = 4\lambda^2/(D\pi^2) = 0.4053\lambda^2/D$, which is equivalent to the relaxation timescale found numerically by *Roering et al.* [2001] for hillslopes whose sediment flux is a linear function of slope. The effect of different wavenumbers on the erosion rate of a hillslope whose channel incision rate has been perturbed is plotted in Figure 5.

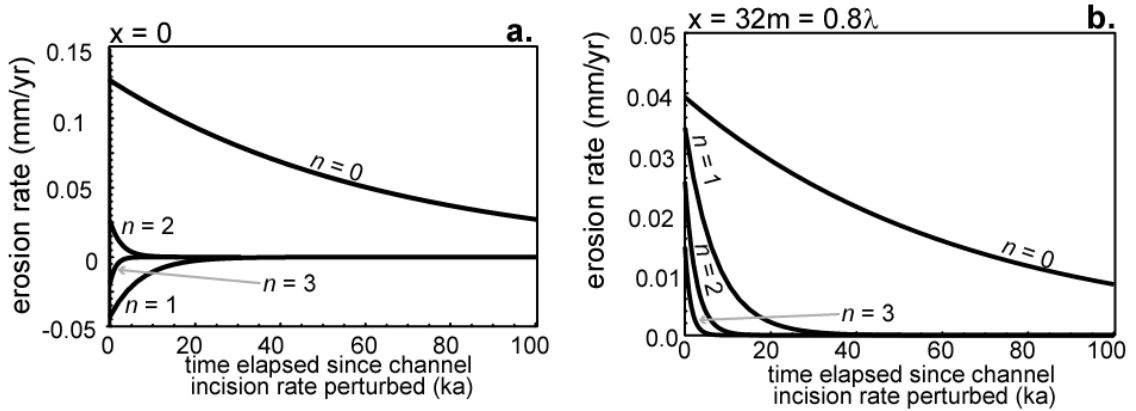


Figure 5. Erosion rate due to individual harmonics on a perturbed hillslope as a function of time. Plot **a.** shows harmonics at the divide ($x = 0$) and plot **b.** shows harmonics at a point near the channel ($x = 32\text{m} = 0.8\lambda$). Note that the total erosion rate is the sum of all harmonics minus the perturbed incision rate I (see equation 10).

Because signals propagate away from the channel, the transient response of the hillslope due to the effects of higher wavenumbers (i.e., $n > 0$) varies as a function of distance from the channel (Figure 5). Near the channel, the effects of the harmonics with higher wavenumber (e.g., $n > 0$) combine to cause the hillslope to respond rapidly to the change in the rate of channel incision; this rapid incision is not captured by equation (9) (see Figure 4b). On the other hand, the effect of the harmonics with higher wavenumbers is to reduce the erosion rate near the divide (Figure 5a). This reduction in the erosion rate due to the harmonic functions with the higher wave numbers, and therefore more rapid response timescales, is what causes the delay in the response of the erosion rate at the divide (Figure 4a).

The relative importance of individual harmonic functions, and therefore the relative importance of different response timescales (i.e., equation 10), may be determined by comparing the coefficients that multiply the time-varying exponential term

in equation (8). We define a function:

$$M_E(n, x) = \frac{(-1)^n}{(1 + 2n)} \cos\left[\frac{(1 + 2n)\pi x}{2\lambda}\right] \sec\left[\frac{\pi x}{2\lambda}\right], \quad (11)$$

where M_E is the ratio of the coefficients that multiply the time varying exponential term of equation (8) for a wavenumber n to the coefficient when the wavenumber, n , is zero. By definition, M_E is equal to one when $n = 0$. For $n \neq 0$, M_E reflects the proportion of the erosion rate (M_E) signal that is contributed by the harmonic with wavenumber n . Because each harmonic function decays over the timescale described by equation (10), M_E measures the importance of higher harmonics ($n > 0$) while t is less than τ_n .

The magnitude of the harmonics as a function of position is plotted in Figure 6. Recall from Figure 5 that if M_E takes a negative value, this causes a delayed response in the erosion rate. This effect is most pronounced near the divide ($x = 0$). Positive values of M_E indicate that fast moving signals are accelerating the response of the hillslope to the change in channel incision. This occurs in locations near the channel. Near the divide, the harmonic of $n = 1$ is a significant fraction of the total response of the hillslope (Figure 6). Because this harmonic is the principal cause of the delay between the time the channel incision rate is perturbed and the time the divide ‘feels’ this signal, the time of delay can be estimated by the timescale of this harmonic. By equation (10), the delay in the response of the divide after the channel incision rate is perturbed is $\tau_0/9$. So, for example, in the hillslope depicted in Figures 3,4, and 5, which has a length of 40m and a diffusivity of $0.01\text{m}^2/\text{yr}$, τ_0 is approximately 65ka, and τ_1 is approximately 7ka. Examination of Figure 4b reveals that the divide begins responding to the transient incision signal at approximately 7ka.

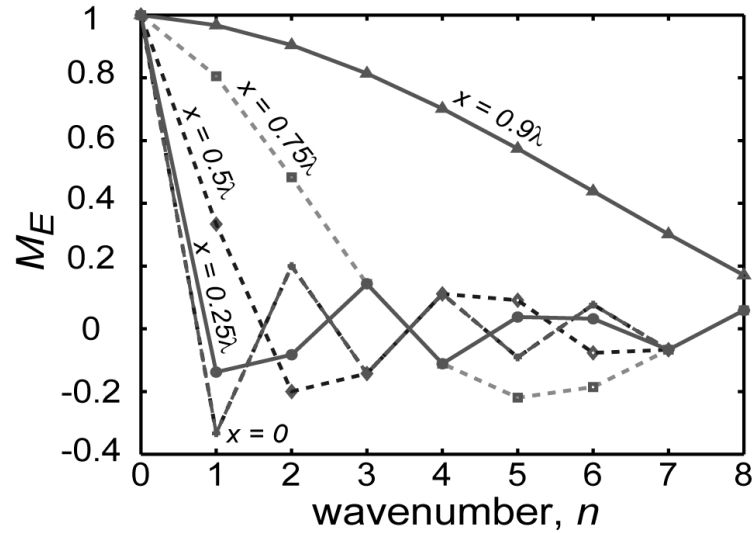


Figure 6. Values of M_E (see equation 11) as a function of wavenumber.

4. Timescales of Hillslope Response for Soil Thickness, Soil Production, and Hillslope Erosion Rate

The analysis in section 2 focuses on analytic solutions for idealized hillslopes where soil production and soil thickness are not considered. We now extend our analysis to include these, and other, factors. Returning to equations (2-4) to describe the soil mantled hillslope, we assume that the soil may have a different dry bulk density than the soil (i.e., $\rho_s \neq \rho_\eta$). In addition, the soil production rate, p_η , is described by a function of the soil thickness (h). In several field locations [e.g., *Heimsath et al. 1997; Heimsath et al. 2000; Heimsath et al. 2001*], the soil production rate has been found to be a decreasing function of increasing soil thickness:

$$p_\eta = W_0 e^{-\frac{h}{\gamma}} \quad (12)$$

where W_0 ($L T^{-1}$) is the nominal rate of soil production when the soil thickness is zero and γ (L) is a length scale that characterizes the rate of decline in the soil production rate with increasing soil thickness. Others have argued for a soil production function that peaks at some intermediate soil thickness [*Ahnert, 1976; Anderson, 2002; Carson and Kirkby, 1972; Furbish and Fagherazzi, 2001; Wilkinson et al. 2005*]. Here we limit our analysis to a soil production function that takes the form of equation (12).

Because the soil production as described by equation (12) is a nonlinear function of soil thickness, equations (2) and (4) must be solved numerically. In addition, the relationship between slope and sediment flux may be nonlinear. Examples include sediment flux that increases asymptotically as the hillslope approaches a critical gradient [*Andrews and Bucknam, 1987; Roering et al. 1999; Roering et al. 2001 Roering, 2004*], sediment flux that varies nonlinearly with slope due to biogenic effects [e.g., *Gabet, 2000; Gabet et al. 2003; Yoo et al. 2005*], an effective sediment diffusivity that is a nonlinear function of soil thickness [*Anderson, 2002*], and sediment transport that is a function of the product of the hillslope gradient and the soil thickness [*Heimsath et al. 2005*].

For example, *Roering et al. [2001]* examined the adjustment timescale of hillslopes whose sediment flux was a nonlinear function of the hillslope gradient of the form

$$h \bar{v}_x = -D \frac{\partial \zeta}{\partial x} \left[1 - \left(\frac{1}{S_c} \frac{\partial \zeta}{\partial x} \right)^2 \right]^{-1}, \quad (13)$$

where S_c (dimensionless) is a critical slope. They found that the hillslopes experiencing

sediment flux governed by equation (13) had lower values of τ (see equation 9) than did hillslopes where sediment transport was a linear function of slope (e.g., equation 5). The response became more rapid (e.g., τ decreases) as hillslope gradients increased [Roering *et al.* 2001]. Here we investigate the timescales of hillslope response as affected by the soil production and sediment flux that is proportional to the product of soil thickness and hillslope gradient.

4.1. Numerical Simulations

As we have demonstrated in section 2, changes in channel incision rates lead to signals that move away from the channels with different characteristic timescales (equation 10). We now concentrate on the timescale, τ , that may be extracted using equation (9) as described by Howard [1988] and Roering *et al.* [2001]. We again note that when $t = 3\tau$, the value of the function being analyzed (which could be topography, soil thickness, erosion rate, etc.) is within 5% of its final value if the new channel incision rate is steady in time.

Two sets of model runs were carried out. The model solves equations (2-4) using a finite difference scheme. In the first set of model runs, sediment transport was assumed to be a linear function of slope (equation 5) and in the second set of model runs the sediment flux was assumed to be proportional to the product of the soil thickness and the hillslope gradient:

$$h \bar{v}_x = -D_L h \frac{\partial \zeta_{bl}}{\partial x}, \quad (14)$$

where D_L is a transport coefficient of units $L T^{-1}$. We call equation (14) the depth-slope

sediment flux law.

4.1.1. Linear Flux Law

Response timescales for hillslopes whose sediment flux is linearly proportional to slope are plotted in Figure 7. Figure 7a plots the ratio between the timescale extracted by equation (9) (τ) and the timescale τ_0 predicted as the long term adjustment timescale by equation (10). This plot illustrates that the ratio between the density of the soil and the density of the soil's parent material can have a significant influence on the relaxation time of the hillslope.

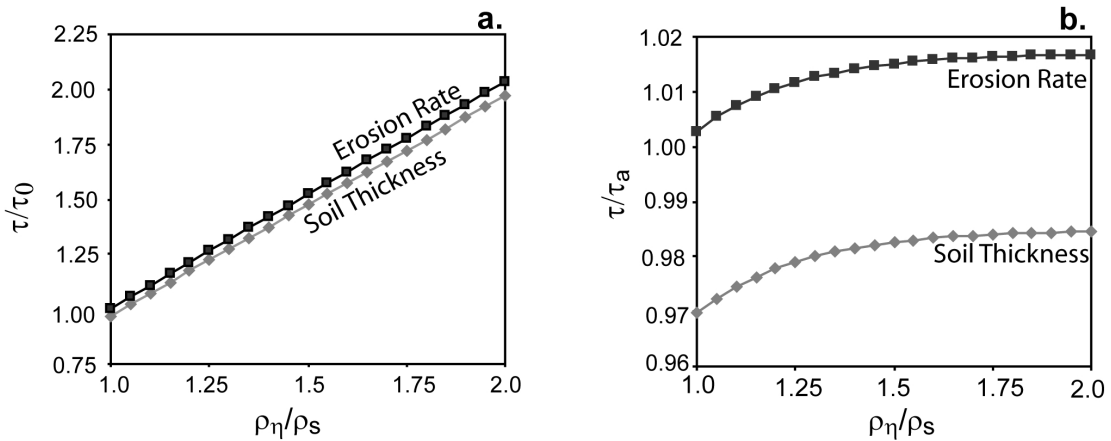


Figure 7. Plots of normalized (by τ_0 in **a.** and τ_a in **b.**) response timescale for the soil thickness and erosion rate. Other parameters from these model runs are $D = 0.005\text{m}^2/\text{yr}$, $\gamma = 0.3\text{m}$, $\lambda = 20\text{m}$, $W_0 = 0.0003\text{m}/\text{yr}$, $I_0 = -0.0001\text{m}/\text{yr}$, and $I = -0.0002\text{m}/\text{yr}$.

Figure 7b plots the ratio $\tau_p/\rho_\eta\tau_0$ for the erosion rate and the soil thickness. These curves are approximately equal to one, such that the relaxation timescale of a hillslope where the dry bulk density of the soil is different from that of its parent material can be approximated by:

$$\tau_a = \frac{4 \rho_\eta \lambda^2}{\rho_s \pi^2 D} \quad (15)$$

where τ_a is an approximate timescale of adjustment for hillslopes that experience a linear sediment flux law and experience soil production such that the hillslope is modeled using equations (2-4) and (5).

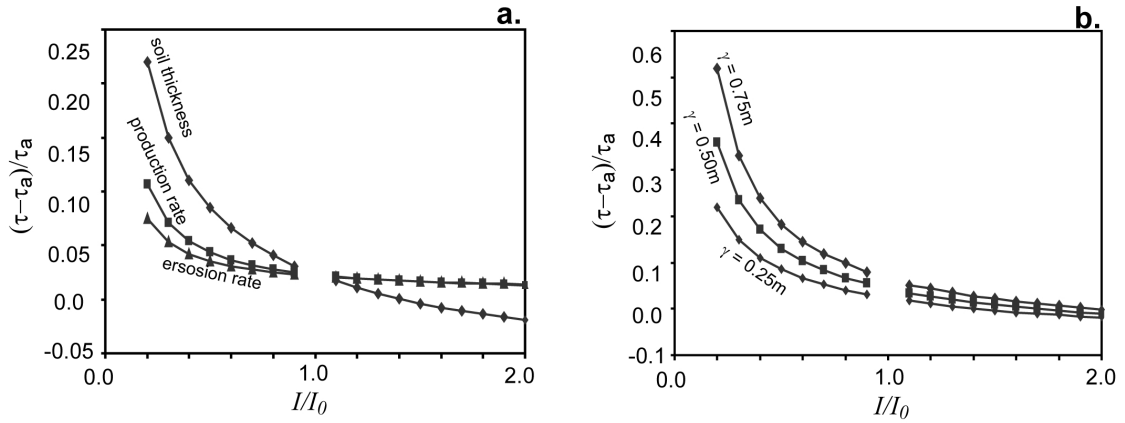


Figure 8. Difference between hillslope response timescale τ and approximate hillslope response timescale τ_a normalized by τ_a for hillslopes whose sediment flux is linearly proportional to the hillslope gradient. Plot **a.** shows the difference in response timescales for soil thickness, soil production rate, and erosion rate for a hillslope with parameters $\rho_\eta/\rho_s = 1.5$, $D = 0.005\text{m}^2/\text{yr}$, $\gamma = 0.25\text{m}$, $\lambda = 20\text{m}$, $W_0 = 0.0006\text{m}/\text{yr}$, $I_0 = -0.0001\text{m}/\text{yr}$. Plot **b.** shows the normalized response timescale of soil thickness for different values of γ on a hillslope with parameters $\rho_\eta/\rho_s = 1.5$, $D = 0.005\text{m}^2/\text{yr}$, $\lambda = 20\text{m}$, $W_0 = 0.0006\text{m}/\text{yr}$, $I_0 = -0.0001\text{m}/\text{yr}$. Note the change in scale on the vertical axes between **a.** and **b.** There is no data for I/I_0 because, trivially, there is no change in the hillslope under these conditions.

In Figure 8, we plot the difference between the adjustment timescale τ extracted using equation (10) and the approximated timescale τ_a , normalized by τ_a . As observed by *Furbish and Fagherazzi* [2001] and *Mudd and Furbish* [2005], soil thickness responds on a different timescale than does the erosion rate (Figure 7b, 8a). In addition, soil

production also responds on a different timescale, although the timescale of response for production more closely matches that of erosion than does the soil thickness. Our numerical experiments have shown W_0 has negligible influence on the timescale of hillslope response, but both the ratio between the timescale of response in the erosion rate and the timescale of response of the soil thickness is sensitive to the difference between the initial and final channel incision rates and also the depth over which soil production decays (γ) (Figure 8).

As the difference between the initial incision rate grows, the discrepancy between the approximate timescale τ_a and the timescale of response of the hillslope τ grows for the soil production rate, the erosion rate, and the soil thickness. This effect is most pronounced for the soil thickness, such that for hillslopes where there is a large (e.g., $I/I_0 < 0.2$) difference in the channel incision rates before and after the change in the channel incision rate the response timescale of the soil thickness can be different from the timescale of response in the erosion rate by 20%. When channel incision rates are increased, the soil thickness responds to the change in channel incision more slowly than the surface topography, whereas when the channel incision rate increases the soil thickness adjusts more rapidly than the hillslope erosion rate. As seen in Figure 8b, the timescale of response will be more poorly predicted by τ_a for thicker soils than for thinner soils (because γ sets the soil thickness for a given erosion rate).

4.1.2. Depth-Slope Flux Law

In the case of hillslopes where sediment flux is governed by equation (14), τ_a is inappropriate for comparing to the timescale, τ , which is measured by equation (9), because D_L is of different units than D . Instead, the D in equation (15) may be replaced

by $D \sim D_L h$, which is equivalent to stating that the diffusivity of the soil is depth dependant [e.g., *Anderson, 2002*]. Figure 9 plots the ratio of τ to this modified τ_a where in these plots $\tau_a = 4\rho_\eta \lambda^2 / (\pi^2 D_L h \rho_s)$ and the soil thickness is evaluated when it is in equilibrium with the lowest channel incision rate (e.g., the slowest possible hillslope response timescale for a given model run).

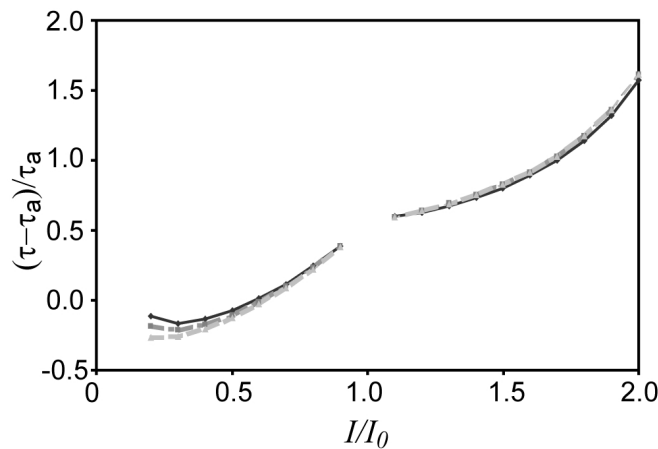


Figure 9. Difference between hillslope response timescale τ and approximate hillslope response timescale τ_a normalized by τ_a for hillslopes whose sediment flux is proportional to the hillslope gradient times the soil thickness. The hillslopes modeled have parameters $\rho_\eta/\rho_s = 1.5$, $D = 0.005\text{m}^2/\text{yr}$, $\gamma = 0.75\text{m}$, $\lambda = 20\text{m}$, $W_0 = 0.00025\text{m}/\text{yr}$, and $I_0 = -0.0001\text{m}/\text{yr}$. There is no data for I/I_0 because, trivially, there is no change in the hillslope under these conditions.

Several features of response timescales for hillslopes whose sediment flux is proportional to the product of the soil thickness and the hillslope gradient contrast with hillslopes whose sediment flux is linearly proportional to slope. First, the response timescales of hillslopes with the depth-slope sediment flux law are similar for soil thickness, soil production, and erosion rate (Figure 9), unlike the hillslopes experiencing a linear sediment flux law. In addition, in the case of the depth-slope sediment flux law,

hillslopes where the initial incision rate (I_0) is slower than the final incision rate (I) have much greater adjustment timescales as a percentage of τ_a than the hillslopes in which the opposite is true. This effect is accentuated if τ_a is calculated using the soil thickness that is in equilibrium with I . The reason for this difference is that if the incision rate is initially slow, and then accelerates, there is initially a greater thickness of soil that allows for larger sediment flux and faster propagation of transient incision signals away from the channel. When channel incision rates increase, the response timescale for hillslopes that experience a depth-slope product sediment flux law can be several times greater than the approximated timescale τ_a , such that in the case of increased channel incision, signals from the channel can be stored in these hillslope soils for a much greater period of time than a similar hillslope that experiences a linear sediment flux law.

5. Conclusions

Channel incision drives the evolution of soil mantled hillslopes. When channel incision rates change, signals from such changes propagate away from the channel. These signals operate on a number of timescales. We have demonstrated that for soil mantled hillslopes two timescales are particularly important. The first timescale, which we call τ_0 , determines how much time must pass after a change in the channel incision rate before the entire hillslope equilibrates to this new condition. For hillslopes that experience sediment flux that is linearly proportional to slope and whose soil is the same density as the material from which the soil is derived, this timescale is approximated by $4\lambda^2/(\pi^2 D)$ where λ is the length of the hillslope and D is the sediment diffusivity. At a time of $3\tau_0$ after a perturbation on the channel incision rate, the topography and erosion rate of the

hillslope are within 5% of their final values, and the hillslope can be reasonably considered to be at steady state. An additional timescale is the time it takes a signal caused by a change in the channel incision rate to propagate from the channel to the divide. This timescale is approximated by $\tau_0/9$.

As described by both *Furbish* [2003] and *Roering et al.* [2004], measurement of several spatially and temporally varying soil properties can be used to constrain the dynamic response of hillslopes to changes in the channel incision rate. The strongest spatial variation in soil properties can be expected to occur within the time after channel perturbation of $0 < t < \tau_0/9$, when the hillslope near the channel has begun to adjust to the new channel incision rate but the divide has not yet ‘felt’ this disturbance.

On hillslopes where soil is not the same density as the material from which the soil is derived (i.e., when $\rho_s \neq \rho_\eta$), the ratio between the two densities is of first order importance in determining the hillslope response to a change in the channel incision rate. In this case, the response timescale can be approximated by $4\rho_\eta\lambda^2/(\pi^2D\rho_s)$ if sediment flux is linearly proportional to slope. The difference in the adjustment timescales for soil thickness and soil erosion rate is sensitive to the ratio between the initial channel incision rate (I_0) and the channel incision rate after it has been perturbed (I). The difference between τ and τ_a is greater as the difference between I and I_0 increases for hillslopes that experience a linear sediment flux law, whereas this relationship is reversed for hillslopes experiencing sediment flux that is proportional to the product of the soil thickness and the hillslope gradient.

6. List of Symbols

D	Sediment diffusivity ($L^2 T^{-1}$)
η	Elevation of soil-bedrock boundary (L)
γ	Soil production decay lengthscale (L)
h	Soil thickness (L)
I, I_0	Channel incision rate and initial incision rate, respectively ($L T^{-1}$)
λ	Length of the hillslope (L)
M_E	Ratio determining the magnitude of the time vary component of the erosion rate as a function of position and wavenumber
n	Wave number (dimensionless)
p_η	Soil production rate ($L T^{-1}$)
$\bar{\rho}_s$	Depth averaged dry bulk density of hillslope soil ($M L^{-3}$)
ρ_η	Dry bulk density of parent material ($M L^{-3}$)
S_c	Critical slope for linear-critical flux law (dimensionless)
t	Time (T)
τ	Decay timescale (T)
τ_a	Approximate hillslope response timescale for hillslopes where $\rho_s \neq \rho_\eta$.
τ_n	Decay timescale for individual harmonic functions with wavenumber n .
\bar{v}_x	Depth averaged sediment velocity in the x direction ($L T^{-1}$)
W_0	Nominal rate of soil production ($L T^{-1}$)
x	Distance from the divide (L)
ζ	Elevation of soil surface (L)
ζ_{bl}	Elevation of soil surface relative to the channel (L)

7. References

- Ahnert, F. (1976), Brief description of a comprehensive three-dimensional process-response model of landform development, *Z. Geomorph. Suppl. Bd.*, 25, 29-49.
- Ahnert, F. (1987), Approaches to Dynamic Equilibrium in Theoretical Simulations of Slope Development, *Earth Surface Processes and Landforms*, 12 (1), 3-15.
- Anderson, R.S. (2002), Modeling the tor-dotted crests, bedrock edges, and parabolic profiles of high alpine surfaces of the Wind River Range, Wyoming, *Geomorphology*, 46 (1-2), 35-58.
- Andrews, D.J., and R.C. Bucknam (1987), Fitting Degradation of Shoreline Scarps by a Nonlinear Diffusion-Model, *Journal of Geophysical Research-Solid Earth and Planets*, 92 (B12), 12857-12867.
- Carslaw, H.S., and J.C. Jaeger (1959), *Conduction of Heat in Solids*, 510 pp., Oxford University Press, Oxford
- Carson, M.A., and M.J. Kirkby (1972), *Hillslope Form and Process*, 475 p. pp., Cambridge University Press, Cambridge.
- Culling, W.E.H. (1960), Analytical Theory of Erosion, *Journal of Geology*, 68 (3), 336-344.
- Culling, W.E.H. (1963), Soil Creep and the Development of Hillside Slopes, *Journal of Geology*, 71 (2), 127-161.
- Culling, W.E.H. (1965), Theory of erosion on soil-covered slopes, *Journal of Geology*, 73, 230-254.
- Davis, W.M. (1899), The geographical Cycle, *Geographical Journal*, 14, 481-504.
- Deen, W.M. (1998), *Analysis of Transport Phenomena*, 597 pp., Oxford University Press, Oxford.
- Dietrich, W.E., D.G. Bellugi, L.S. Sklar, and J.D. Stock (2003), Geomorphic transport laws for predicting landscape form and dynamics, in *Prediction in Geomorphology*, edited by P.R. Wilcock, and R.M. Iverson, American Geophysical Union, Washington, D. C.
- Fernandes, N.F., and W.E. Dietrich (1997), Hillslope evolution by diffusive processes: The timescale for equilibrium adjustments, *Water Resources Research*, 33 (6), 1307-1318.
- Furbish, D.J., and S. Fagherazzi (2001), Stability of Creeping Soil and Implications for

- Hillslope Evolution, *Water Resources Research*, 37 (10), 2607-2618.
- Furbish, D.J. (2003), Using the dynamically coupled behavior of the land-surface geometry and soil thickness in developing and testing hillslope evolution models, in *Prediction in Geomorphology*, edited by P.R. Wilcock, and R.M. Iverson, pp. 169-182, American Geophysical Union, Washington, D. C.
- Gabet, E.J. (2000), Gopher Bioturbation: Field Evidence for Non-Linear Hillslope Diffusion, *Earth Surface Processes and Landforms*, 25 (13), 1419-1428.
- Gabet, E.J., O.J. Reichman, and E.W. Seabloom (2003), The Effects of bioturbation on soil processes and sediment transport, *Annual Reviews of Earth and Planetary Science*, 31, 249-73.
- Gilbert, G.K. (1877), Report on the geology of the Henry Mountains: U.S. Geographical and Geological Survey of the Rocky Mountain Interior Region, pp. 160, U.S. Government Printing, Washington D.C.
- Gilbert, G.K. (1909), The convexity of hilltops, *Journal of Geology*, 17, 344-350.
- Hack, J.T. (1960), Interpretation of erosional topography in humid temperate region, *American Journal of Science*, 258-A, 80-97.
- Heimsath, A.M., W.E. Dietrich, K. Nishiizumi, and R.C. Finkel (1997), The Soil Production Function and Landscape Equilibrium, *Nature*, 388 (6640), 358-361.
- Heimsath, A.M., J. Chappell, W.E. Dietrich, K. Nishiizumi, and R.C. Finkel (2000), Soil Production on a Retreating Escarpment in Southeastern Australia, *Geology*, 28 (9), 787-790.
- Heimsath, A.M., J. Chappell, W.E. Dietrich, K. Nishiizumi, and R.C. Finkel (2001), Late Quaternary Erosion in Southeastern Australia: a Field Example Using Cosmogenic Nuclides, *Quaternary International*, 83-5, 169-185.
- Heimsath, A.M., J. Chappell, N.A. Spooner, and D.G. Questiaux, Creeping soil, *Geology*, 30 (2), 111-114, 2002.
- Heimsath, A.M., D.J. Furbish, and W.E. Dietrich (2005), The illusion of diffusion: Field evidence for depth-dependent sediment transport, *Geology*, 33 (12), 949-952.
- Howard, A.D. (1988), Equilibrium models in geomorphology, in *Modeling in Geomorphic Systems*, edited by M.G. Anderson, pp. 49-72, John Wiley, New York.
- Jyotsna, R., and P.K. Haff (1997), Microtopography as an indicator of modern hillslope diffusivity in arid terrain, *Geology*, 25 (8), 695-698.

- King, L.C. (1953), Canons of landscape evolution, *Bulletin of the Geological Society of America*, 64, 721-752.
- Kirkby, M.J., Measurement and theory of soil creep, *Journal of Geology*, 75 (4), 359-&, 1967.
- Mudd, S.M., and D.J. Furbish (2004), The Influence of chemical denudation on hillslope morphology, *Journal of Geophysical Research*, 109 (F02001), doi:10.1029/2003JF000087.
- Mudd, S.M., and D.J. Furbish (2005), Lateral migration of hillcrests in response to channel incision in soil mantled landscapes, *Journal of Geophysical Research*, 110 (12), F04026, doi:10.1029/2005JF000313.
- Penck, W. (1972), *Morphological analysis of land forms; a contribution to physical geology*, translated by Hella Czech and Katharine Cumming Boswell, 429 pp., Hafner, New York (reprint of the 1953 edition)
- Roering, J.J., J.W. Kirchner, and W.E. Dietrich (1999), Evidence for Nonlinear, Diffusive Sediment Transport on Hillslopes and Implications for Landscape Morphology, *Water Resources Research*, 35 (3), 853-870.
- Roering, J.J., J.W. Kirchner, and W.E. Dietrich (2001), Hillslope Evolution by Nonlinear, Slope-Dependent Transport: Steady State Morphology and Equilibrium Adjustment Timescales, *Journal of Geophysical Research-Solid Earth*, 106 (B8), 16499-16513.
- Roering, J.J., P. Almond, P. Tonkin, and J. McKean, Soil transport driven by biological processes over millennial time scales, *Geology*, 30 (12), 1115-1118, 2002.
- Roering, J.J. (2004), Soil creep and convex-upward velocity profiles: Theoretical and experimental investigation of disturbance-driven sediment transport on hillslopes, *Earth Surface Processes and Landforms*, 29 (13), 1597-1612.
- Roering, J.J., P. Almond, P. Tonkin, and J. McKean (2004), Constraining climatic controls on hillslope dynamics using a coupled model for the transport of soil and tracers: Application to loess-mantled hillslopes, South Island, New Zealand, *Journal of Geophysical Research-Earth Surface*, 109, F01010, doi: 10.1029/2003JF000034.
- Small, E.E., R.S. Anderson, and G.S. Hancock (1999), Estimates of the Rate of Regolith Production Using Be-10 and Al-26 From an Alpine Hillslope, *Geomorphology*, 27 (1-2), 131-150.
- Wilkinson, M.T., J. Chappell, G.S. Humphreys, K. Fifield, B. Smith, and P. Hesse (2005), Soil production in heath and forest, Blue Mountains, Australia: influence of

lithology and palaeoclimate, *Earth Surface Processes and Landforms*, 30 (8), 923-934.

Yoo, K., R. Amundson, A.M. Heimsath, and W.E. Dietrich (2005), Process-based model linking pocket gopher (*Thomomys bottae*) activity to sediment transport and soil thickness, *Geology*, 33 (11), 917-920.

Young, A., A twelve-year record of soil movement on a slope, *Z. Geomorph. Suppl. Bd.*, 29, 104-110, 1978.

CHAPTER VI

CONCLUSIONS AND FUTURE DIRECTIONS

The four manuscripts that make up this thesis have two components that constitute both important advances in hillslope geomorphology and the framework upon which my work in the future will be based. In chapter II and III, I have derived statements of mass conservation for a hillslope soil, and constituent phases of the soil, that are far more robust than those used in the past because: (i) they are derived from local statements of mass conservation and can be modified to suit a wide variety of hillslope conditions, and (ii) they incorporate, for the first time, effects of chemical denudation in addition to mechanical processes of sediment transport. These mass conservation equations, when applied to a hillslope soil, allow geomorphologists to be more explicit about the assumptions used in hillslope analysis than was previously possible.

In addition, I have investigated the timescales of response to different disturbances influencing the evolution of hillslope soils, and have characterized the timescale over which these disturbances propagate through a landscape (Chapters IV and V). Landscapes are dynamic: faults move at different rates, tectonic uplift rates are not constant in time, and climate, which can drive erosion, varies dramatically over geomorphically significant timescales. Whereas in the past much geomorphic research was carried out by using the simple and illustrative ‘steady state’ hypothesis, in which erosion rates are assumed to be constant in time and landscapes obtain a steady topographic form, I am now poised to move beyond this limiting scenario and explore the full dynamic behavior of the landscape.

I have quantified the duration over which signals induced by changes in landscape erosion rates persist in hillslope soils. An important next step is to find suitable field areas where various soil properties and their variations over space serve as signatures of transient channel incision rates. In this way hillslope soils function as recording devices for a landscape's dynamic history of erosion. This avenue of research will combine my interest in conserving mass of numerous soil properties (e.g., Chapters II and III) and my interest in how long term changes in soil properties may persist in an evolving hillslope soil (e.g., Chapters IV and V).

My future research direction involves two primary goals. The first is to use the methods that have been developed for this thesis to try to understand how chemical denudation rates vary as a function of topographic position. Constraining these denudation rates will involve combining the statements of mass conservation derived in chapters II and III. This work is currently in progress and has resulted in a collaboration with Kyungsoo Yoo at the University of Delaware. Once we can quantify the spatial distribution of chemical denudation rates, the perhaps more pertinent question of what causes chemical denudation rates to vary in space can then be addressed. To this end I have been developing discrete particle simulations that can be used to test weathering laws for hillslope soils.

The fundamental coupling of mechanical and chemical denudation rates may be caused by strong relationship between chemical weathering rates and the period of time that particles reside in the 'weathering engine,' as described in section 4.2 of chapter III. This weathering engine is the hillslope soil, and the time particles spend in hillslope soils is fundamentally related to the rates of erosion and soil production in a landscape. By investigating how transient channel incision rates affect the age distribution of particles that make up hillslope soil, I hope to be able

to gain an understanding of the close relationship between physical and chemical denudation rates.